MODELLING THE POTENTIAL IMPACTS OF FORESTATION ON EXTREME CLIMATE EVENTS OVER WEST AFRICA

ODOULAMI, ROMARIC CHRISTEL

MET/12/2035

JUNE, 2016

MODELLING THE POTENTIAL IMPACTS OF FORESTATION ON EXTREME CLIMATE EVENTS OVER WEST AFRICA

ODOULAMI, Romaric Christel

(B.Sc., M.Eng.)

MET/12/2035

A THESIS

IN THE DEPARTMENT OF METEOROLOGY AND CLIMATE SCIENCE IN PARTNERSHIP WITH THE WEST AFRICAN SCIENCE SERVICE CENTRE ON CLIMATE CHANGE AND ADAPTED LAND USE (WASCAL) SUBMITTED TO THE SCHOOL OF POSTGRADUATE STUDIES, IN PARTIAL FULFILLMENT OF THE REQUIREMENT FOR THE AWARD OF THE DEGREE OF DOCTOR OF PHILOSOPHY IN METEOROLOGY AND CLIMATE SCIENCE OF THE FEDERAL UNIVERSITY OF TECHNOLOGY, AKURE ONDO STATE IN NIGERIA

JUNE, 2016

CERTIFICATION

a) By the student:

This work has not been presented elsewhere for the award of a degree, or any other purpose.

Candidate's name: ODOULAMI, Romaric Christel

Signature:  Date: 15/07/2016

b) By the Supervisor(s):

I certify that this work has been carried out by Mr. ODOULAMI, Romaric Christel under my supervision and that to the best of my knowledge, it has not been submitted elsewhere for the award of a degree.

Supervisor's Name: Dr. Babatunde J. ABIODUN

Signature:  Date: 20/07/2016

Co-supervisor's Name: Dr. Eng. Ayodele E. AJAYI

Signature:  Date: 20/07/2016

ACKNOWLEDGEMENTS

I would like to express my sincere gratitude to my supervisor, Dr. Babatunde J. Abiodun. More than a supervisor, you are a brother and a friend. I want to thank you for always motivating me, for the invaluable advice, the guidance, the support, and the encouragement throughout this journey.

I am also grateful to my co-supervisor, Dr.-Eng. Ayodele E. Ajayi, for his collaboration, advice and contribution to make this Ph.D. work a success. My regard also goes to Dr. Dominikus Heinzeller for his collaboration and assistance.

This Ph.D. programme is fully sponsored by the German Ministry of Education and Research (BMBF) through the West African Service Centre on Climate Change and Adapted Land Use (WASCAL). I am grateful to WASCAL for granting me all the required financial support for the successful completion of my Ph.D. studies, including my research visit at the University of Cape Town (UCT), South Africa.

I would like to show my gratitude to the Director of the WASCAL GRP-WACS in FUTA, Prof. Kehinde Ogunjobi and the entire staff. My respect also goes to the former director of the WASCAL centre, Prof. Jerome A. Omotosho, with whom we have started this Ph.D. Programme. I would like to express my gratitude to the head of the Department of Meteorology and Climate Science, Dr. E. C. Okogbue, and to all his assisting staff.

The computational facilities used in this study are provided by the Centre of High Performance Computing (CHPC) in Cape Town, South Africa. My regards go to the CHPC for its support in the accomplishment of this Ph.D. thesis. I would like to thank Mr.

Sibusiso E. Mbele and Mr. Sticks Mabakane for their continuous assistance with training on how to use the CHPC resources and for helping me to solve problems I encountered while using the CHPC resources.

My regards go to the Climate System Analysis Group (CSAG) in the Department of Environmental and Geographical Science (EGS) at UCT for having hosted me and also for providing me parts of the computational resources used in this study. I would like to particularly thank Mr. Phillip Mukwenha for his permanent availability and willingness to help with software installations and IT-related issues and to; Dr. Chris Lennard and Dr. Chris Jack for their suggestions and advice. I am also grateful to Mrs Sharon Adams for helping with general administrative issues.

I also want to thank all EGS students and staff I encountered during my stay at UCT. A special thank you goes to the "Monday Morning Peer Reviewing Team", to all my office mates and all those in the departmental 'donjon'. I would like to specially thank Dr. Arlindo Meque, Sabina Abba Omar, Myra Naik, Roland Takong, Mariam Nguvava, Stefaan Conradie, Temitope Egbebiyi and Teboho Nchaba for their availability and assistance and for the shared knowledge, memories and frustrations.

My recognition goes to all West African students I came across within and around Cape Town. I want to show my respect to Dr. Chabi Djagoun, Ms Flora Assogbadjo, Ulrich Gaba, Ruben Aza-Gnandji, Constant Labitan, Dr. Ousman Sawadogo and his family, Dr. Lougue Siaka and his family and all the others.

My regards also go to former WASCAL students, especially Dr. Ulrich Diasso and Dr. Moussa Mounkaila Saley. Your assistance has been of great importance in the achievement of this work. My gratitude also goes to all my fellow WASCAL comrades, mainly to those in the second batch of the GRPs WACS: Peter Gibba, Michel Nikiema, Edward Naabil, Ibouraima Kébé, Kouakou Kouadio, Amadou Coulibali, Vincent Ojeh, and Mrs Christiana Talabi.

I would like to express my gratitude to my family, to my parents for having given me all the best they can and also for their unconditional support, prayers and blessings. This work is fully dedicated to you. I also want to thank my sisters for their support. To my uncle, Emeritus Prof. Honoré Odoulami, I am grateful for your advices and support.

I would also like to thank some of my former lecturers for their contribution to this Ph.D. work. The best of my regards go to Dr. Christoph Chrysostome, Dr. Frederick Houndonougbo, Dr. Achille Assogbadjo and Prof. Romain Kakai-Glele for their advice and support.

To all of you who have in a way or another contributed to the successful completion of my Ph.D. work, thank you to you all.

DEDICATION

In the memory of Kenneth Conrad PADONOU: You are not here to contemplate this achievement of your little brother. I strongly believe that you know an endless happiness and that this piece of work also brings to you more joy. Rest in Peace Brer Kenneth

To my father, Roger A. ODOULAMI, and to my mother, Julienne A. BABADOUDOU, for the endless sacrifices you made and continue to make for the sake of your children.

ABSTRACT

Previous studies on climate change projections over West Africa did not include the influence of on-going forestation activities on future climate extremes over the region. The present study aimed to examine the potential impacts of a large scale forestation activity on the future characteristics of extreme climate events (extreme rainfall and heatwaves) over West Africa using Regional Climate Models (RCMs). The specific objectives of the study were to: (i) examine RCMs ability to simulate extreme climate events over West Africa; (ii) investigate the potential impacts of climate and forestation on extreme rainfall events over West Africa; and (iii) examine the potential impacts of climate and forestation on heatwaves characteristics over West Africa. The study applied two RCMs (RegCM and WRF) to simulate the present day (PRS, 1970-2004) and the future (2030-2064) climates, with and without forestation (GHG and FRS, respectively). The simulations account for the potential impacts of forestation over the Savannah zone (8°N - 12°N) in West Africa. In this study, an extreme rainfall event is said to occur when the daily rainfall amount exceeds a threshold value (*i.e.* 95^{th} percentile of the daily rainfall) and a Widespread Extreme Rainfall Event (WERE) is defined as the simultaneous occurrence of extreme rainfall that covers at least 50% of a given area. Heatwaves are identified using two metrics: the excess heat factor (EHF) and a percentile based index (TXI: 90^{th} percentile of daily maximum temperature). The RCMs ability to simulate the characteristics of extreme events for PRS is assessed against observed datasets: the Global Precipitation Climatology Project (GPCP) and Tropical Rainfall Measurement Mission (TRMM) for extreme rainfall events analysis; and the Princeton University Global Meteorological Forcing Dataset (PGFD) for heatwaves analysis. The results show that both RCMs reproduce well the extreme rainfall threshold

values (95th percentile) over West Africa and WEREs over Savannah in comparison with the observation datasets (GPCP and TRMM), though with some notable discrepancies. The RCMs generally overestimate the threshold of extreme rainfall over coastal areas and highlands, and simulated WEREs earlier than observed. For heatwaves, the two methods (EHF and TXI) generally produce similar patterns of heatwave characteristics over West Africa, except that heatwave number and days are substantially greater with TXI than with EHF. Also, the models give a realistic simulation of extreme temperature thresholds and heatwave characteristics over West Africa, although with some apparent biases. The results agree with previous studies that the Representative Concentration Pathway (RCP4.5) emission scenario would increase the frequency and intensity of extreme climate events over West Africa in future. In fact climate change would increase the frequency of extreme rainfall events over parts of the Guinea coast (and lower it over the Sahel zone), and heatwave number, days and duration over the whole region in future. The results further indicate that forestation would enhance the characteristics of extreme events over West Africa in future. Forestation generally increases the frequency and intensity of extreme rainfall events over the forested zone and decreases it elsewhere. Also, both models suggest that forestation would increase WERE frequency in parts of the Savannah zone. Similarly, forestation would also increase heatwave number and days over the forested area as the forestation would decrease surface albedo which during the dry season would increase the net solar radiation making more energy available at the surface. The outcomes of the present study suggest that the use of forestation to mitigate the impacts of climate change over West Africa might induce undesirable climatic impacts (increase in extreme rainfall and heatwave events) over some locations of the subcontinent, thereby increasing the

climatic risk on human health and security. Therefore, the results of this study may guide decision makers in improving the resilience of West African countries to the consequences of climate and weather extremes and also in choosing appropriate climate change mitigation and adaptation options.

TABLE OF CONTENTS

LIST OF TABLES

LIST OF FIGURES

LIST OF ACRONYMS

AEJ	African Easterly Jet
AEW	African Easterly Wave
AOGCM	Atmosphere-Ocean General Circulation Model
AUC	African Union Commission
BATS	Biosphere Atmosphere Transfer Scheme
CCM	Community Climate Model
CCWR	Climate Change and Water Resources
CMIP5	Coupled Model Intercomparison Project phase 5
CORDEX	Co-ordinated Regional Downscaling Experiment
CSAG	Climate System Analysis Group
CRED	Centre for Research on the Epidemiology of Disasters
CS	Central Savannah
DJF	December-January-February
ECHAM6	European Centre/Hamburg (Sixth Generation Atmospheric General Circulation) Model (of the Max Planck Institute for Meteorology)
EHF	Excess Heat Factor
EHI	Excess Heat Index
EHIaccl	Acclimatisation Excess Heat Index
EHIsig	Significant Excess Heat Index
EGS	Environmental and Geographical Science Department
ES	East Savannah
ETCCDI	Expert Team on Climate Change Detection and Indices

EVT Extreme Value Theory

FAO United Nations Food and Agriculture Organisation

FRS Future climate experiment with forestation

FUTA Federal University of Technology, Akure

GCAM Global Change Assessment Model

GCM General Circulation Model

GEV Generalised Extreme Value

GHG Future climate experiment without forestation

GPCP Global Precipitation Climatology Project

GRP Graduate Research Programme

HADGEM1 Met Office Hadley Centre Global Earth System Model version 1

HADGEM2-ES (or **HAD**) Met Office Hadley Centre Global Earth System Model version 2

HAMOCC Hamburg Ocean Carbon Cycle Model

HWD Heatwave duration

HWF Heatwave days

HWN Heatwave number

ICTP International Centre for Theoretical Physics

IFRC International Federation of Red Cross and Red Crescent Societies

IPCC Intergovernmental Panel on Climate Change

ITCZ Intertropical Convergence Zone

ITD Intertropical Discontinuity

JSBACH Land Vegetation Model of the Max-Planck-Institute Earth System Model

LFI Local Fit and Interpolation

LHF Latent Heat Flux

MAM March-April-May

MCC Mesoscale Convective Complex

MCS Mesoscale Convective System

MPI-ESM-LR (or **MPI**) Max-Planck-Institute Earth System Model Low Resolution

MPI-OM Max-Planck-Institute Ocean General Circulation Model

NCEP-NCAR National Centre for Environmental Prediction – National Centre for Atmospheric Research

PBL Planetary Boundary Layer

PGFD Princeton University Global Meteorological Forcing Dataset for land surface modelling

POT Peaks-Over-Threshold

PRS Present-day climate experiment

QAS Near surface air specific humidity

RCM Regional Climate Model

RCP Representative Concentration Pathway

RegCM ICTP Regional Climate Model

RH Near surface relative humidity

RSNL Surface net longwave energy flux

RSS Surface net shortwave energy flux

SHF Sensible Heat Flux

SMLE Spatial Maximum Likelihood Estimation

SMOIS Moisture content of the soil layers

SST Sea Surface Temperature

STWJ Subtropical Westerly Jet

SUBEX SUB-grid EXplicit moisture scheme

T95 95^{th} percentile of Daily Mean Temperature

TEJ Tropical Easterly Jet

TF Foliage Canopy Temperature

T_i Daily Mean Temperature

Tmax Daily Maximum Temperature

Tmin Daily Minimum Temperature

TRMM Tropical Rainfall Measuring Mission

TS Ground Surface Temperature

TX90 90^{th} percentile of Daily Maximum Temperature

TXI Percentile based heatwave index

UCT University of Cape Town

UN United Nations

USD United States Dollar

USGS United States Geological Survey

WAM West African Monsoon

WACS West African Climate System

WASCAL West African Science Service Centre on Climate Change and Adapted Land-Use

WERE Widespread Extreme Rainfall Event

WMO World Meteorological Organisation

WRF Weather Research and Forecast

WS West Savannah

WSM5 WRF single-moment 5-class scheme

CHAPTER ONE

INTRODUCTION

1.1 BACKGROUND

The anthropogenic (man-made) influences on the climate have affected the frequency and intensity of extreme events (extreme temperatures, extreme precipitation, droughts) in some regions of the world (IPCC, 2013). Considering the growing threat of climate change to human and natural systems, there is a need for climate change information, at the regional to local scale, to assess the impacts of climate change and to develop suitable adaptation and mitigation strategies at the national level (Giorgi *et al.*, 2009). This need is especially important in Africa, one of the most vulnerable regions to the impacts of climate change because of the susceptibility of its population to the impacts of climate change, climate variability and extreme climate events. Providing useful and reliable climate information at the regional and local scale enables the formulation of climate projections, which provides end-users and policy makers a solid foundation to guide response options (Giorgi *et al.*, 2009). This may help to enhance the adaptive capability of the population to the impacts of climate change, to lower the negative impacts of climate change on society, human health and security.

This study aims to provide a detailed projection of the potential impacts of climate change on extreme climate events over West Africa in future. The study uses dynamical downscaling of general circulation models (GCMs) outputs by regional climate models

(RCMs) to project the potential impacts of climate change and the potential impacts of forestation on extreme rainfall events and heatwaves.

The World Meteorological Organisation (WMO, 2014) produced a comprehensive report on the damages (lives and economic losses) related to climate extremes between 1970 and 2012. From 1970 to 2012, 8,835 weather and climate-related disasters globally (Figure 1.1) claimed 1.94 million human lives and caused economic losses estimated at USD 2.4 trillion. In terms of human lives lost, the 10 worst reported climate disasters during that period represented only 0.1% of the total number of climate events, but accounted for 69% (1.34 million) of the total deaths from climate-related disasters.

In Africa, during the same period, up to 1,319 disasters were reported (Figure 1.2), claiming about 698,380 lives and USD 26.6 billion of economic losses (Figure 1.3). While floods were the most frequent disaster type (61%) over the continent, drought was the deadliest type of disaster; with up to 91% of all human lives lost due to climate-related disasters.

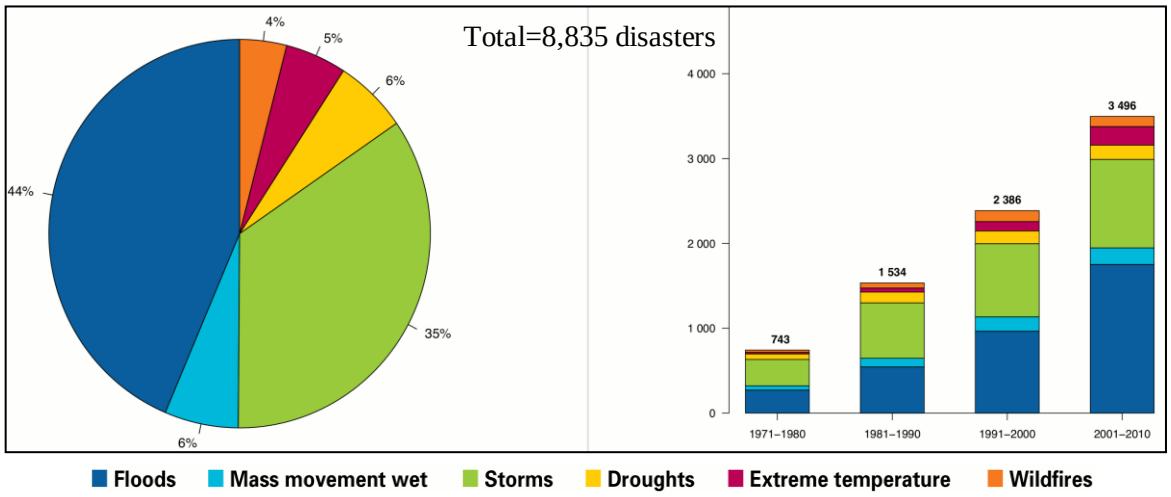

Figure 1.1: Global distribution of reported climate-related disasters (1970 - 2012)

Source: WMO (2014)

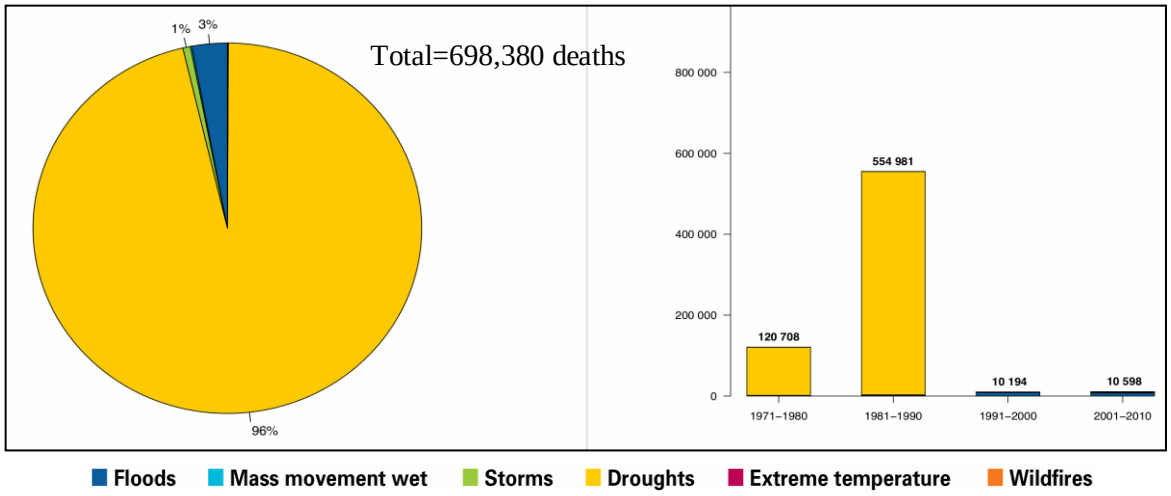

Figure 1.2: Distribution of climate disaster-related deaths in Africa (1970 - 2012)

Source: WMO (2014)

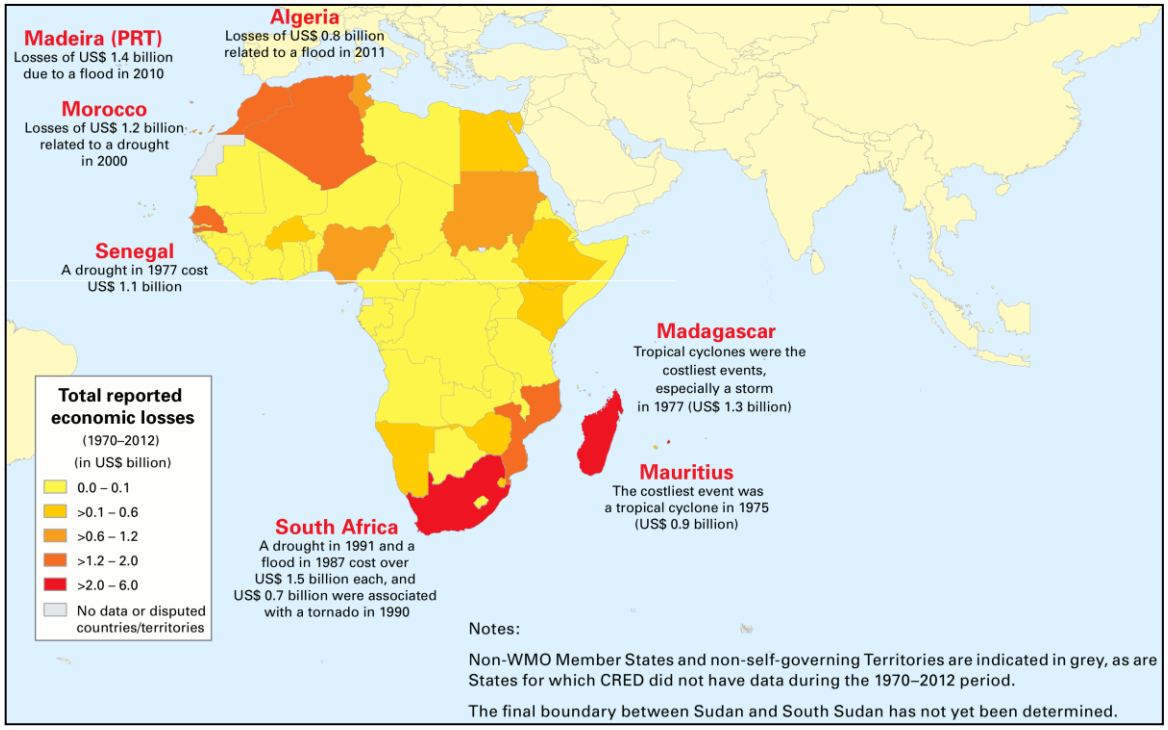

Figure 1.3: Economic losses associated with climate disasters in Africa (1970 - 2012)

Source: WMO (2014)

1.1.1 Extreme Rainfall Events

Extreme rainfall events are generally associated with flooding that can be devastating for the environment and human communities' economy and infrastructure. Estimates from the International Federation of Red Cross and Red Crescent Societies (IFRC, 2014) indicate that, for the decade 2004-2013, floods affected more than 943 million people in the world and claimed more than 63,207 lives. During the same period, flood-related damage totalled more than USD 312 billion globally, which represents nearly 20% of all economic damage attributable to natural disasters (IFRC, 2014).

In West Africa, extreme rainfall events can be especially destructive to property and life due to the low adaptive capacity of the region to cope with weather extremes. Tschakert *et al.* (2010) report that in 1995, 1998 and 1999, extreme rainfall events in West Africa affected more than one million people from five, eight and eleven countries respectively, including Sudan. Extreme rainfall events and associated damages were also recorded in 2007 in West Africa, with 56 killed and a community of 28,000 displaced in Ghana, 46 killed in Burkina Faso, and 23 people killed in Togo (Tschakert *et al.*, 2010). In September 2009, an extreme rainfall of over 260 mm day produced floods that destroyed about 300 hectares of crops, wrecked almost 25,000 houses, and rendered more than 100,000 people homeless in Burkina Faso (FAO, 2009). Similarly, in 2010, more than USD 260 million damages were attributed to extreme rainfall events in the Republic of Benin. Figure 1.4 provides a detailed map of floods and their impacts across West Africa experienced in 2007.

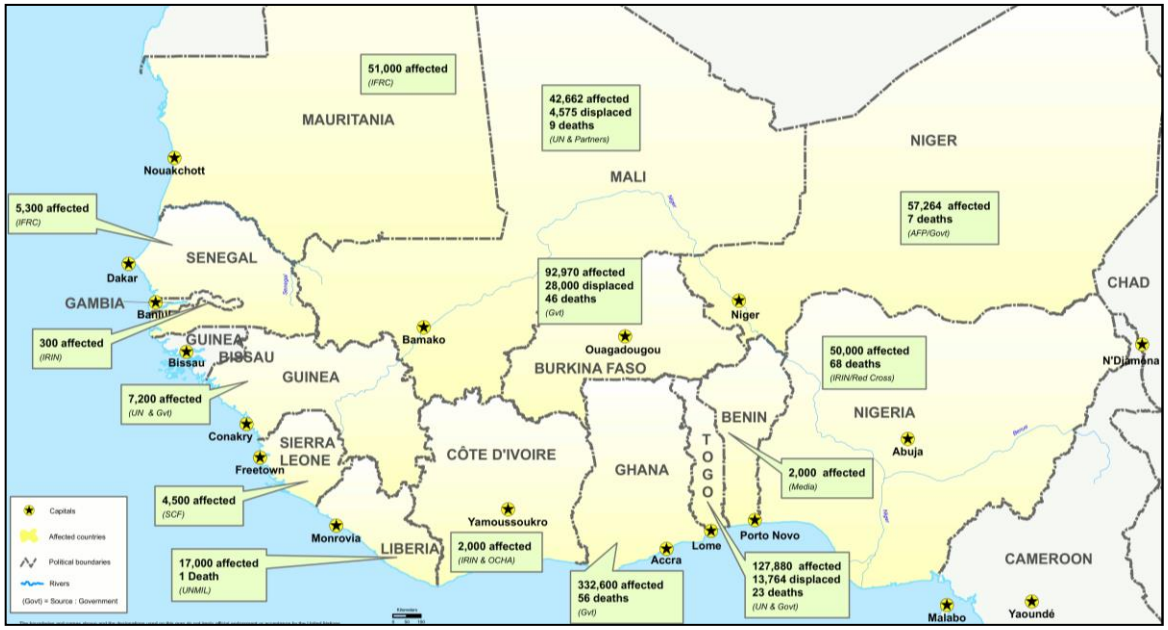

Figure 1.4: Floods and their impacts across West Africa, July to September 2007

Source: UN Office for the Coordination of Humanitarian Affairs (http://reliefweb.int/map/ghana/west-africa-floods-17-oct-2007)

Many studies show that, due to the impacts of climate change, the recent increase in frequency of extreme rainfall events may continue into the future (Abiodun *et al.*, 2013; Christensen *et al.*, 2007; Sylla *et al.*, 2012). Christensen *et al.* (2007) project an increase of 20% in the frequency of extreme rainfall events over West Africa in the coming decades. Sylla *et al.* (2012) project that future extreme rainfall events will be more intense and frequent during the boreal summer (June-August) of the mid and late 21st century, especially over the Guinea Highlands and Cameroon Mountains. An increase in extreme rainfall events is also projected over various ecological zones in Nigeria (Abiodun *et al.*, 2013).

Previous studies on extreme rainfall events in West Africa usually focus on localised (*i.e.* grid-scale) extreme rainfall events, but a Widespread Extreme Rainfall Event (WERE) would induce more devastating impacts on people and communities. While much is known about the atmospheric circulation systems that produce localised extreme rainfall events, little is known about which of the systems usually produce WERE in West Africa. The risk for damaging floods due to the changing climate in West Africa remains an issue of great importance. However, high quality projections from RCMs may help to reduce the future environmental and socio-economic impacts of extreme rainfall events in West Africa by assisting to find suitable mitigation/adaptation strategy to lower impacts on human security and health.

1.1.2 Heatwaves

Heatwaves can have devastating impacts on society, the economy and the environment. Commonly, heatwaves induce increases in human morbidity and mortality rates among elderly and infants (Anderson & Bell, 2011; Basu & Samet, 2002). Heatwaves can also increase stress on crops and animals, with considerable economic impacts, such as price increase of agricultural products (Chung *et al.,* 2014; Ciais *et al.,* 2005; Lanning *et al.,* 2011). This can increase the vulnerability of populations in developing countries to food security by limiting their access to food.

In Europe, more than 40,000 heat-related deaths were recorded during the devastating heatwaves of 2003 (García-Herrera *et al.,* 2010; Hémon *et al.,* 2003). A severe heatwave event also occurred in Russia during 2010 (Dole *et al.,* 2011). More recently, between April and May 2015, India and Pakistan experienced prolonged and deadly heatwave events that induced thousands of deaths, predominantly among the poorest populations – more than 2,500 in India and 1,100 in Pakistan (Rafferty, 2015). In West Africa, there are fewer recorded instances of deadly heatwaves as is the case in other parts of the world. However, extremely hot events were reported over the region during the boreal summer of 2002, with abnormally high temperatures of up to 50.6°C in the Sahara (WMO, 2013).

The frequency, duration and intensity of heatwaves are expected to increase in the future due to climate change (IPCC, 2014). For example, Russo *et al.* (2014) report that more areas globally have been affected by heatwaves over the period 1980-2012. They project that extreme and very extreme heatwave events are likely to occur as often as every 2 years in certain regions of the world, including Africa, by the end of the 21st century. Likewise,

there is a general warming trend observed throughout West Africa over the period 1960-2010, with more frequent warm days and warm spell events (Mouhamed *et al.*, 2013). Moreover, Vizy and Cook (2012) project that climate change may increase the frequency of heatwave days in West Africa during the mid-21st century, and Abiodun *et al.* (2013) project increases in future occurrence of extreme temperature events over all ecological zones of Nigeria.

1.1.3 Forestation

Forestation is a sustainable way to mitigate the effects of global warming (IPCC, 2007). It is a geo-engineering option as, by sequestering carbon dioxide in the biomass of trees, it alters the surface properties that are relevant for the climate (IPCC, 2007). Forestation can increase rainfall (Enger & Tjernstrom, 1991) and lower temperature (Abiodun *et al.*, 2012a; Abiodun *et al.*, 2012b). Moreover, forestation may improve soil's physical properties; increasing the soil infiltration rate, porosity and water retention capacity (Mapa, 1995). This may lower the risk for flooding and inundation.

However, arguments exist on the specific impacts of forestation land-cover modification activity in Africa on climate change projections over the region (AUC 2006). For instance, while Abiodun *et al.* (2012a) and Abiodun *et al.* (2012) claim that forestation reduces the projected warming over the forested area in West Africa, Naik and Abiodun (2016) show that forestation increases the projected warming over the forested area in Southern Africa. However, both studies agree that forestation increases rainfall over the forested areas. Mounkaila Saley (2015) showed that a large-scale forestation across the Savannah zone in

West Africa induces earlier onsets of rainfall over some areas, but delayed onsets of rainfall over other areas. Diasso (2015) also shows that forestation alters the projected changes in the patterns and intensity of drought over West Africa, but at varying degree over the sub-continent. Abiodun *et al.* (2012b) found that, while forestation increases the frequency of extreme rainfall events over the Guinean zone in Nigeria, it decreases the extreme rainfall events elsewhere within the country. Likewise, forestation lowers the number of heatwave events and days over some areas, while others experience increase. However, it is not appropriate to generalise this result over the entire West Africa, because Nigeria is not representative of the entire region. In addition, while many countries in West Africa are embarking on widespread forestation under the Green Sahel initiatives, an African Union programme (AUC, 2006), Abiodun *et al.* (2012b) only considered the impacts of a national-scale forestation. Hence, the result of Abiodun *et al.* (2012b) might underestimate the potential impacts of the large-scale forestation. Furthermore, as the result of Abiodun *et al.* (2012b) is based on simulations of a single regional climate model, there is uncertainty associated with the results.

There is clearly significant potential in forestation as a climate change mitigation strategy, but the inconclusive and in some instances contradictory, conclusions as to its effects requires further investigation.

1.2 JUSTIFICATION FOR THE STUDY

The anthropogenic influences on climate is progressively affecting the frequency and intensity of extreme climate events (extreme temperatures, extreme precipitation, droughts)

in some regions of the world (IPCC, 2013, 2014). In Africa, especially in West Africa, many studies project increases in extreme rainfall and heatwave events (Christensen *et al.*, 2007; Sylla *et al.,* 2012; Vizy and Cook, 2012; Abiodun *et al.,* 2012b). This may increase the vulnerability of populations living in that region due to the low adaptive capacity of West African countries to the impacts of climate change; increasing the risks for human health and security. The IPCC (2014) identifies West Africa as one of the most vulnerable areas in the world to the effects of global warming. As a result of the rapid population growth in West Africa, of around 2.35%, projected to exceed 500 million by 2035 (West Africa Gateway, 2011), coupled with the increases in population needs and their high dependency on the environment for subsistence, makes the threat of environmental changes very serious (Diasso, 2015). Therefore there is a need for reliable climate information for accurate projections, to assist decision makers in the choice and implementation of suitable climate change mitigation or adaptation strategies to lower its impacts on human communities. Amongst the potential climate change mitigation strategies, forestation stands out as a practical and potentially effective approach, but the inconclusive state of current literature as to its effects justifies further investigation.

Climate change would increase the frequency and intensity of extreme climate events over West Africa in future, increasing the vulnerability of people living in that region to the impacts of extreme climate events. However, none of the previous studies on extreme climate events have considered the influence of the ongoing forestation activities in the region in their projections. Therefore, there is a need to provide policy makers with appropriate regional- and local-scale climate information, which can be used to enhance the

resilience of West African countries to the impacts of climate change on extreme climate events through mitigation and/or adaptation.

1.3 AIM AND OBJECTIVES OF THE STUDY

This study aims to examine the potential impacts of a large scale forestation activity on the characteristics of extreme climate events over West Africa in future using two regional climate models.

The specific objectives of the thesis can be summarised as follows

i. to examine the regional climate model‘s ability to simulate extreme climate events over West Africa;
ii. to examine the potential impacts of climate change and land cover change (forestation) on extreme rainfall events over West Africa; and
iii. to examine the potential impacts of climate change and forestation on heatwaves characteristics over West Africa.

1.4 RESEARCH QUESTIONS

The study considers climate change dynamics in West Africa, focusing on the extreme climate events of extreme rainfall events and heatwaves. To achieve this, the following research questions are addressed:

i. What is the capability of two regional climate models to simulate extreme climate events over West Africa?

ii. What are the potential impacts of climate change and land cover change (forestation) on extreme rainfall events over West Africa?

iii. What are the potential impacts of climate change and forestation on heatwave characteristics over West Africa?

1.5 THESIS STRUCTURE

This thesis is organised into five chapters. Chapter 2 presents literature relevant to the research areas. It defines extreme climate events, discusses the West African climate system and the impacts of land cover modification (forestation) on the regional climate. Chapter 3 presents the methodology used in the study and discusses in detail the regional climate models (RCMs) used to answer the research questions, and the data used. Chapter 4 presents and discusses the findings of the study relative to extreme rainfall events and heatwaves characteristics. The chapter also discusses the capabilities of the RCMs to simulate characteristics of climate extremes over West Africa, the projected changes in the characteristics of extreme climate events over West Africa due to the impacts of climate change, and the potential future impacts of forestation on characteristics of extreme climate events over West Africa. Chapter 5 presents the conclusions to the research, the limitations, and suggestions for further studies.

CHAPTER TWO

LITERATURE REVIEW

2.1 INTRODUCTION

This chapter presents a comprehensive review of previous studies on climate simulation approaches, and extreme climate events over West Africa. The review discusses definitions used in identifying and characterising extreme climate events, atmospheric features and conditions that induce them and also gives an insight into the simulation of extreme events and the impacts of forestation on extreme climate events.

2.2 DEFINITIONS OF EXTREME CLIMATE EVENTS

Various definitions of extreme climate events have been used in previous studies (Zhang et al., 2011; Vizy and Cook, 2012; Abiodun *et al.*, 2012b; Abiodun *et al.*, 2013; Abiodun *et al.*, 2015; Browne Klutse *et al.*, 2015). For example, Zhang *et al.* (2011) define an extreme climate event as the occurrence of a value in the observation of climate variables, such as temperature or precipitation, which is above (or below) a specific threshold value near the upper (or lower) end of the distribution of the observed variables in that region (see Figure 2.1). The higher the black curve line, the more likely weather with those characteristics occurs; which implies that extreme weather events are exponentially less likely to occur than common weather events.

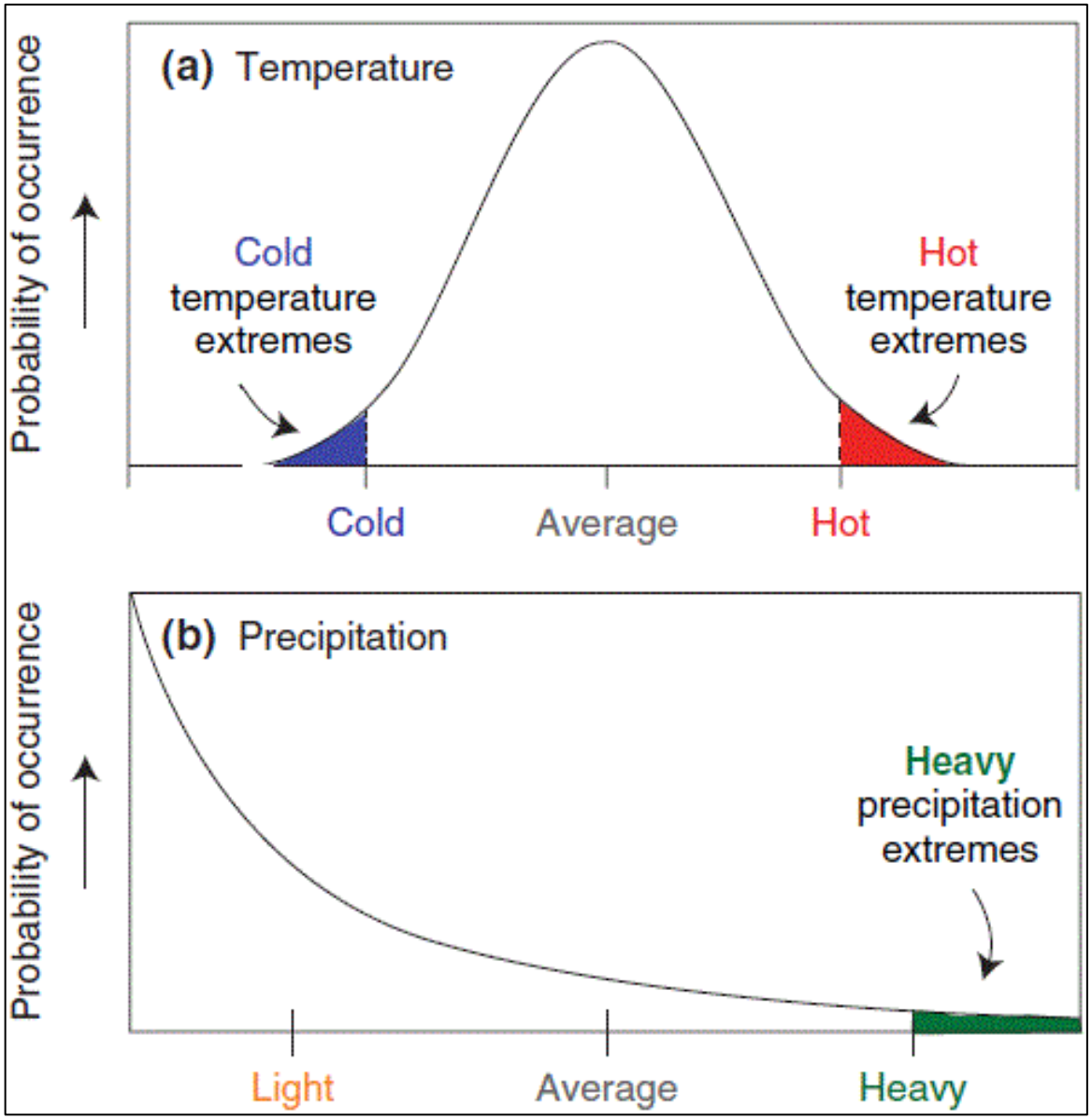

Figure 2.1: The probability distributions of daily temperature and precipitation

Source: Zhang *et al.*, (2011)

This simple definition of extreme climate events implies that an event which is considered as an extreme in one location might be normal in another location. However, the definition only considers extreme events that can be measured based on the daily observation of meteorological surface variables, such as temperature, precipitation and wind. It does not cover those events that are generally the result of the combination of different climatic factors and usually referred to as "compound extreme events" (*e.g.* drought, tropical cyclones) (Zhang *et al.*, 2011).

There is debate as to what constitutes an extreme climate event. The difficulties associated with the definition of an extreme climate event are various. For instance, Stephenson (2008) found that there are a multiplicity of definitions of what constitutes an 'extreme' relative to context, and that there are similarities between a 'severe event', 'rare event', 'extreme event' and 'high impact event'. Furthermore, Zwiers *et al.* (2013) explain that climate extremes can be referred to either using characteristics of a climate variable or that of an impact of an event. The IPCC (2001) defines an extreme climate event as an event that is as rare as, or rarer than, the 10^{th} or 90^{th} percentile of a particular distribution of an atmospheric variable, such as temperature and precipitation. Beniston and Stephenson (2004) however argue that this definition is problematic as, for example, in the case of extreme temperatures the heat stress on the organism will differ depending on the climatology of each location. The second problem with this definition is that a damaging natural hazard can also happen in the absence of an intense or rare climatic event.

Previous studies identify extreme events in many different ways. An investigation of the available literature on climate extreme reveals two main methods that are used to identify

climate extremes. The first approach uses descriptive indices of extremes based on different thresholds and the second uses statistical modelling of extremes.

2.2.1 Descriptive Indices used to Identify Extreme Weather Events

Generally, extreme events are identified using indices that describe particular characteristics of extreme events, such as frequency, amplitude and persistence (Klein Tank *et al.*, 2009; Zhang *et al.*, 2011). Most of those indices tend to examine 'moderate extremes' that occur once or a few times each year (Klein Tank *et al.*, 2009; Zhang *et al.*, 2011; Zwiers *et al.*, 2013). Most of these indices are derived from the Expert Team on Climate Change Detection and Indices (ETCCDI) which define a core set of 27 extremes indices for temperature and precipitation (APPENDIX A).

The key approach of these indices is to establish thresholds for frequency of occurrence of extreme events (Klein Tank *et al.*, 2009). The extreme indices usually use two different types of thresholds to define extremes: (i) fixed absolute thresholds, and (ii) fixed relative thresholds (percentile thresholds) (Klein Tank *et al.*, 2009). The fixed absolute thresholds indices identify an extreme climate event using a threshold value appropriate to the area of focus, and any event with a climate variable (*e.g.* rainfall or temperature) exceeding that value is defined as an extreme climate event (Abba Omar, 2014). Generally, the focus is on the number of days with rainfall or temperature above (or below) the threshold value. Different threshold values can be applied for different parts of the world (Dyson, 2009). For example, Houze *et al.* (1990) define a 'major rainfall event' over a location of the United States as a 24 hours period with at least 25 mm of rainfall over an area of 12,500

km^2 or greater, while Groisman *et al.* (2001) define a heavy rainfall event over the United States as 50.8 mm day^{-1} and a very heavy rain event as 101.6 mm per day. In Taiwan, (Chen *et al.*, 2007) define a heavy rainfall event when a fixed threshold of 50 mm is exceeded in 24 hours for at least one weather station, and an extremely heavy rain event as at least 130 mm recorded in one day. Over southern Portugal, Fragoso and Tildes Gomes (2008) identify an extreme rainfall event using a fixed threshold of 40 mm day. The fixed relative thresholds (or percentile thresholds) based indices define an extreme climate event using a percentile threshold which is determined from a climatological base period, such as 1961-1990. An event is considered as extreme when it is in the range of a defined percentile of the daily meteorological data distribution (rainfall or temperature).

In West Africa, studies on climate extremes using fixed absolute thresholds are lacking. This may be the results of various reasons, such as the large size of the region and the diversity in the regions' climatology; making the use of fixed absolute threshold based indices more complex. Moreover, according to Klein Tank *et al.* (2009) and Zhang *et al.* (2011), over large areas, fixed thresholds are less suitable for spatial distribution of number of days exceeding the threshold than the percentile thresholds. However, Browne Klutse *et al.* (2015) define a fixed threshold of 20 mm to identify heavy rainfall events over West Africa. Moreover, Vizy and Cook (2012) used a fixed threshold of 41°C of the daily maximum to define heatwave days. Studies over West Africa commonly use the percentile thresholds to define extreme climate events. However, there is considerable variation in the percentiles used. For instance, Abiodun *et al.* (2012b; 2013) defined an extreme rainfall day and extreme temperature day over Nigeria as days with rainfall or maximum temperature above the 99.5^{th} percentile of daily rainfall or maximum temperature of the climatological

base reference, while Sylla *et al.* (2012), Vizy and Cook (2012) and Browne *et al.* (2015) used the 95th percentile threshold to define extreme rainfall events over the West African region. Unlike fixed absolute thresholds, the percentile thresholds indices are more suitable for spatial comparisons of extreme events and meaningful for all regions (Klein Tank *et al.*, 2009; Zhang *et al.*, 2011).

2.2.2 Statistical Modelling of Extreme Weather Events

The statistical modelling of extreme weather events uses the extreme value theory (EVT) to evaluate the intensity and frequency of events that are rare; situated in the margins of the probability distribution of weather variables (Klein Tank *et al.*, 2009). The EVT is the most widely used statistical method to study weather extremes, and is based on the analysis of series of maximal values over a specified period of time, that are theoretically described by the generalised extreme value (GEV) distributions (Panthou *et al.*, 2012). This method generally defines climate extremes using return periods. For a given extreme event of a defined size or intensity, its return period is an estimate of the average interval of time required for the reoccurrence of such an event (size or intensity). According to Coles (2001), the extreme value analyses usually require to estimate the probability of events that are more extreme than any that have already been observed. Klein Tank *et al.* (2009) identify two methods generally used in the extreme value analysis. The first approach is the 'peaks-over-threshold' (POT) method which is used to represent the behaviour of events that exceed a high threshold and the threshold crossing process. In addition, under appropriate conditions, the extremes identified using the POT method will have a generalized Pareto distribution when the threshold used is high enough. The second

approach is the ‘block maximum’ method in which the sample of extreme values considered is obtained through the selection of the maximum (or the minimum) value observed in each block of time (season of year).

Many studies use the EVT to define climate extremes. Zwiers and Kharin (1998), analysing changes due to CO_2 doubling in extremes of the surface climate variables (temperature, precipitation and near-surface wind), calculated the magnitude of events with 10, 20 and 50-year return periods using GEV distribution for 20-year simulations of the second-generation circulation model of the Canadian Centre for Climate Modelling and Analysis. Paeth *et al.* (2011) used the Generalised Pareto distribution to calculate the return periods of flood-producing precipitation in 2007 over West Africa from a 10-year satellite derived dataset. Galiano and Osorio (2011), in a study aiming to calculate the annual maximum daily rainfall for various return periods over the Senegal River Basin, used the Generalized Additive Models for Location, Scale and Shape for gridded observed daily rainfall and RCMs datasets. Panthou *et al.* (2012) compared two approaches based on the extreme value theory for extreme rainfall mapping in West Africa. The first approach is a local fit and interpolation (LFI) consisting of a spatial interpolation of the GEV distribution parameters estimated independently at each station, and the second a spatial maximum likelihood estimation (SMLE) which directly estimates the GEV distribution over the entire region by a single maximum likelihood fit using jointly all measurements combined with spatial covariates. More recently, Hounkpè *et al.* (2015) implemented a statistical model with a time-dependent and/or covariate-dependent GEV distribution to analyse the frequency of non-stationary floods in the Oueme River Basin in the Republic of Benin (West African country).

2.2.3 Challenges of Defining a Heatwave Event

There is no universal definition of a heatwave event (Nairn and Fawcett, 2013; Keggenhoff *et al.*, 2015; Nairn and Fawcett, 2015). However, many studies define heatwaves using a fixed or percentile threshold of temperature calculated over a given reference period. Then, a heatwave occurs as conditions above the defined threshold persist for a required number of days (Vizy and Cook, 2012; Abiodun *et al.*, 2012a; Russo *et al.*, 2014). The main limitation of this definition of a heatwave is the variation, across locations in the threshold value and the minimum number of days above the threshold required to be considered as a heatwave. For example, Frich *et al.* (2002) define a heatwave as a period of at least 5 consecutive days with maximum temperature 5°C above the climatological daily normal. The threshold of 5°C above the climatological daily normal may be difficult to obtain in some locations, such as tropical regions, where the day-to-day variability in temperature is very small (Zhang *et al.*, 2011). Also, the threshold may vary significantly across locations of the same country or region depending on their respective climatology. Finally, the use of 5 consecutive days excludes shorter heatwaves (less than 5 days) as the death rate increase due to heat is generally highest during the first few days of a heatwave (Kalkstein and Davis 1989), and that acclimatisation factors (possibly both behavioural and physiological) also seem to be important (IPCC 1996). Hence, there is a need to develop a heatwave definition applicable to any location. To help in solving this issue, Nairn and Fawcett (2013) suggest a new heat index, the excess heat factor (EHF). EHF is the combined effect of excess heat and heat stress calculated as an index that provides a comparative measure of intensity, load, duration and spatial distribution of a heatwave event (Nairn and Fawcett 2013; Nairn and Fawcett 2015). This study employs both the EHF as defined by Nairn and

Fawcett (2013) as a heat index and a percentile based threshold to define heatwaves and to measure the potential impacts of forestation on heatwave characteristics over West Africa in future.

2.3 WEST AFRICAN CLIMATE SYSTEMS

2.3.1 West African Monsoon

The climate of West Africa is influenced by the West African Monsoon (WAM) which is characterised by summer rainfall and winter drought (Cornforth, 2012). The WAM is a large scale circulation system characterised by the seasonal fluctuations of two distinct air masses (Abiodun *et al.*, 2008; Afiesimama *et al.*, 2006; Sylla *et al.*, 2013). The first is the dry, hot and dusty tropical continental air mass from the Saharan region, blowing from the northeast over most of the West African countries, generally known as the 'harmattan'. It is characterised by dry and hot conditions over land and reaches its southernmost position (about 7°N) in January over the Guinean zone (Peter and Tetzlaff 1988). Second is the warm and moist tropical maritime air mass of the Atlantic region from the south-west, transporting moisture over land from the Atlantic Ocean providing the West African countries with rainfall and moisture. According to Peter and Tetzlaff (1988) the tropical maritime air mass reaches its northernmost position (about 22°N) in August. The zone of convergence of the two air masses (tropical continental and tropical maritime) is referred to as the Inter Tropical Discontinuity (ITD) when it occurs over continental West Africa at the surface and the Inter Tropical Convergence Zone (ITCZ) over the ocean areas (see Figure 2.2).

The WAM circulation has a major social and economic importance for local populations in West African Countries whose economy depends mostly on rain-fed agriculture (Sylla *et al.,* 2013). It accommodates the primary rain-producing systems – the African easterly jet (AEJ), tropical easterly jet (TEJ), African easterly waves (AEW) and mesoscale convective systems (MCSs) – during the summer months and provides West African countries with more than 75% of their annual rainfall (Omotosho, 1985). There is a complex interaction between all those phenomena and the monsoon flow (at low level) which ensures the transport of moisture from the Atlantic over land, providing the region with the main proportion of its moisture for rainfall (Abiodun *et al.*, 2008) (see Figure 2.3). The WAM is subjected to the influence of diverse factors that control its variability. Among them are the variability of ocean Sea Surface Temperatures (SSTs) (Fontaine *et al.*, 1998), continental land surface conditions (Wang and Eltahir, 2000) and atmospheric circulation (Nicholson and Grist, 2001; Jenkins *et al.*, 2005).

2.3.2 Conditions causing Extreme Climate Events over West Africa

Previous studies on climate extremes over West Africa have used observed extreme climate events to investigate the relationships between these extreme events and atmospheric features over the region. For example, Paeth *et al.* (2011) investigated the flood-producing rainfall in 2007 by assessing and comparing the spatial and temporal characteristics and intensity of the floods with the associated rain events using satellite datasets. The results further showed that the floods were limited to the main river basins in Sub-Saharan West Africa and among the potential causes identified were a La Niña event in the tropical Pacific, anomalous heating in the tropical Atlantic accompanying a greater depth of the

monsoonal south-westerly's, and an enhanced activity of African Easterly Waves (Paeth *et al.*, 2011). Browne *et al.* (2015) characterised extreme rainfall events in West Africa using an observation dataset; they associated observed heavy rainfall events in Sahel with the occurrence of deep convection events. Rainfall over Sahel is mostly convective and about 95% of the annual rainfall is produced by the MCSs (Laurent *et al.*, 1998; Mathon *et al.*, 2002; Guy, 2012). Laing *et al.* (1999) estimated that mesoscale convective complexes (MCCs) contribute nearly 22% of the boreal summer (July-September) rainfall in Sahel. All these studies show the importance of MCSs for extreme rainfall events and floods in the Sahel region of West Africa.

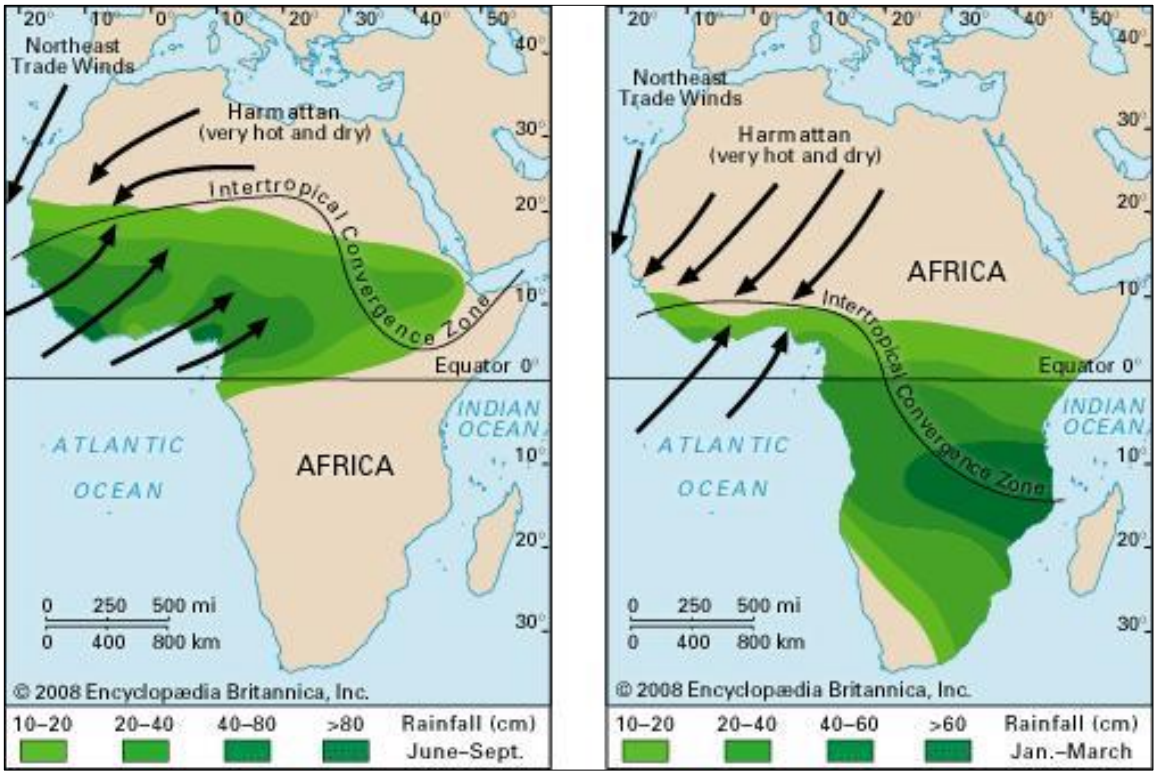

Figure 2.2: The West African Monsoon

Source: Britannica Encyclopaedia (2016)

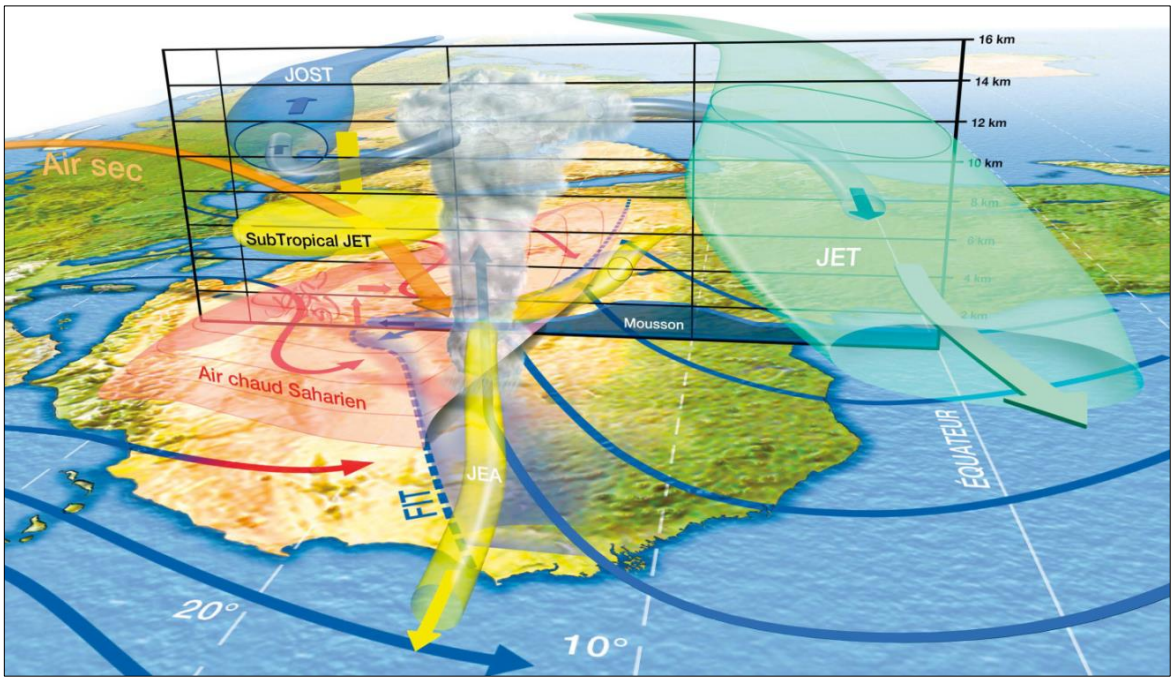

Figure 2.3: Interaction of phenomena resulting in West African Monsoon. FIT = ITD: Inter-Tropical Discontinuity; JET: Tropical Easterly Jet; STWJ: Subtropical Westerly Jet; JEA: African Easterly Jet

Source: Lafore *et al.* (2010)

2.4 SIMULATING EXTREME CLIMATE EVENTS OVER WEST AFRICA

There is general agreement that climate change as a result of anthropogenic influences will influence the frequency and intensity of extreme climate events affecting both human society and the natural environment (Easterling *et al.*, 2000; IPCC, 2013). Russo *et al.* (2014) report more areas globally affected by heatwave events in the past decades (1980-2012) and project that extreme and very extreme heatwave events are likely to occur as often as every 2 years in different regions of the world, including Africa, by the end of the 21st century. Mouhamed *et al.* (2013) found that extreme rainfall events have become more frequent in the West African Sahel during the last decades (1991-2010) compared to the 1961-1990 period. Moreover, for the period 1960 to 2010, a general warming trend is observable throughout the region during the period 1960-2010 with warmer nights and more frequent warm days and warm spells (Mouhamed *et al.*, 2013).

This reality has motivated the development of a considerable number of modelling approaches using regional climate models (RCMs) and general circulation models (GCMs) to project the potential impacts of future climate change on extreme climate events. Broadly speaking, GCMs provide climate projections on a larger scale, while RCMs provide more detailed climate projections on a regional scale. Previous studies of climate dynamics in West Africa have projected changes in climate extremes based on RCM and GCM simulations. Christensen *et al.* (2007) projected that the frequency of extremely wet seasons and extreme rainfall events in West Africa is expected to increase by about 20% in the coming decades due to the impacts of climate change. More recently, studies over West Africa project increases of extreme climate events due to ongoing global warming. Sylla *et al.* (2012) project, using an RCM, that extreme rainfall events will increase significantly

and become more frequent and more intense in the boreal summer (June-August) over West Africa during the mid and late 21st century, especially over the Guinea Highlands and Cameroon Mountains. Similarly, Vizy and Cook (2012) report a projected increase of the number of extremely wet days and heatwave days over West Africa. Abiodun *et al.* (2013) statistically downscaled outputs from different GCMs and observed that global warming increased the occurrence of days with extreme climate events (extreme rainfall and heatwaves) over different ecological zones of Nigeria.

Most of these studies are based on the use of a single RCM simulation, which makes it difficult to assess the uncertainty associated with results. To overcome this, the present study uses two RCMs to simulate the impacts of climate change and forestation on extreme climate events over West Africa.

2.5 IMPACTS OF VEGETATION DYNAMICS ON THE CLIMATE IN WEST AFRICA

This section discusses the impacts of land cover change (including forestation) on the climate in West Africa, and its implications for extreme climate events. Past studies have shown how sensitive the climate in West Africa is to vegetation changes (Charney 1975; Charney *et al.*, 1977; Xue and Shukla, 1993; Zheng and Eltahir, 1997; Afiesimama *et al.*, 2006; Abiodun *et al.*, 2008; Abiodun *et al.*, 2012a; Abiodun *et al.*, 2012b; Diasso, 2015; Mounkaila Saley, 2015).

2.5.1 Desertification and Deforestation

The potential impact of human-induced land cover change on regional climate strongly depends on the location and type of the vegetation change (Zheng and Eltahir 1997; Abiodun *et al.*, 2008). While desertification in West Africa may have a minor impact on the simulated monsoon circulation; deforestation in the coastal region may cause its collapse and drastically influence the regional rainfall regime (Zheng and Eltahir 1997). However, Abiodun *et al.* (2008) projected that both desertification in the Sahel and coastal deforestation have strong local impacts on the climate in West Africa and that, while desertification induces more warming at the surface, deforestation reduces the surface friction. Moreover, in contrast to Zheng and Eltahir's (1997) results, they found that land cover modification increases the flow of the monsoon over West Africa, and that desertification decreases rainfall over the Sahel region and increases it near the coastal regions, while deforestation lowers the rainfall across the whole region. In addition, Xue and Shukla (1993) demonstrated that changing the land surface in the Sahel region to desert conditions, would decrease the June-August rainfall amount in the degraded area by about 22%. Likewise, Charney (1975) argued that rainfall in the Sahel is associated with the surface albedo (the proportion of sunlight reflected) and hypothesised that the increase of land surface albedo as the result of desertification in the Sahel region of West Africa would induce sinking motion, additional drying, and would therefore perpetuate the arid conditions. To support this hypothesis, Charney *et al.* (1977) used GCM simulations to increase the albedo (as a result of vegetation degradation) of the Sahel region and indicated decreases in rainfall.

2.5.2 Forestation

The impact of forestation on the climate is well documented. By sequestering the atmospheric carbon into trees biomass, forestation contributes to the reduction of the atmospheric greenhouse gases concentration that induces global warming and therefore alters surface properties that are relevant for the climate (Abiodun *et al.*, 2012). Forestation is therefore considered as a geo-engineering option, a large scale manipulation of the earth's environment, in order to offset the harmful consequences of anthropogenic climate change (National Academy of Sciences 1992; The Royal Society 2009; IPCC 2007; Scheer and Renn 2014). According to Lenton and Vaughan (2009), forestation is one of the most promising geo-engineering options because of its capacity for cooling the global climate. Forestation can also increase the amount of rainfall (Enger and Tjernstrom 1991) and improves soil's physical properties (Mapa, 1995).

Previous studies have proven that forestation, an ongoing land-cover modification activity in Africa (AUC, 2006), would alter the future climate over the continent. However, the direction of the alteration may vary across the continent. For example, Abiodun *et al.* (2012a; 2012b) support that forestation would lower the projected warming over forested areas in West Africa, while Naik and Abiodun (2016) found that forestation would increase the projected warming over forested areas in Southern Africa. However, both studies projected that forestation would increase rainfall over the forested areas. Mounkaila Saley (2015) showed that a large-scale forestation across the Savannah could induce earlier onset of rainfall over some areas, but later onset of rainfall over other areas. Similarly, Diasso (2015) also showed that forestation would alter the projected changes in the patterns and

intensity of drought over West Africa, but the degree of the alteration varies over the sub-continent.

Among these studies, only Abiodun *et al.* (2012b) consider the potential impacts of forestation on extreme climate events, including extreme rainfall and heatwave events. The study shows that forestation in Nigeria may lower the number of heatwave events and days over some areas, while others may experience increase. However, the study focuses on Nigeria which may not be representative of the entire West African region. In addition, while many countries in West Africa are embarking on widespread forestation under the Green Sahel initiatives, Abiodun *et al.* (2012b) only considered the impacts of a national-scale forestation. Hence, the result of Abiodun *et al.* (2012b) might underestimate the potential impacts of large-scale forestation. This study builds on the work of Abiodun et al (2012b) to overcome the above limitations by investigating the potential impacts of a large-scale forestation activity on climate extremes in West Africa.

CHAPTER THREE

RESEARCH METHODOLOGY

3.1 INTRODUCTION

This chapter provides a description of the two regional climate models (RCMs) used in this study and their respective forcing GCMs. The models description is followed by the presentation of the observation datasets used and the numerical experiments conducted. The chapter discusses the definitions used to identify extreme rainfall and heatwave events over West Africa, the presentation of their characteristics and the methods used to quantify changes in climate extremes over West Africa in future.

3.2 STUDY DOMAIN

The model domain included for performing simulations of extreme climate events covers West Africa (Figure 3.1) which extends from about 37°W to 32°E and 27°S to 27°N. The horizontal domain is large enough to fully capture the main processes controlling the annual cycle of the West African Monsoon (WAM), and to reduce lateral boundary conditions problems over the study domain. The study domain on which the analyses of projected impacts of extreme climate events are performed, extends from 0°N to 20°N and 20°W to 20°E as indicated by the red box in Figure 3.1. The study domain encompasses three selected ecological zones: Guinea (4°N - 8°N), Savannah (8°N - 12°N) and Sahel (12°N - 16°N). The simulations and study domain used here are identical to those of Diasso (2015) and Mounkaila Saley (2015).

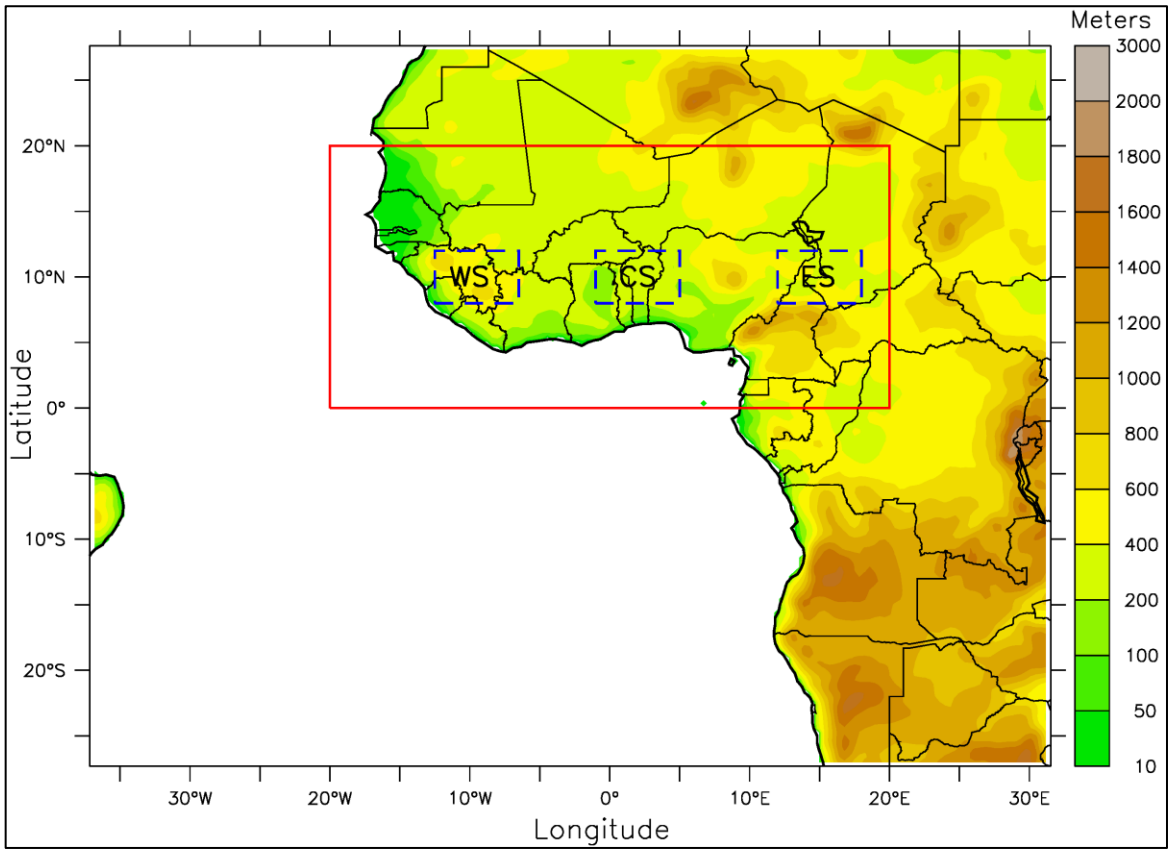

Figure 3.1: Model domain showing the topography of West Africa, the study domain (red box) and the areas designated as West Savannah (WS), Central Savannah (CS) and East Savannah (ES)

3.3 OBSERVATION DATASETS

For this study, rainfall and temperature observation datasets were used. The observation datasets for rainfall were obtained from two satellite-derived rainfall datasets, while the temperature dataset is a hybrid observation-reanalysis dataset. The observation data are used in the study to evaluate the capability of the RCMs in simulating climate extremes.

3.3.1 Rainfall Observation Datasets

The two rainfall observation datasets used in this study are the Global Precipitation Climatology Project (GPCP) and the Tropical Rainfall Measuring Mission (TRMM). GPCP is the first satellite-derived observation rainfall product used in this study. It estimates rainfall at daily intervals and at $1° \times 1°$ latitude-longitude resolution using a combination of geosynchronous satellite infrared readings and a low earth polar orbit satellite (Huffman *et al.*, 2001). The TRMM dataset provides rainfall estimates using a merged microwave-infrared product computed at 3-hourly intervals and at $0.25° \times 0.25°$ latitude-longitude resolution (Huffman *et al.*, 2007).

The satellite data were used to evaluate the model simulations of extreme rainfall events over West Africa. Both GPCP and TRMM incorporate surface precipitation gauge data as much as possible (Huffman *et al.*, 2007). However, GPCP produces rainfall values that are closer to rain gauge products than TRMM over Africa (Sylla, Giorgi, *et al.*, 2013). The use of the two observation datasets for the evaluation of the RCMs helped to assess the level of uncertainty among observation datasets in obtaining extreme rainfall events over the study

area. Both GPCP and TRMM have been widely used over West Africa to evaluate simulations from RCMs (Browne & Sylla, 2012; Browne *et al.*, 2015; Cook & Vizy, 2012).

3.3.2 Temperature Dataset

The temperature dataset used is the Princeton University Global Meteorological Forcing Dataset (PGFD) for land surface modelling, produced by the Terrestrial Hydrology Research Group at Princeton University (Sheffield et al., 2006). This study used PGFD maximum and minimum daily temperatures for the period 1971-2004 to evaluate the RCM simulations of heatwave characteristics over West Africa. The PGFD is an observational-reanalysis hybrid dataset which provides near-surface meteorological data for driving land surface models and other terrestrial modelling systems (Sheffield et al., 2006). PGFD consists of a global 50-year (1948-2008), 3 hourly dataset at 1° × 1° resolution. It is constructed from reanalysis of the combination of a set of global observation datasets with the National Centre for Environmental Prediction – National Centre for Atmospheric Research (NCEP-NCAR) (Sheffield et al., 2006). The biases in the precipitation and near-surface meteorology reanalysis are corrected using observation-based datasets of precipitation, air temperature, and radiation (Sheffield et al., 2006). Table 3.1 gives a brief summary of the contributing datasets used in the development of the PGFD. The temporal resolutions given here are those used in Sheffield et al. (2006) but the original data may be available at finer temporal resolutions.

Table 3.1: Summary of datasets used in the construction of the PGFD

Dataset	Variables	Temporal coverage	Spatial coverage
NCEP–NCAR reanalysis	P, T, SW, LW, q, Ps, w	1948–present, 6 hourly	Global, ~2.0° × 2.0°
CRU TS2.0	P, T, Cld	1901–2000, monthly	Global land excluding Antarctica, 0.5° × 0.5°
GPCP	P	1997–present, daily	Global, 1.0° × 1.0°
TRMM	P	Feb 2002–present, 3 hourly	50°S–50°N, 0.25° × 0.25°
NASA Langley SRB	LW, SW	1983–95, monthly	Global, 1.0° lat × 1.0°–120° lon

Source: Sheffield *et al.* (2006)

Note: Variables are precipitation (P), surface air temperature (T), downward shortwave radiation (SW), downward longwave radiation (LW), surface air pressure (Ps), specific humidity (q), wind speed (w), and cloud cover (Cld)

3.4 EXTREME RAINFALL CHARACTERISTICS AND MEASUREMENT

This study uses the percentile threshold to identify extreme rainfall events at each grid point over West Africa. The extreme rainfall threshold is computed at any grid point as the 95^{th} percentile of the daily rainfall using all wet days of the year. A wet day is defined as a day with rainfall greater or equal to 0.5 mm. At a given grid point, any rainfall amount equal or greater than this threshold is considered an extreme rainfall event, while any rainfall value less than the threshold (but higher than 0.5 mm) is considered a non-extreme rainfall event at that point. For each dataset, the spatial distribution of extreme event thresholds over West Africa was analysed. This allowed for the evaluation of the intensity of the simulated extreme rainfall events over West Africa.

Following Abiodun *et al.* (2015), a Widespread Extreme Rainfall Event (WERE) over any of the three Savannah areas (shown in Figure 3.1) is defined as a simultaneous occurrence of extreme rainfall events over at least 50% (*i.e.* 102 grid points) of the area. This definition helps to eliminate localised extreme rainfall events and retain those induced by synoptic scale features. For each dataset, all WERE days over the area were extracted. The characteristics of the simulated WEREs were evaluated against observations. The evaluation includes how well the models reproduce the total number, seasonal variation, and annual variability of WEREs.

3.5 HEATWAVES CHARACTERISTICS AND MEASUREMENT

The calculation of the excess heat factor (EHF) index required both daily maximum and minimum temperatures. As stated earlier, the EHF combines the effects of excess heat and

heat stress. The former measures how hot a three-day period is with respect to a long-term climatic reference (daily mean temperature threshold) calculated for the period 1971-2004. The latter is a measure of how hot a three-day period is compared to the recent past (previous 30 days), to measure the short term acclimatisation.

In addition to the EHF index, a second heatwave index is defined using a percentile threshold of the daily maximum temperature (TXI). For this, the 90th percentile threshold (TX90) of daily maximum temperature (Tmax) is calculated for the period 1971-2004 using all days of the year. At any grid point, a day with Tmax greater than TX90 (Tmax > TX90) is considered as an extreme temperature day at that point. This offers a basis for comparison of results from both heatwave indices (EHF and TXI).

For each heatwave index, EHF and TXI, a heatwave event is defined, at any grid point, when the respective threshold value is exceeded (EHF > 0 or Tmax > TX90) for at least three consecutive days. Furthermore, both indices are defined using a framework with different characteristics. The framework is based on that of (Perkins *et al.*, 2012) and focused only on: HWN – the total number of heatwave events; and HWF – the total number of days satisfying the index criteria.

In addition, a third heatwave characteristic is defined as the average heatwave duration (HWD) that is obtained by dividing the total number of heatwave days by the total number of heatwave events (HWF/HWN).

Both excess heat and heat stress are measured using two excess heat indices (EHIs). The first index is the significant excess heat index (EHI_{sig}) which compares a three-day-average

of daily mean temperature to the 95th percentile (T95) of the daily mean temperature (T_i, daily average of maximum and minimum temperature on day i) for the climate reference period 1971-2004 calculated using all days of the year. The EHI_{sig} is calculated following Nairn and Fawcett (2013):

$$\mathbf{EHI_{sig}} = \frac{\mathbf{T_i + T_{i+1} + T_{i+2}}}{\mathbf{3}} - \mathbf{T95} \qquad (3.1)$$

The second index is the acclimatisation excess heat index (EHI_{accl}) which measures the short-term acclimatisation to heat. It describes the anomaly over a three-day period against the preceding 30 days and is calculated following Nairn and Fawcett (2013):

$$\mathbf{EHI_{accl}} = \frac{\mathbf{T_i + T_{i+1} + T_{i+2}}}{\mathbf{3}} - \frac{\mathbf{T_{i-1} + \cdots + T_{i-30}}}{\mathbf{30}} \qquad (3.2)$$

The calculation of the EHF values requires the combination of these two EHIs. Therefore, the EHF is calculated as the product of the two indices and is obtained as follows (Nairn & Fawcett, 2013):

$$\mathbf{EHF} = \mathbf{EHI_{sig}} \times \mathbf{max}(\mathbf{1}, \mathbf{EHI_{accl}}) \qquad (3.3)$$

The EHF ($°C^2$), by using the mean rather than the maximum daily temperature, integrates the effect of humidity on heat tolerance; and also provides a comparative measure of intensity, load, duration and spatial distribution of a heatwave and has a strong signal to noises (Nairn and Fawcett 2013). A positive EHF at a given grid point indicates heatwave conditions for the first day of the three-day period considered in the calculation of the index at that point.

3.6 REGIONAL CLIMATE MODELS UTILISED

The two regional climate models used in the study are the International Centre for Theoretical Physics (ICTP) Regional Climate Model version 4 (RegCM) (Pal *et al.*, 2007; Giorgi *et al.*, 2012) and the Weather Research Forecasting Model version 3.5.1 (WRF) (Skamarock *et al.*, 2008). Using two models provides the opportunity to compare simulation results and determine whether the results obtained are model-dependent or can be assessed to be objectively accurate. Both RCMs are suitable for downscaling global climate datasets over the West African region (see Co-ordinated Regional Downscaling Experiment (CORDEX) Africa initiative) (Browne *et al.*, 2015) and for examining the potential impacts of forestation on regional climate (Abiodun *et al.*, 2012a; Trail *et al.*, 2013). However, the two models differ in their dynamics; RegCM is a hydrostatic model while WRF is a non-hydrostatic model.

3.6.1 RegCM Regional Climate Model

The ICTP RegCM is a hydrostatic, terrain-following (sigma) coordinate model with various physics and parameterisation options (Giorgi *et al.*, 2012). For the present study, the Community Climate Model (CCM3) scheme of Kiehl *et al.* (1996) is used for radiative transfer, and the Holtslag *et al.* (1990) parameterisation is used for the planetary boundary layer. Emanuel's (1991) scheme is used for convective parameterisation and the SUB-grid EXplicit moisture scheme (SUBEX) (Pal *et al.*, 2000) for grid-scale precipitation processes. Land surface processes are represented with the Biosphere Atmosphere Transfer Scheme (BATS) (Dickinson *et al.*, 1993). BATS uses 20 different vegetation/land cover types, 3 soil categories (sand, loam and clay) and different soil colours (ranging from light to dark).

Its calculations of sensible heat, water vapour and momentum transfer rely on surface drag coefficients, roughness length, and stability in the boundary layer. Canopy and foliage temperature are calculated diagnostically from radiative, sensible and latent heat fluxes (Elguindi *et al.*, 2011). Soil moisture is a function of surface runoff and saturation and influences evapotranspiration at the surface. A full description of how BATS represents the exchange of momentum, energy and water between the surface, vegetation, soil and the atmosphere can be found in Dickinson *et al.* (1993) and Elguindi *et al.* (2011). RegCM simulations were set up with a horizontal grid space of 40 km using a rotated Mercator projection and 18 vertical levels from the surface to a 50 hPa level.

3.6.2 WRF Regional Climate Model

WRF is a non-hydrostatic, fully compressible and terrain-following (sigma) coordinate model (Skamarock *et al.*, 2008; Skamarock and Klemp, 2008). For the simulation used in the present study, parameterisations for radiative transfer follow the Rapid Radiative Transfer Model scheme (Mlawer *et al.*, 1997) for long waves and the Dudhia (1989) scheme for short waves. The WRF single-moment 5-class scheme (WSM5) (Hong *et al.*, 2004) is used for cloud microphysics and Kain–Fritsch mass flux scheme (new Eta scheme) (Kain, 2004) for convection processes. The planetary boundary layer (PBL) scheme follows that of Hong *et al.* (2006). Land surface processes were represented with the Unified Noah land-surface model (NOAH) (Chen and Dudhia, 2001). NOAH predicts soil texture, temperature and moisture for four soil categories (10, 30, 60 and 1000 cm thick). It includes a rooting zone, soil drainage, and runoff, different vegetation categories and a monthly vegetation fraction. The model calculates the surface water budget, surface

evaporation, vegetation transpiration, canopy resistance and moisture. Surface emissivity properties are represented and the sensible and latent heat fluxes are included in the boundary-layer scheme. The surface data is taken from the United States Geological Survey (USGS 24 category land dataset). The implementation of NOAH in WRF can be obtained in Skamarock *et al.* (2008). The horizontal resolution for WRF simulations is the same as that of RegCM, except that in WRF, 40 vertical grid points are used.

3.7 DESCRIPTION OF THE FORCING GENERAL CIRCULATION MODELS

The RCM simulations were forced using two GCMs outputs. The two GCMs are the Met Office Hadley Centre Model (HADGEM2-ES, hereafter HAD) (Collins *et al.*, 2011; Jones *et al.*, 2011; Martin *et al.*, 2011) and the Max-Planck-Institute for Meteorology Earth System Model (MPI-ESM-LR, hereafter MPI) (Giorgetta *et al.*, 2013a; Giorgetta *et al.*, 2013b; Stevens *et al.*, 2013). The simulations for both GCMs (HAD and MPI) were obtained from the Coupled Model Intercomparison Project (CMIP5) and were used to provide the initial and lateral boundary conditions for the two RCMs.

3.7.1 HAD Earth System Model

In this study, the HAD is utilised for initial and lateral boundary conditions for all the experiments performed with RegCM to simulate over West Africa the impacts of climate change and forestation on climate extremes. The description of the HAD model presented here is based on previous works (Collins *et al.*, 2011; Jones *et al.*, 2011; Martin *et al.*, 2011). The HAD is an Earth system model which is appropriate for the simulation and

understanding of the centennial scale evolution of climate including biogeochemical feedbacks (Collins *et al.*, 2011). It is a coupled Atmosphere-Ocean general circulation model (AOGCM) with an atmospheric horizontal grid spacing resolution of 1.875° × 1.25° with 38 vertical levels (from the surface to over 39 km in height). However, the model resolution is not uniform all over the globe. Over ocean, the model uses a horizontal zonal resolution of 1° × 1° except from the poles to 30° latitude – where it uses a meridional resolution of 1° – which increases up to 1/3° at the equator with 40 vertical levels. As an improvement on HADGEM1, the model incorporates many forcings – aerosols, greenhouse gases emissions, solar irradiance and ozone – and components, such as atmosphere, land surface and hydrology, aerosols, ocean and sea ice, terrestrial carbon cycle, atmospheric chemistry, and ocean biogeochemistry (Jones *et al.*, 2011). HAD is used by the Met Office Hadley Centre for the core climate simulations carried out for the account of the Coupled Model Intercomparison Project (CMIP5). Therefore the historical simulations (present day climate) extends from 1950 to 2005 and the future climate projections under the representative concentration pathway (RCPs) emission scenarios (future climate simulation) from 2006 to 2100.

3.7.2 MPI Earth System Model

In this study, the MPI is used for initial and lateral boundary conditions for all the experiments performed with WRF to simulate the impacts of climate change and forestation on climate extremes in West Africa. The MPI consists of the coupled GCMs for the atmosphere and the ocean (Giorgetta *et al.*, 2013b). The atmospheric component is ECHAM6 (Stevens *et al.*, 2013), while the ocean component is the MPI-OM (Jungclaus *et*

al., 2013). The MPI also includes the land surface model JSBACH (Reick *et al.*, 2013; Schneck *et al.*, 2013) and the ocean biogeochemistry model HAMOCC (Ilyina *et al.*, 2013). Figure 3.2 gives a schematic view of the MPI. The coloured boxes represent the components of the model: ECHAM6 is the atmospheric general circulation model, which is directly coupled to the land surface model JSBACH (describes physical and biogeochemical aspects of soil and vegetation). The ocean general circulation model MPI-OM includes the HAMOCC model for the marine biogeochemistry. OASIS is the coupler program, which aggregates, interpolates, and exchanges fluxes and state variables once a day between ECHAM6+JSBACH and MPI-OM+HAMOCC. The coupler exchanges fluxes for water, energy, momentum, and CO2 (Giorgetta *et al.*, 2013a).

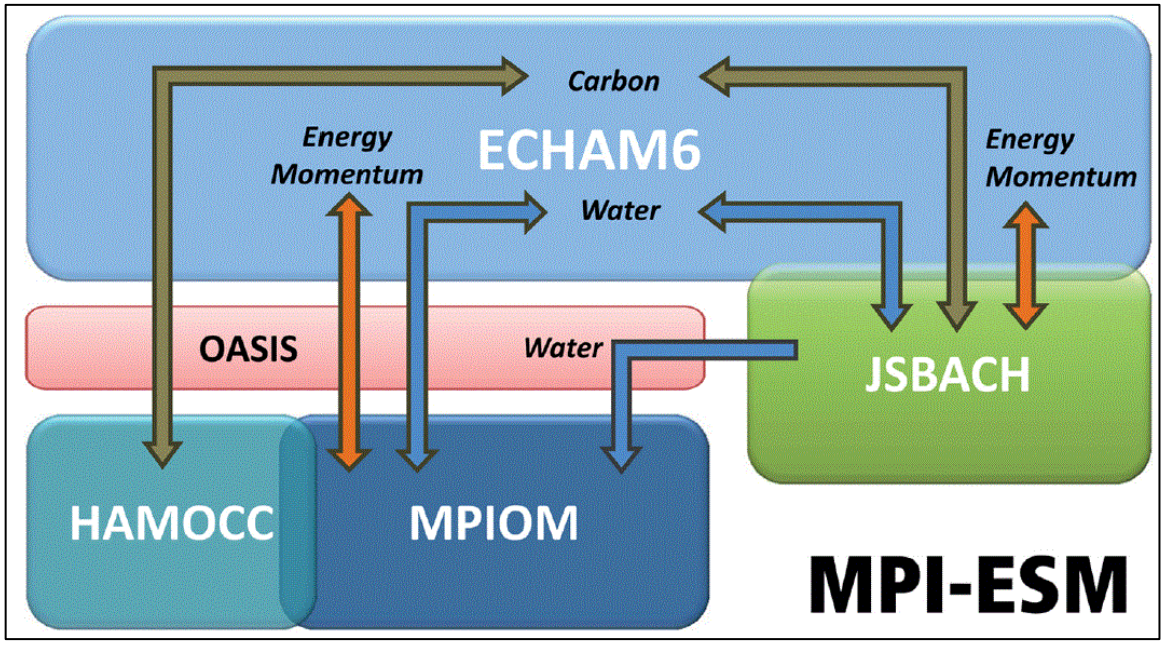

Figure 3.2: Schematic view of the Max-Planck-Institute for Meteorology Earth System Model (MPI-ESM)

Source: (Giorgetta *et al.*, 2013a)

This study uses the Coupled Model Intercomparison Project phase 5 (CMIP5) simulations for observations and future simulations (using the Representative Concentration Pathway (RCP 4.5 scenarios). ECHAM6 is developed for the following resolutions T63L47, T63L95 and T127L95. The MPI simulations used in the present study are performed at low resolution T63 (1.9°) with 47 vertical levels for ECHAM6, over ocean (MPI-OM) the horizontal resolution is 1.5° with 40 vertical levels and the land surface model (JSBACH) which shares the horizontal grid of the atmospheric model.

3.8 NUMERICAL SIMULATION EXPERIMENTS

Three numerical experiments were performed using two different land cover patterns with each RCM. The first experiment (PRS) simulated the present-day climate (1970-2004). The second experiment simulated the future climate (2030-2064) without forestation (GHG). The third experiment simulated the future climate with forestation (FRS). Table 3.2 illustrates the experiments performed with each RCM.

The first two experiments (PRS and GHG) employed the present-day land-cover pattern (Figure 3.3a and Figure 3.4a) to simulate the present-day (1970-2004) climate and the future (2030-2064) climate. The third experiment (FRS) simulated the impact of forestation on the future climate (2030-2064). The FRS is identical to the GHG experiment with the exception that the land-cover pattern over the Savannah (area between 8°N and 12°N) is replaced by broad leaf trees (Figure 3.3b and Figure 3.4b).

In general, the land-use pattern used in WRF and RegCM are similar (Figure 3.3a and Figure 3.4a). The future simulations for GHG and FRS (Figure 3.3b and Figure 3.4b) are

based on the increasing greenhouse gas concentration under the intermediate-range Representative Concentration Pathway (RCP) 4.5 scenario (Thompson *et al.*, 2009; Thomson *et al.*, 2011). The RCP is simulated using the Global Change Assessment Model (GCAM) and includes long-term, global emissions of greenhouse gases, short-lived species, and land-use-land-cover in a global economic framework (Thomson *et al.*, 2011).

Each RCM simulation was initialised and forced with the corresponding GCM simulation (*i.e.* RegCM with HAD, and WRF with MPI). All the simulations were 35 years long, starting from 1970 to 2004 for the PRS simulations and 2030 to 2064 for the GHG and FRS. The first years of all simulations are discarded as spin-up and the remaining 34 years (1971-2004 for PRS, and 2031-2064 for GHG and FRS) are analysed for the study.

The extreme rainfall threshold of PRS was used as reference in obtaining the extreme, non-extreme, and widespread-extreme rainfall events for the three simulations (PRS, GHG, and FRS). This study also quantified the impacts of climate change and forestation on extreme rainfall characteristics. PRS simulations were used to evaluate the capability of the models to simulate characteristics of extreme climate events over West Africa. The difference between PRS and GHG (*i.e.* GHG minus PRS) results were used to obtain the projected future climate change while the difference between GHG and FRS (*i.e.* FRS minus GHG) results were used to assess the impacts of the forestation on the future climate extremes. The difference in the thresholds of PRS and GHG (GHG and FRS) was used to quantify the impacts of climate change (forestation) on extreme rainfall intensity in future. The analyses on changes in extreme rainfall characteristics also accounted for extreme and non-extreme rainfall events, WEREs and total annual rainfall over West Africa.

Table 3.2: Summary of experiments performed with each regional RCM

S/No.	Experiments	Initial and boundary condition data	Land cover pattern
1	PRS	Present day (1970-2004)	Present day (Figure 3.3a and Figure 3.4a)
2	GHG	Future period (2030-2064) RCP 4.5	Present day (Figure 3.3a and Figure 3.4a)
3	FRS	Future period (2030-2064) RCP 4.5	Savannah zone (8°-12°N) forestation (Figure 3.3b and Figure 3.4b)

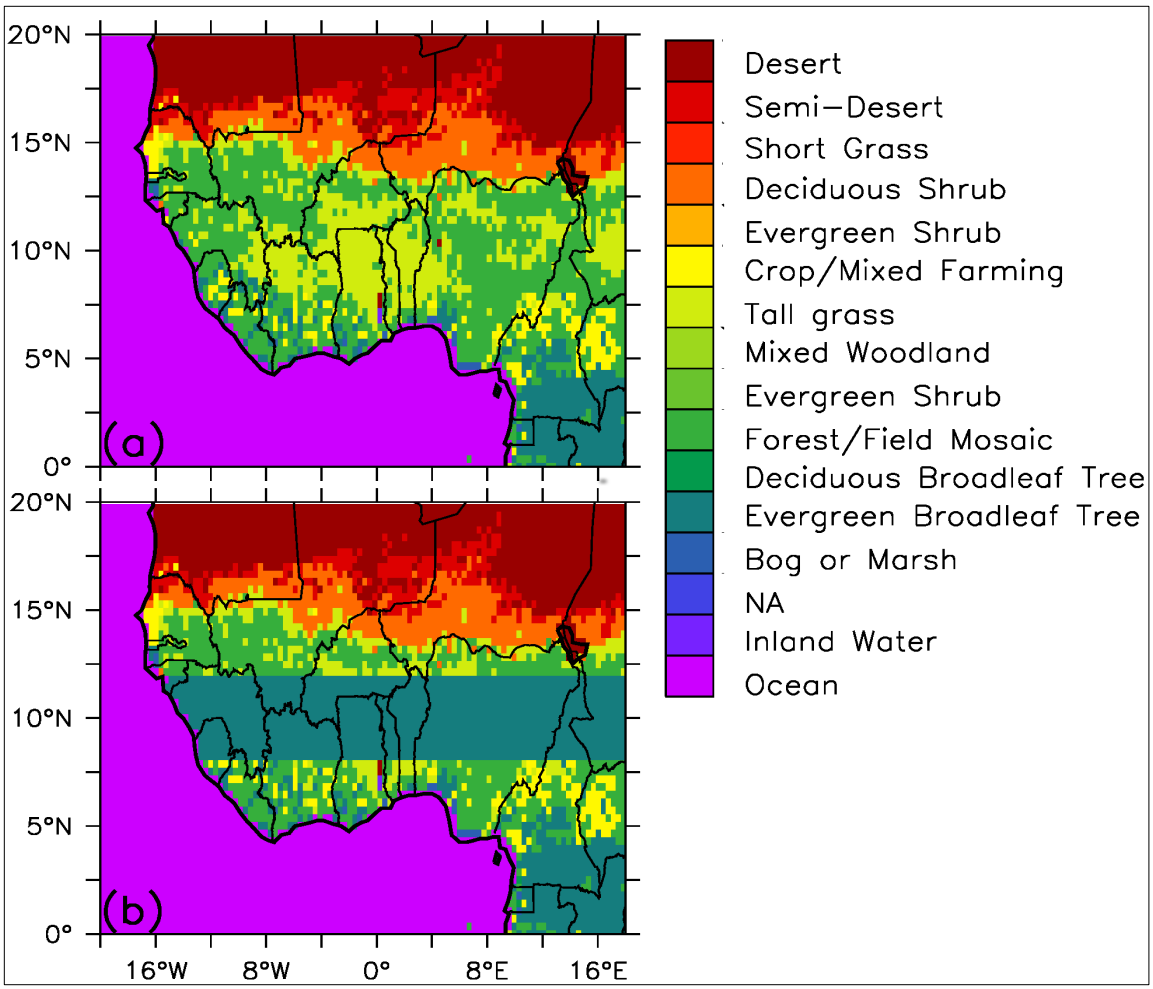

Figure 3.3: Land-cover types used for (a) the present-day climate (PRS) simulations and (b) the future climate (FRS) simulations for RegCM

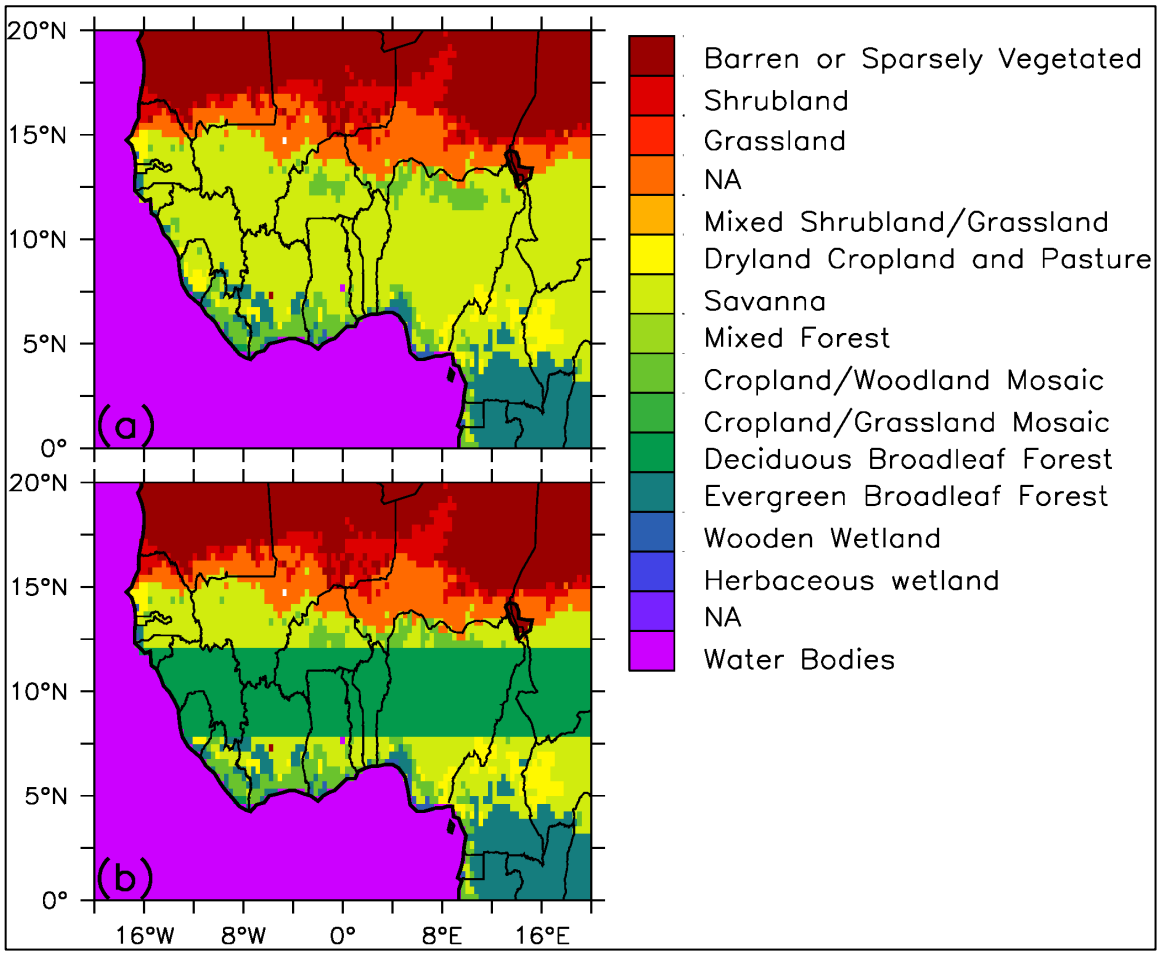

Figure 3.4: Land-cover types used for (a) the present-day climate (PRS) simulations and (b) the future climate (FRS) simulations for WRF

In the study, the main focus is on the spatial distribution of heatwave characteristics and the impact of the climate change and forestation on heatwave events in future over West Africa. The T95 and TX90 from PRS are respectively used to compute EHF and extreme temperature days for the three simulations (PRS, GHG, and FRS). The characteristics of the simulated heatwaves (PRS) are evaluated against observations. The evaluation includes how well the models simulate T95 and TX90 and reproduce heatwave number (HWN), heatwave days (HWF) and heatwave duration (HWD) over West Africa. Similarly to extreme rainfall characteristics, this study quantifies the impacts of climate change (forestation) on heatwave characteristics. The difference in the T95 and TX90 for PRS and GHG (GHG and FRS) were used to quantify the impacts of climate change (forestation) on extreme temperature days in future. The analyses of future changes on heatwave characteristics also accounted for HWN, HWF and HWD over West Africa.

CHAPTER FOUR

RESULTS AND DISCUSSIONS

4.1 INTRODUCTION

In this chapter, the research findings are presented relative to the impacts of climate change and forestation on climate extremes over West Africa. First, the ability of the RCMs to reproduce some characteristics of extreme rainfall and heatwave events over West Africa for the present-day climate is evaluated. Then, the projected impacts of climate change on extreme rainfall and heatwave characteristics are presented and discussed. Lastly, the projected impacts of forestation on extreme climate events are presented.

4.2 EXTREME CLIMATE EVENTS FOR THE PRESENT-DAY CLIMATE

This section evaluates the RCMs simulation of extreme rainfall characteristics in the present-day climate over West Africa. The ability of RegCM and WRF) to simulate the extreme rainfall threshold and the seasonal distribution of WEREs frequency over the Savannah zone in West Africa in comparison with the observation datasets (Global Precipitation Climatology Project – GPCP and Tropical Rainfall Measuring Mission – TRMM) is analysed.

4.2.1 Threshold of Extreme Rainfall over West Africa

Figure 4.1 presents the spatial distribution of observed (GPCP and TRMM) and simulated (RegCM and WRF) extreme rainfall threshold over West Africa. The figure shows that the

two observation datasets (GPCP and TRMM) generally produce similar patterns of extreme rainfall threshold (*i.e.* 95th percentile) over West Africa, but with some notable discrepancies. While the spatial correlation between the threshold patterns is high (r = 0.7), the threshold value is generally higher in TRMM than in GPCP. However, both datasets feature maximum threshold values at the west coast (*i.e.* over Guinea and Sierra Leone) and the south coast (*i.e.* at the border of Nigeria and Cameroon). The major discrepancy between the two observed datasets occurs along the coastal region (from the west coast to the south coast), where their extreme rainfall threshold values differ by almost 30 mm day^{-1}. The discrepancy may be attributed to the difference in the spatial resolution of the two datasets (1° x 1° and 0.25° x 0.25°, respectively). However, the discrepancy is less than 20 mm day^{-1} over the Savannah zone (8°N to 12°N) and Sahel zone (12°N to 16°N).

The two models simulate conflicting threshold patterns (Figure 4.1c and Figure 4.1d) that generally differ from the observed datasets. The correlation between the simulated and observed (GPCP) threshold patterns is weak, although the value is higher in WRF (r = 0.5) than in RegCM4 (r = 0.4). However, the models capture the observed maximum threshold values at the west and south-east coasts, but with some differences in their magnitude and location. For instance, while RegCM centres the western maximum threshold at 6°N, WRF reproduces it at 14°N, but observation datasets (GPCP and TRMM) show it at 9°N. In addition, both models overestimate the magnitudes of the maximum threshold by more 40 mm day^{-1}. Although the location of the south-eastern maximum threshold is well captured by the models, the magnitude is overestimated. The RCMs also generally overestimate extreme rainfall threshold values over mountains (*i.e.* Cameroon Mountains and Jos Plateau). While RegCM underestimates the threshold values (with reference to GPCP) over

the lowlands in West Savannah and in the Sahel by about -10 mm day^{-1}, WRF overestimates it by about 20 mm day^{-1} (Figure 4.1c and Figure 4.1d). All these biases may be attributed to different shortcomings in the models, ranging from the inadequacy in convective parameterisation (Browne *et al.*, 2015), to the insufficiently high resolutions (Druyand and Fulakeza, 2012), lateral boundary condition problems (Sylla *et al.*, 2009; Moufouma-Okia and Rowell, 2010), and the deficiencies in land-cover representation (Sylla *et al.*, 2010). It could also be attributed to differences in the length of the observation and simulations datasets used in the study. The periods of the observed datasets (GPCP: 1997-2004; TRMM: 1998-2004) are shorter than that of the simulations (*i.e.* 1971-2004). A dataset with a longer period would possibly have higher extreme rainfall threshold values than the one with a shorter period. However, the discrepancy among the observation datasets (TRMM and GPCP) also creates uncertainties in the model evaluation.

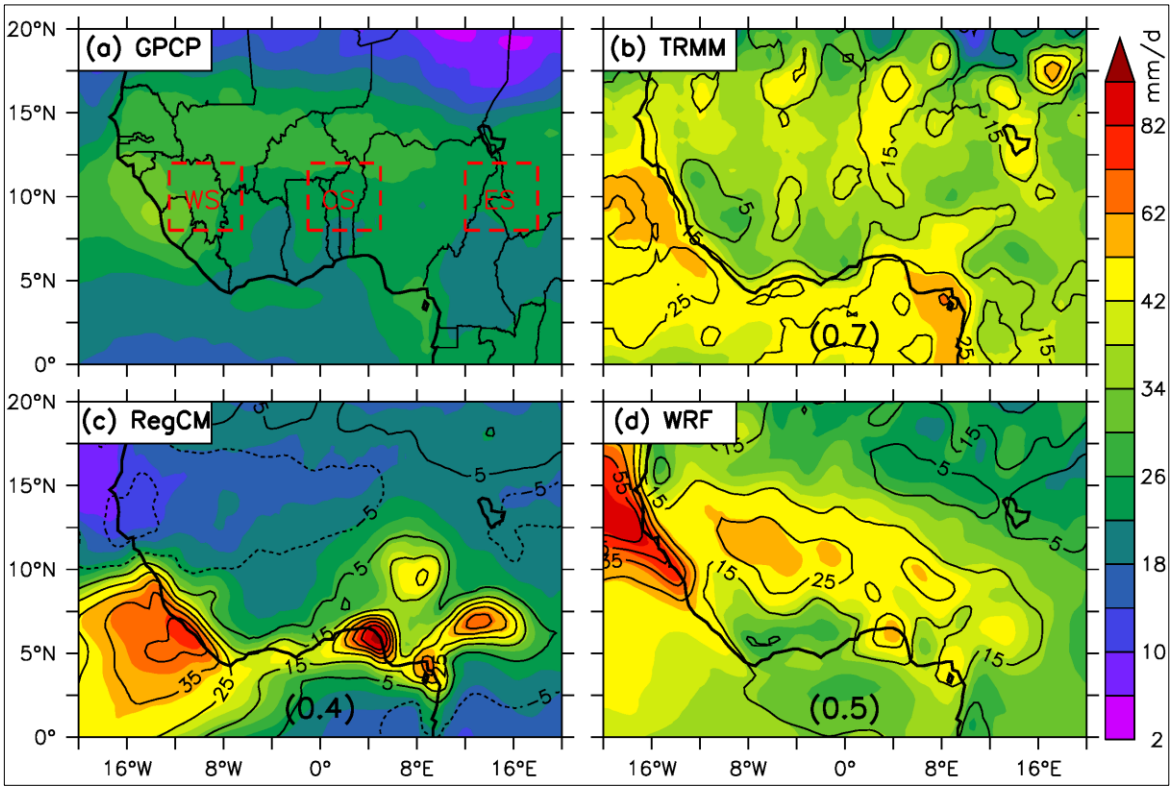

Figure 4.1: The horizontal distribution of extreme rainfall threshold: 95th percentile of daily rainfall (mm day^{-1}) as observed (a) GPCP and (b) TRMM and simulated (c) RegCM and (d) WRF over West Africa. The contours indicate the biases in the observed (TRMM) and simulated (RegCM and WRF) extreme rainfall threshold, in reference to GPCP results. The spatial correlation between the pattern in each panel and that of GPCP is indicated in the bracket

4.2.2 Seasonal Variation of WERE over Savannah

The seasonal distribution of WEREs over the three selected areas in Savannah (west, central and East Savannah) shows that GPCP reports more WEREs than TRMM (Figure 4.2). However, both datasets agree that the WEREs only feature in June-August and September-November, and that the WEREs are more frequent in June-August than in September-November. The WEREs occur in these two seasons because the West Africa Monsoon (WAM), which provides a favourable condition for deep convection (*i.e.* moisture and triggering mechanisms) over this region, traverses the Savannah with its rain-producing systems during these seasons. However, the selected Savannah areas experience more WEREs in June-August than in September-November because, while the WAM slowly moves northward in June-August, it swiftly retreats southward in September-November. Hence, the rainfall producing systems stay longer over the areas in June-August than in September-November. In both TRMM and GPCP, the WEREs are more frequent over west Savannah than over central or East Savannah. This may be a result of the proximity of the west Savannah to the oceans resulting in more influx of moisture from the oceans than the central and East Savannah, which depend mainly on moisture-recharge of the WAM through evaporation.

Despite the poor performances of RegCM and WRF in simulating the extreme rainfall threshold over West Africa, both models realistically reproduce the observed characteristics of WEREs over the three areas. For instance, they simulate the highest frequency of WEREs in June-August, and WRF shows that more WEREs occur over west Savannah than over the central or East Savannah. The major bias in the simulated WEREs is that some WEREs are simulated in March-May contrarily to the observation datasets (GPCP

and TRMM). This suggests that the models simulate the onset of the WAM over the Savannah earlier than observed. However, the total number of the simulated WEREs over each area is within the observed (GPCP and TRMM) values.

To check the sensitivity of WERE computation to extreme rainfall threshold values, the observed and simulated WEREs are recalculated, but using the threshold from GPCP and TRMM. The results indicate that using the threshold from TRMM (Figure 4.3d - f) lowers the WEREs frequency in GPCP because TRMM extreme rainfall threshold is higher than that of GPCP, while using the threshold from GPCP (Figure 4.3a - c) increases WEREs frequency in TRMM but the value is still lower than that of GPCP. This suggests that, regardless of the extreme rainfall threshold value used, the frequency of WEREs in TRMM may always be lower than in GPCP. However, using the threshold from either TRMM or GPCP produces a higher frequency of WEREs in WRF over west and central Savannah, where the model produces higher values of extreme rainfall threshold than the observed, but a lower frequency of WEREs in RegCM over west and East Savannah, where the model produces lower values of extreme rainfall threshold than the observed datasets (GPCP and TRMM).

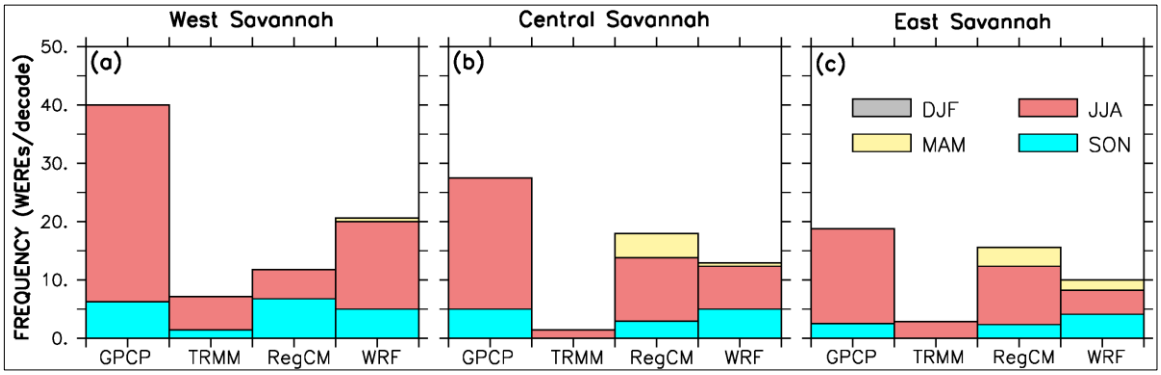

Figure 4.2: The seasonal variations of the frequency of widespread extreme rainfall events (WEREs; events per decade^{-1}) as observed (GPCP and TRMM) and simulated (RegCM4 and WRF) over: (a) West Savannah, (b) Central Savannah, and (c) East Savannah

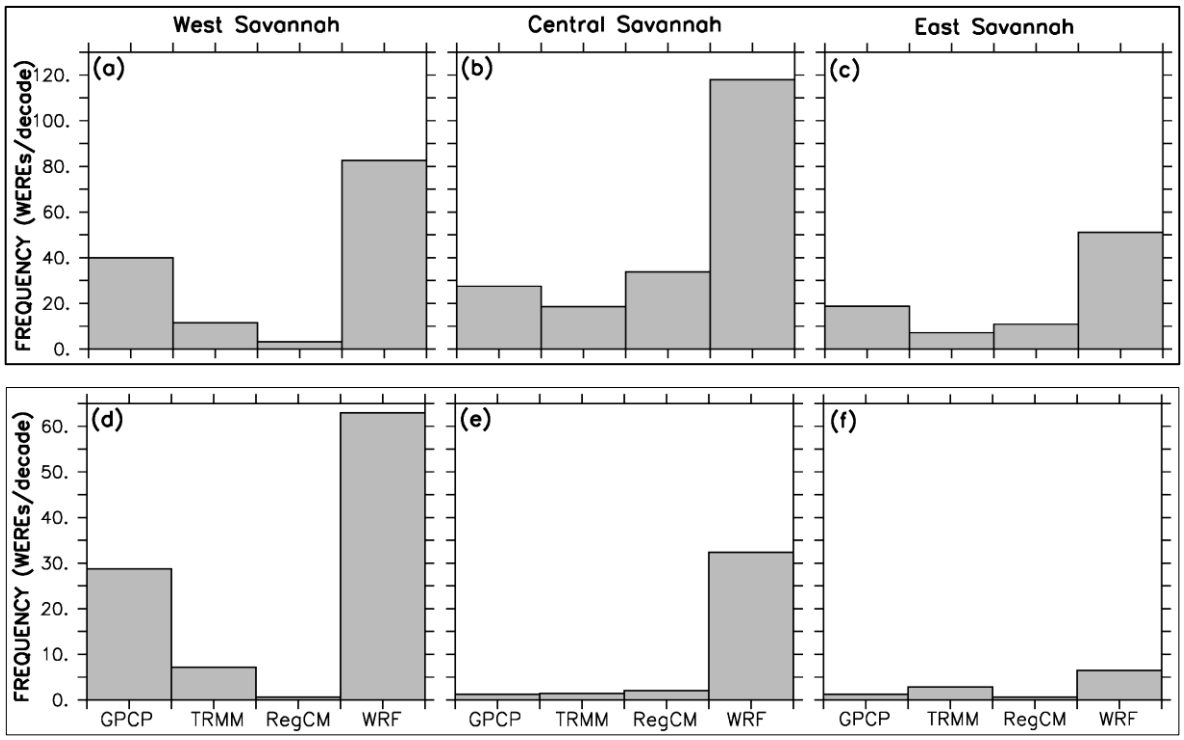

Figure 4.3: The frequency of widespread extreme rainfall events (WEREs). The frequency of WEREs (decade^{-1}) is calculated using the extreme rainfall threshold values of GPCP (a – c) and TRMM (d - f) over: (a) and (d) West Savannah, (b) and (e) Central Savannah, (c) and (f) East Savannah

4.2.3 Characteristics of Heatwaves in Present-Day Climate

Figure 4.4 shows the spatial distribution of the observed (Princeton University Global Meteorological Forcing Dataset: PGFD) and simulated (RegCM and WRF) extreme temperature thresholds (95^{th} percentile of daily mean temperature: T95 and 90^{th} percentile of daily maximum temperature: TX90) over West Africa during the present-day climate. In the observed fields (PGFD), the spatial distributions of both extreme temperature thresholds (T95 and TX90) are comparable over West Africa (Figure 4.4). Their spatial patterns show that the temperature thresholds increased from the south (along the coastal region) to the north, with a local minimum over the Jos Plateau and Cameroon Mountains, and local maximum values over the East Sahel. This pattern is consistent with the spatial distribution of temperature over the region in summer. The minimum temperature along the coastal area is the result of the influence of cooler air from the ocean, while the temperature minimum over Jos Plateau and Cameroon Mountains is associated to the high topography.

The spatial distributions of the observed heatwave events and heatwave days have similar patterns with that of extreme temperature thresholds (Figure 4.5 and Figure 4.6). While the maximum number of heatwave events occurs in the Savannah and Sahel zones (*i.e.* 10° N - 15°N), the minimum occurrence is within the coastal and mountainous areas. Furthermore, the observation shows that the Savannah and Sahel zones may experience up to 2 and 4 heatwave events per year (with Extreme heat factor: EHF, and Percentile based heatwave index: TXI, respectively), and the mean heatwave duration would be about 6 days $event^{-1}$. On the average, the number of heatwave days may be up to 14 days $per\ year^{-1}$ (with EHF) or 30 days $per\ year^{-1}$ (with TXI) in the Savannah and Sahel zones, but it is usually less than 8 days $per\ year^{-1}$ (with EHF) and 15 days $per\ year^{-1}$ (with TXI) along the coasts.

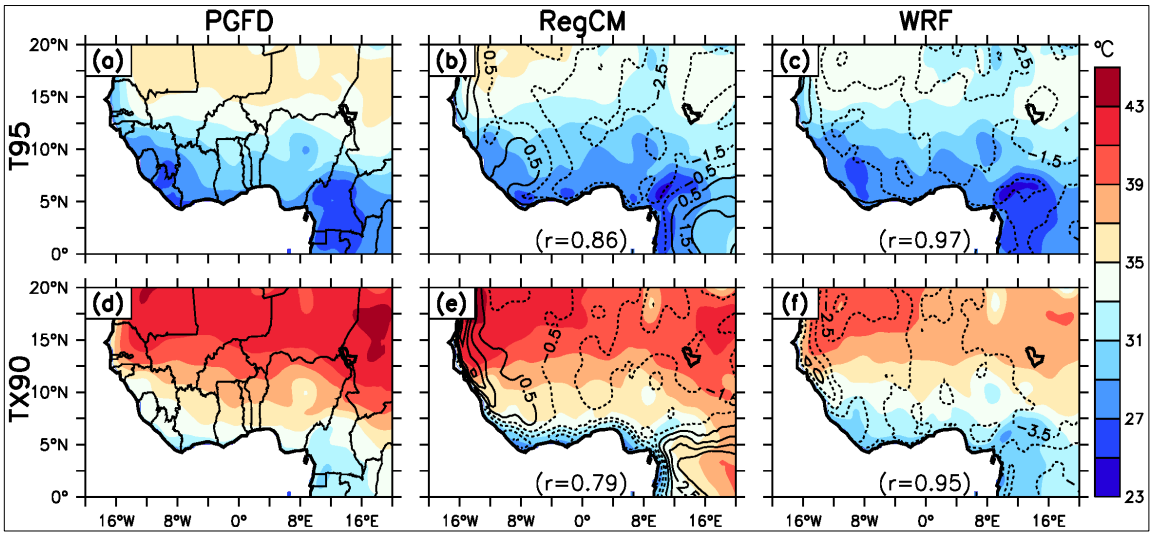

Figure 4.4: The horizontal distribution of extreme temperature thresholds: 95th percentile of daily mean temperature (T95) (a – c) and 90th percentile of daily maximum temperature (TX90) (d – f), as observed (PGFD; a, d) and simulated by RegCM (b, e) and WRF (c, f). The contours indicate the biases in the simulated (RegCM and WRF) extreme temperature thresholds in reference to PGFD results. The spatial correlation between the pattern in each panel and that of PGFD is indicated in the brackets

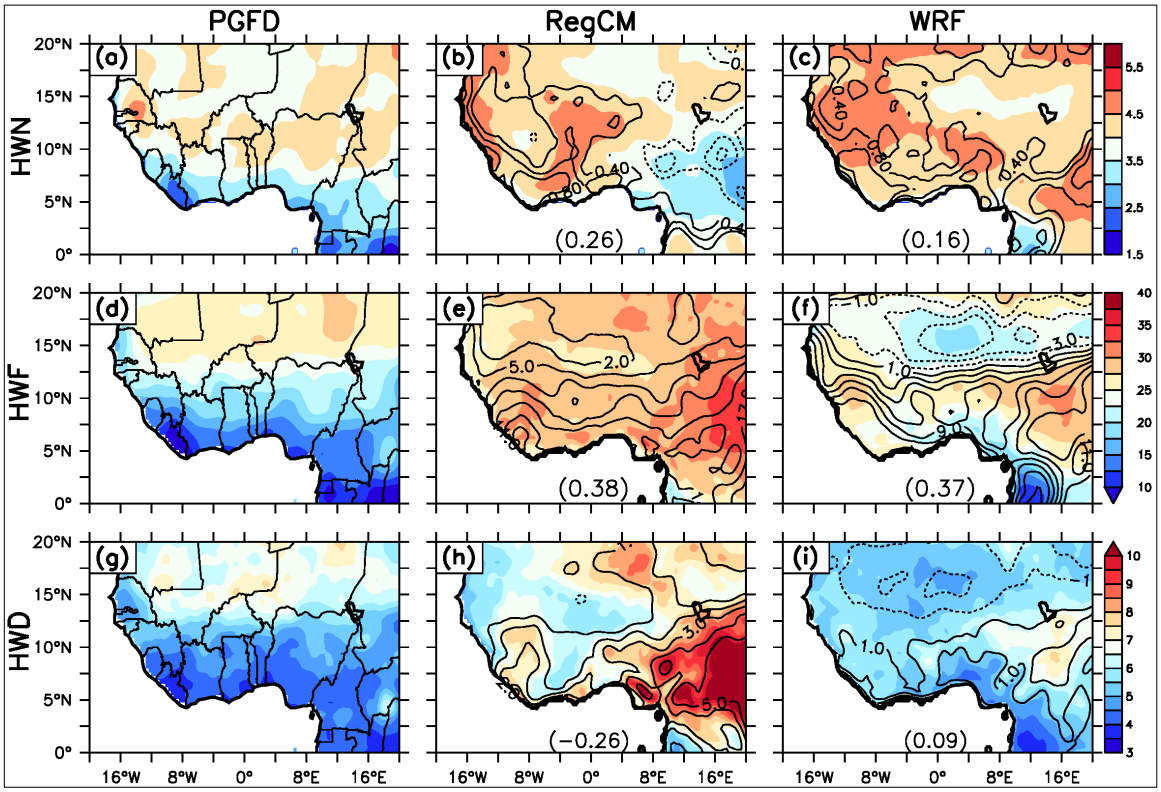

Figure 4.5: The horizontal distribution of heatwave characteristics for the present-day climate (1971-2004) as observed (PGFD; left column) and simulated (RegCM and WRF; middle and right columns respectively) over West Africa using a percentile based index (TXI; 90th percentile of daily maximum temperature). The heatwave characteristics are heatwave number (HWN: event per year^{-1}; a - c), heatwave days (HWF: day year^{-1}; d - f) and heatwave duration (HWD; days event^{-1}; g - i). The contours indicate the biases in the simulated (RegCM and WRF) heatwave characteristics in reference to PGFD results. The spatial correlation between the pattern in each panel and that of PGFD is indicated in the brackets

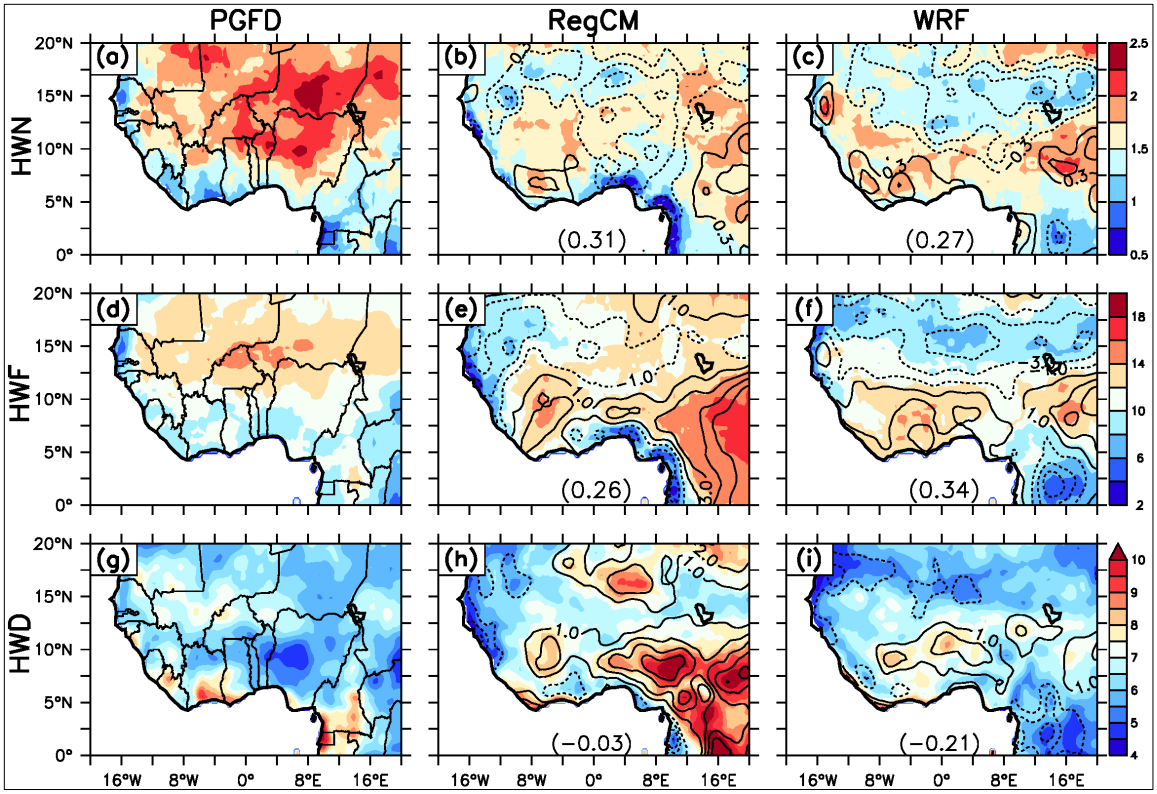

Figure 4.6: The horizontal distribution of heatwave characteristics for the present-day climate (1971-2004) as observed (PGFD; left column) and simulated (RegCM and WRF; middle and right columns respectively) over West Africa using the excess heat factor (EHF) index. The heatwave characteristics are heatwave number (HWN: event per year^{-1}; a - c), heatwave days (HWF: day year^{-1}; d - f) and heatwave duration (HWD: days event^{-1}; g - i). The contours indicate the biases in the simulated (RegCM and WRF) heatwave characteristics in reference to PGFD results. The spatial correlation between the pattern in each panel and that of PGFD is indicated in the brackets

The RCMs simulate some aspects of the heatwave characteristics very well but poorly resolve other aspects. For instance, while the models give a realistic simulation of the spatial variation of the extreme temperature thresholds (T95 and TX90; Figure 4.4), which correlate well with the observation ($0.79 \leq r \geq 0.97$), they do not adequately capture the spatial distribution of the observed heatwave number ($0.16 \leq r \geq 0.31$), heatwave days ($0.26 \leq r \geq 0.38$) and heatwave duration ($-0.26 \leq r \geq 0.09$) (Figure 4.5 and Figure 4.6). In particular, the models weakly reproduce the meridional gradient of the heatwave number as depicted in the observation. While the observation shows the maximum heatwave days and number over Savannah and Sahel zones, the models simulate them over the Savannah alone and produce a minimum heatwave number over the Sahel zone. The largest discrepancy between the simulations and the observation occurs over the eastern part of the Guinean zone (south of 10°N), where the models underestimate the extreme temperature thresholds, and overestimate the heatwave number and days.

The simulated heatwave number and days are generally higher with TXI than with EHF. This may be because, in contrast to TXI, both the Tmax and Tmin (daytime and night-time) are important in defining the heatwave characteristics with EHF. In addition, EHF incorporates the impacts of excess heat and heat stress. While the discrepancy between the observed and simulated heatwave characteristics (heatwave number, days and duration) may be due to the models deficiency, it may also come from the deficiency in the observation dataset (PGFD) used for this evaluation. For example, the PGFD is a hybrid observation-reanalysis dataset created by combining global observation datasets and reanalysis datasets (NCEP-NCAR). Hence, PGFD might reproduce very well the day-to-

day variation of most of the climatological surface variables, but it may not sufficiently capture the temporal and spatial distribution of extreme values among the variables.

4.3 PROJECTED IMPACTS OF CLIMATE CHANGE ON EXTREME CLIMATE EVENTS

4.3.1 Impacts on Extreme Rainfall Events

The RCMs project similar patterns of changes in extreme rainfall frequency over the land (especially north of 10°N), but different patterns over the ocean (especially, south of 5°N; Figure 4.7). Over land, both models generally project a decrease in extreme rainfall frequency in the Savannah and Sahel (*i.e.* north of 10°N), but an increase along the Guinean coast (*i.e.* south of 8°N).

However, there are some notable differences in the projections. First, the maximum decrease of extreme rainfall frequency is located over the East Savannah in RegCM (about 40%; Figure 4.7a), but over the East Sahel in WRF (about 50%; Figure 4.7b). Second, while WRF produces a widespread increase of extreme rainfall frequency over the Guinean coast, RegCM substitutes the increase with a decrease at the southern part of Nigeria and Ghana. Third, the models attribute the decrease of extreme rainfall frequency over Savannah to different reasons. While RegCM attributes it to more frequent non-extreme rainfall events (Figure 4.7c), WRF associates it with a decrease of the number of wet days (*i.e.* extreme *plus* non-extreme rainfall events). Lastly, with RegCM, the intensity of extreme rainfall threshold does not change over Sahel, but with WRF, it decreases by about -4 mm day^{-1} (Figure 4.8). Nevertheless, both models give similar rainfall projections over

the land, except that the magnitude of a decrease in rainfall over Sahel is lower in RegCM because the model projects an increase in number of non-extreme rainfall events over the area (Figure 4.7). Over the Gulf of Guinea, WRF projects an increase in the annual rainfall, but RegCM projects a decrease, despite the increase in frequency non-extreme events (Figure 4.8). The decrease is due to a reduction in the intensity and frequency of extreme rainfall events over the ocean.

In general, RegCM and WRF project an increase in frequency of WEREs over the Savannah (Figure 4.9). The increase is about 3 to 5 events per decade^{-1} over west Savannah and 2 to 7 events per decade^{-1} over central Savannah. However, while WRF projects more frequent WEREs (6 events per decade^{-1}) over East Savannah, RegCM projects fewer because it shows a decrease in the intensity and frequency of extreme rainfall events over the area (Figure 4.9). The seasonal distribution of the changes suggests that the highest increase in WEREs frequency would be in summer (June-August).

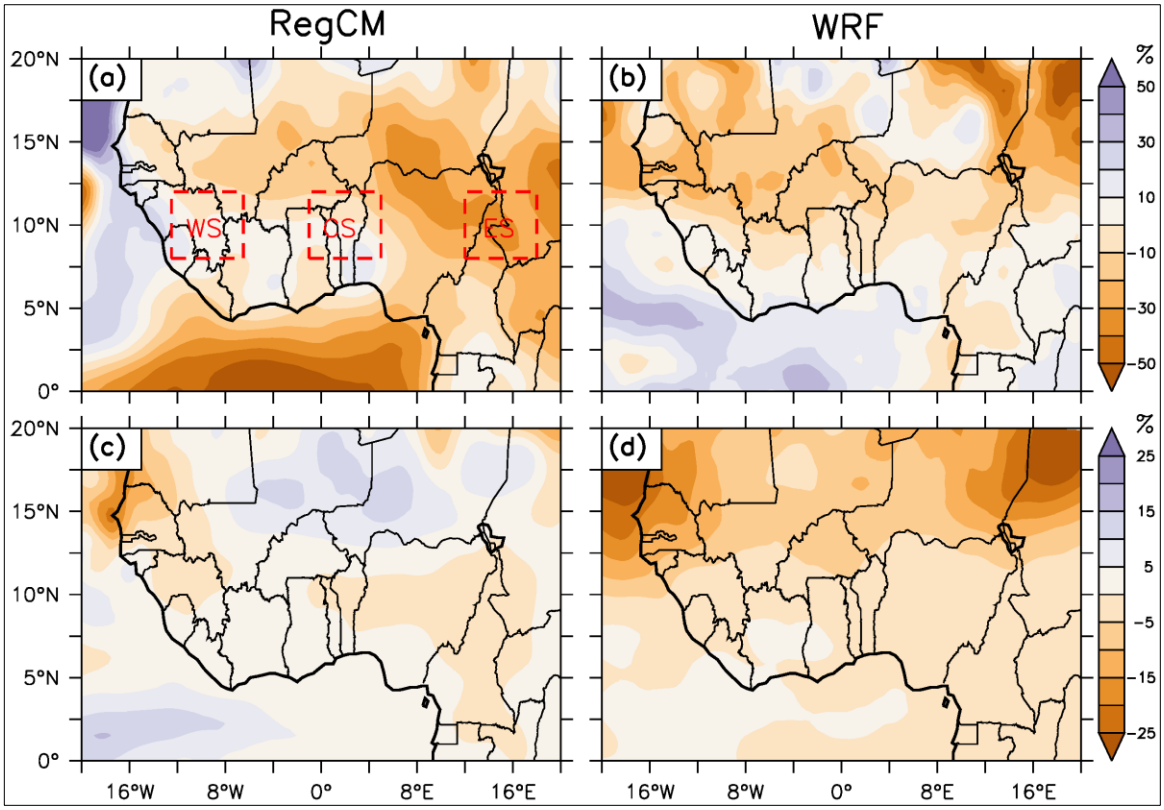

Figure 4.7: Projected future changes (under RCP4.5 scenario) in the frequency of extreme rainfall events (a – b) and frequency of non-extreme rainfall events (c – d)

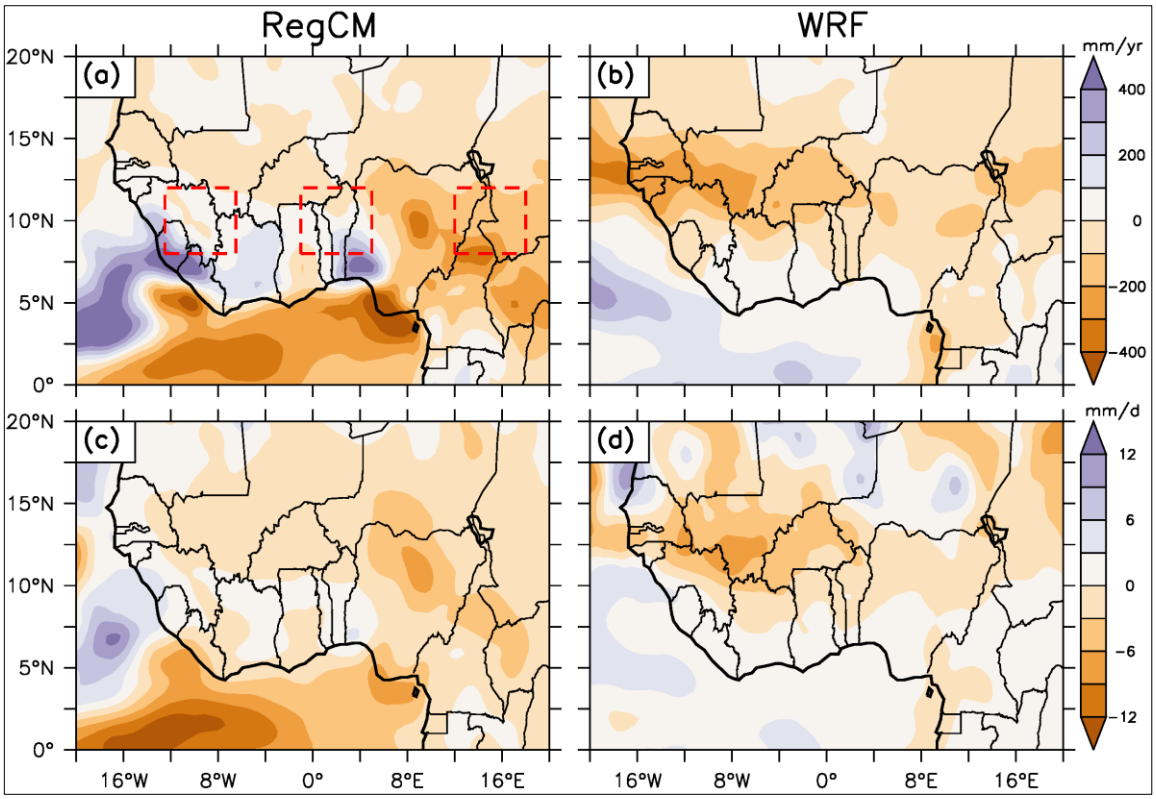

Figure 4.8: Projected future changes (under RCP4.5 scenario) in total annual rainfall (mm per year^{-1}; a - b), and extreme rainfall threshold (mm day^{-1}; c - d)

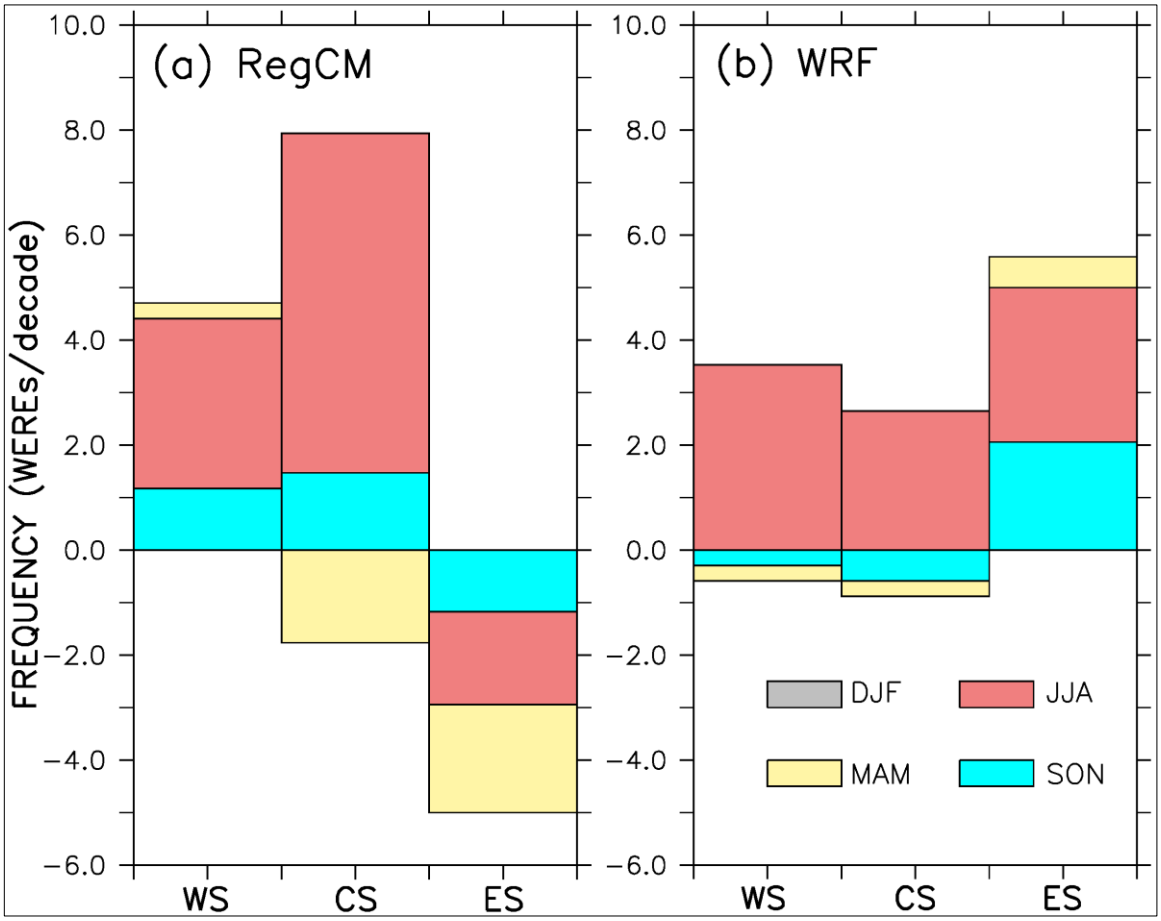

Figure 4.9: Projected future changes in seasonal frequency of Widespread Extreme Rainfall Events (WEREs) over the West, Central, and East Savannah (RCP4.5 scenario)

4.3.2 Impacts on Heatwave Characteristics

Both RCMs project an increase of extreme temperature thresholds (T95 and TX90; Figure 4.10), and heatwave number, days and duration (Figure 4.11 and Figure 4.12) over West Africa in the future (2031 – 2064; under the RCP4.5 climate scenario), although, the magnitude and pattern of the changes slightly differ. This suggests strong and consistent climate change impacts on heatwave characteristics over the region. Both models (RegCM and WRF) agree that the projected increase of extreme temperature thresholds will be highest in the Sahel region (about 2 – 3°C) and lowest (< 2°C) along the coasts. Furthermore, the greatest increase in heatwaves number would also occur in the Sahel zone, although RegCM extends the greatest increase of heatwave number to Savannah zone while WRF shows another peak along the coast. The heatwave duration and heatwave days are also projected to have their greatest increases (6 – 10 days per event^{-1} and 80 – 120 days per year^{-1}, respectively) over the Sahel zone. All these values are generally higher in RegCM than in WRF.

These heatwave projections are consistent with projected temperature changes in West Africa, and agree with some previous studies, especially the Vizy and Cook (2012) mid-21st century heatwave projections under A1B emissions scenario, and the Patricola and Cook (2010) heat index projections for the late-21st century under A2 scenario. Vizy and Cook (2012) also project an increase in maximum and minimum temperatures over West Africa during the mid-21st century, and project an increase of heatwave days north of 8°N with the largest increase (80-120 days per year^{-1}) occurring over the western Sahel between 12° and 18°N.

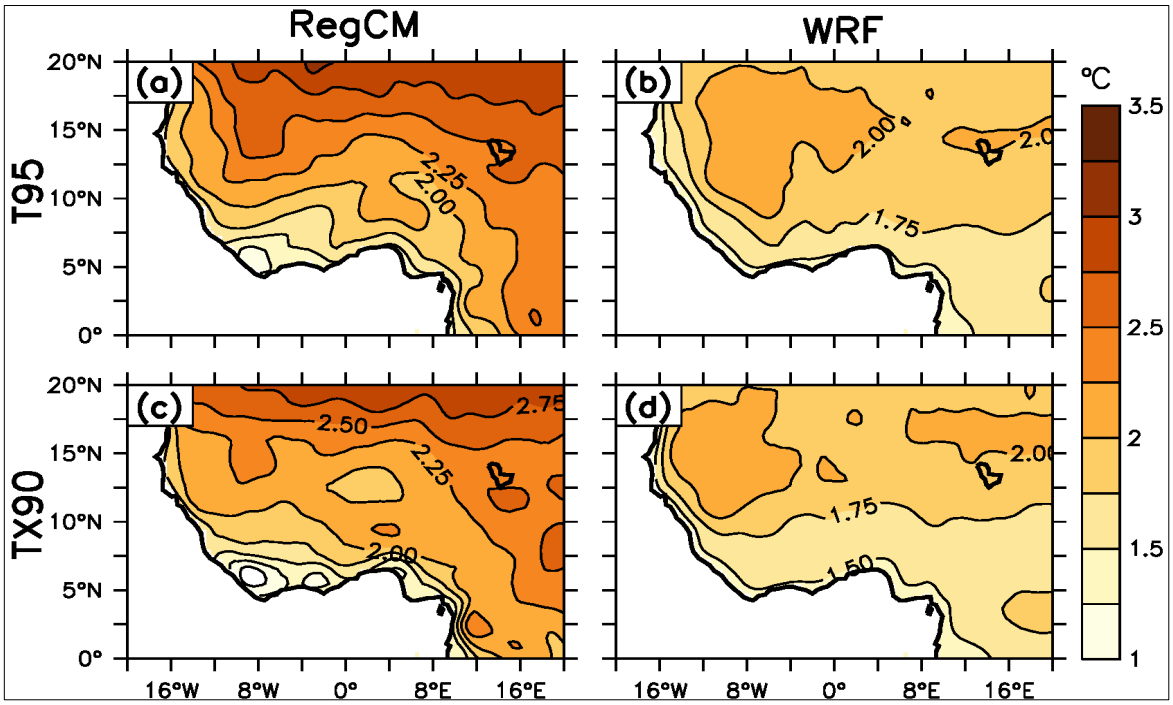

Figure 4.10: Projected future changes in extreme temperature thresholds: T95 (a, b;°C) and TX90 (c, d;°C)

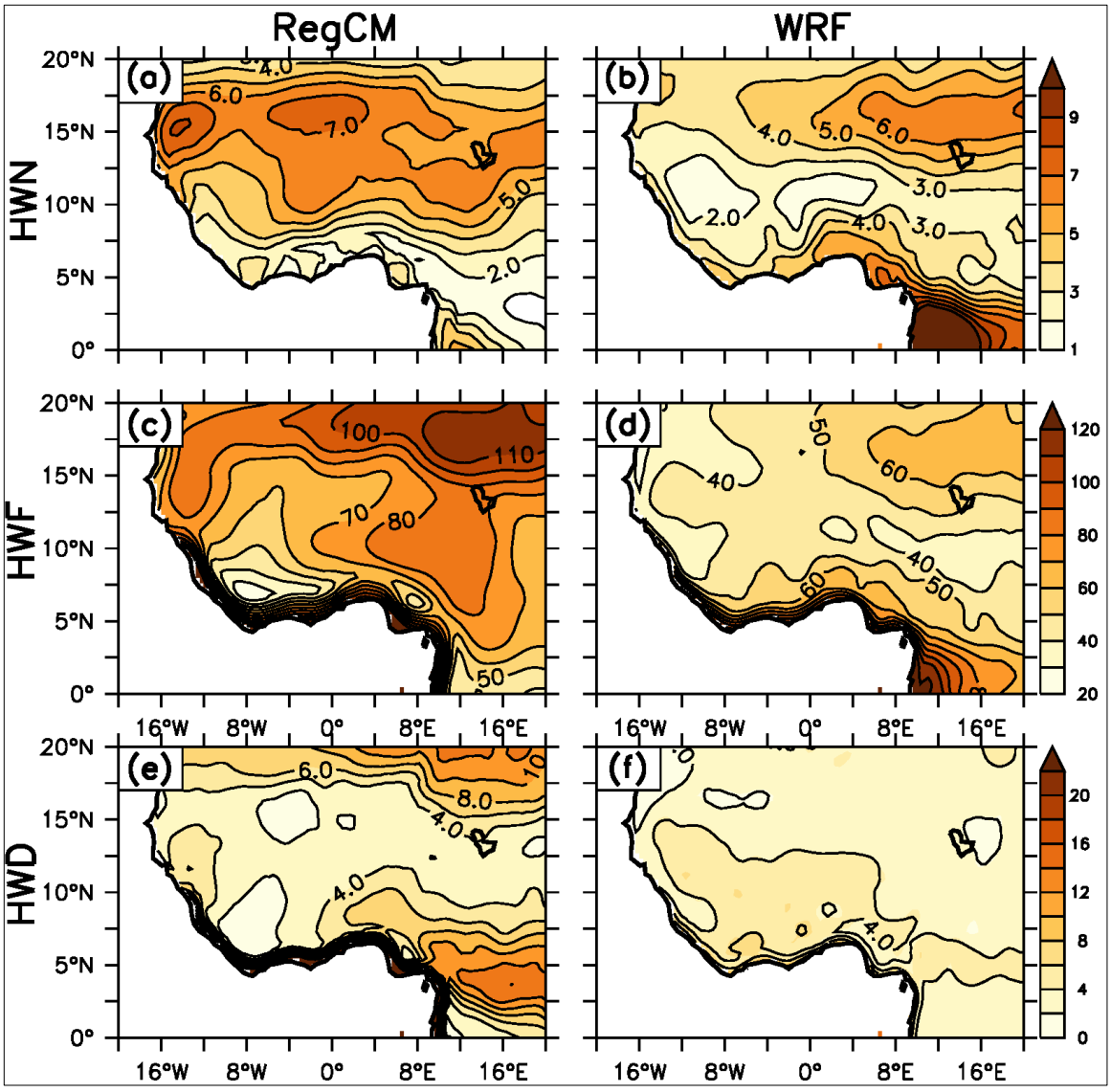

Figure 4.11: Projected future (2031-2064) changes in heatwave characteristics: heatwave number (HWN: event per year^{-1}; a, b), heatwave days (HWF: day year^{-1}; c, d) and heatwave duration (HWD: days event^{-1}; e, f) with TXI

Similarly, Patricola and Cook (2010) project the largest increase of heatwave days (up to 160 days per year^{-1}) with high risk for human health over the Sahel region. However, in these previous studies (Patricola and Cook 2010; Vizy and Cook 2012), the maximum increase of heatwave days over the Sahel region is located between 8°N and 18°N; but, in the present study, the maximum is located north of 15°N (in both models).

Also, along the Guinean coast, both RCMs project another maximum increase of heatwave days and duration, and a minimum increase of heatwave events. This result indicates persistent heatwave conditions over that region. But these conditions may have low to medium risk for human health, as the intensity or magnitude of those heatwave events may be low. Investigating the intensity or magnitude of heatwave events is outside the scope of the present study, which only focuses on heatwave characteristics, such as heatwave number, days and duration. However, results are consistent with that of Patricola and Cook (2010) who project for the late-21st century under A2 scenario, up to 120 heatwave days per year^{-1} with medium risk for human health, which is consistent with the sub-mentioned assumption.

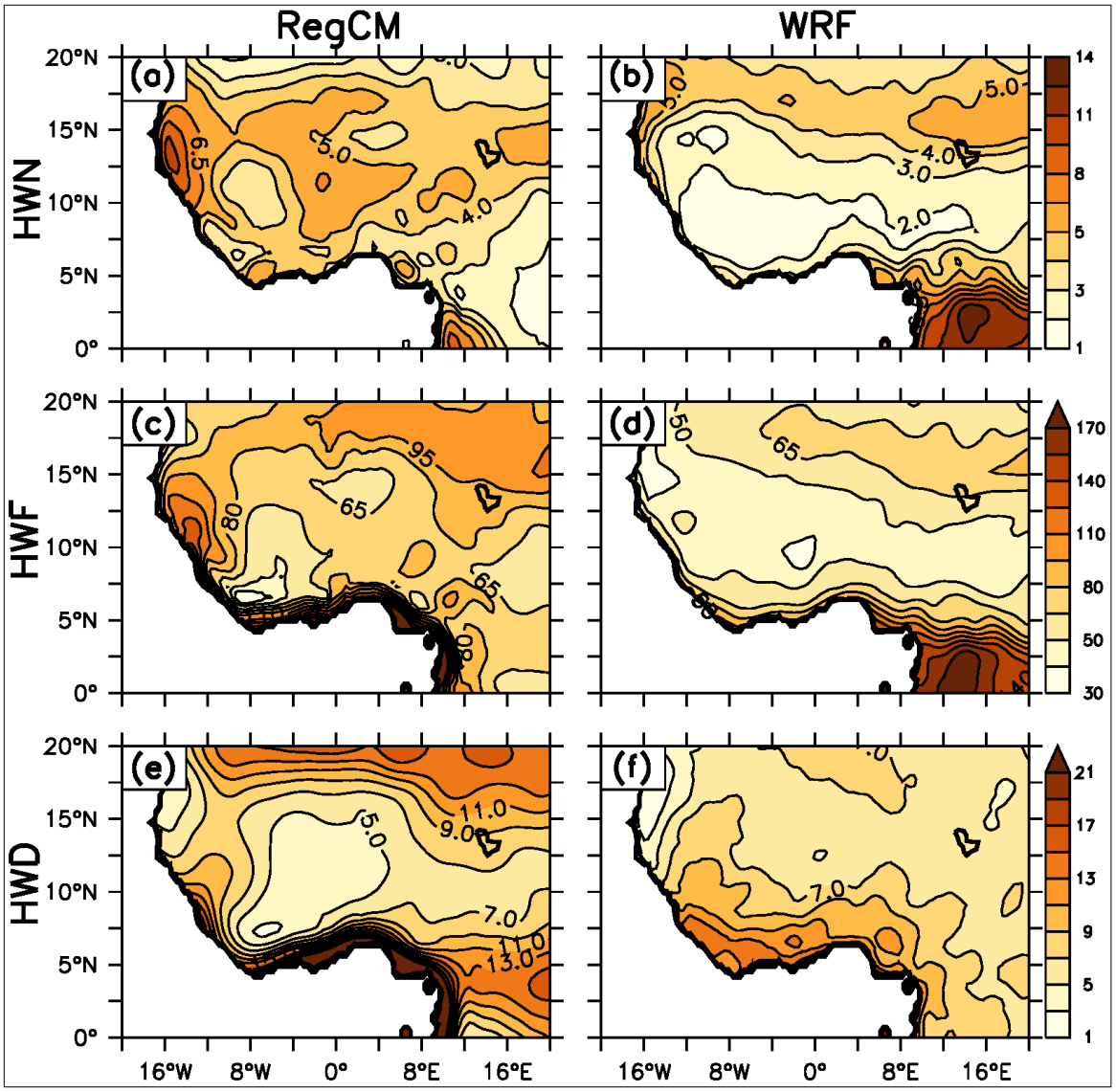

Figure 4.12: Projected future (2031-2064) changes in heatwave characteristics: heatwave number (HWN: event per year^{-1}; a, b), heatwave days (HWF: day year^{-1}; c, d) and heatwave duration (HWD: days event^{-1}; e, f) with EHF

4.4 POTENTIAL IMPACTS OF FORESTATION ON EXTREME CLIMATE EVENTS

4.4.1 Impacts on Extreme Rainfall Events

Both models (RegCM and WRF) show that forestation would alter the characteristics of the projected extreme rainfall events over the forested area (Figure 4.13 and Figure 4.14). Forestation generally increases the intensity and frequency of extreme rainfall events over the forested area (Figure 4.13 and Figure 4.14). However, the magnitude of the increase varies over the area and the patterns of the variation differ in the models. For example, the magnitude of the increase is higher in RegCM (about 10 events per decade^{-1}; Figure 4.13a) than in WRF (about 4 events per decade^{-1}; Figure 4.13b).In RegCM, the maximum increase is located between 10°W and 5°E, but in WRF, two maximum increases (weaker than that of RegCM) are simulated at 10°W and 10°E. Both models simulate an increase in the frequency of non-extreme rainfall events over the forested area, but the value is higher in WRF than in RegCM (Figure 4.13c and Figure 4.13d).

This difference, which may be attributed to the different land model and convection schemes used in the model, suggests that RegCM is more active than WRF in utilising the addition of energy (sensible and latent heat) from the forestation for deep convention (Table 4.1). This also explains why the increase in the threshold of extreme rainfall event is higher in RegCM than in WRF. However, the main message from the results is that forestation would increase the annual rainfall over the forested area (Figure 4.14), partly because the additional latent and sensible energy from forestation would increase the intensity and frequency of extreme rainfall events over the forested area.

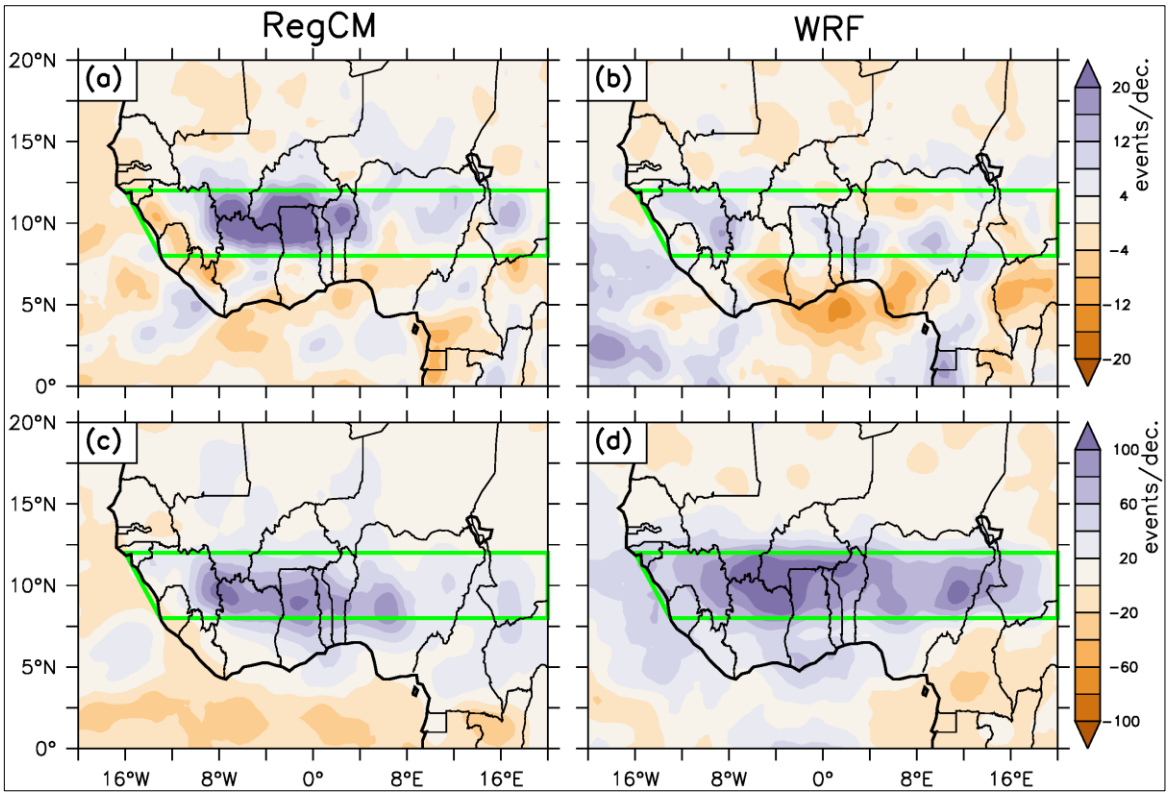

Figure 4.13: Potential impacts of forestation on frequency of extreme rainfall events (events decade^{-1}; a - b) and non-extreme rainfall events (events decade^{-1}; c - d) (RCP4.5 scenario)

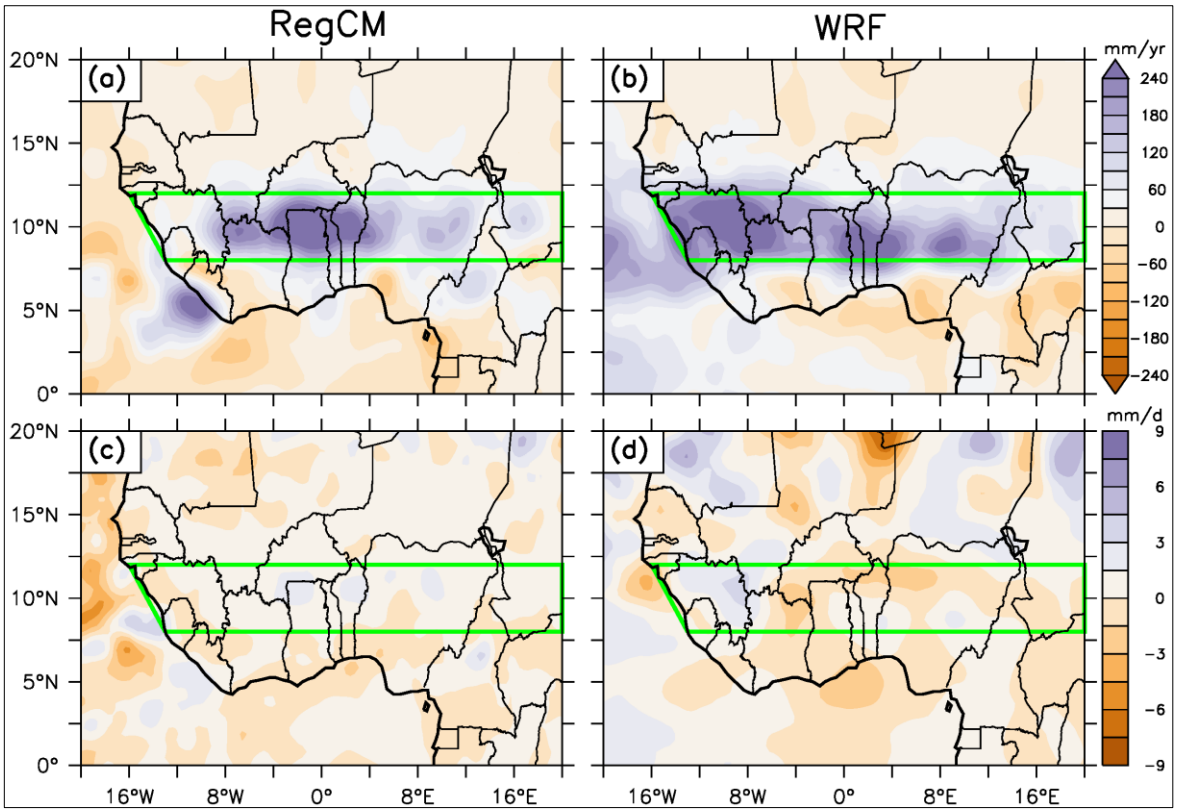

Figure 4.14: Potential impacts forestation on total annual rainfall (mm year^{-1}; a - b), and extreme rainfall threshold (mm day^{-1}; c - d) (RCP4.5 scenario)

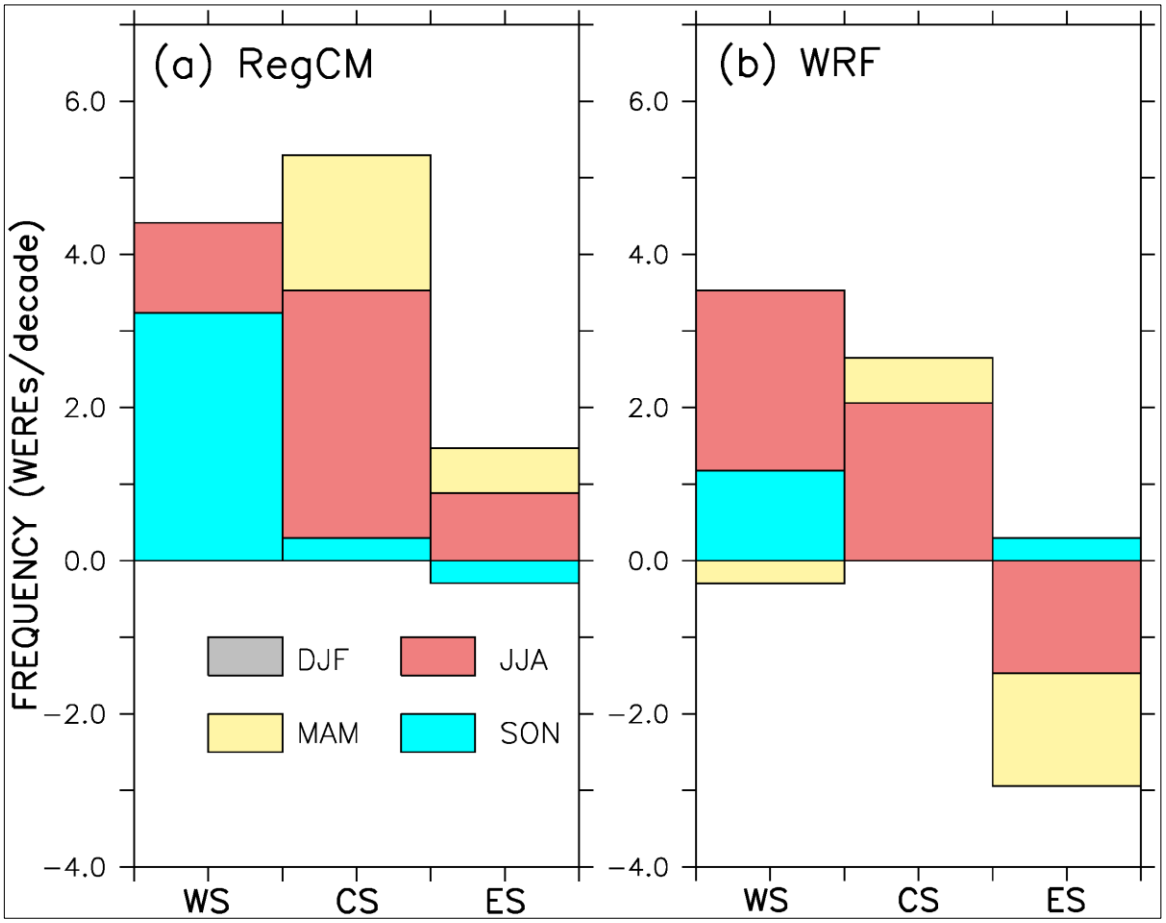

Figure 4.15: Potential impacts of forestation on the seasonal frequency of Widespread Extreme Rainfall Events (WEREs) over the West Savannah, Central, and East Savannah (RCP4.5 scenario)

However, the influence of the forestation on the extreme event is not limited to the forested area; it extends to the surrounding areas (Figure 4.13). For example, both models show that forestation reduces the intensity and frequency of extreme rainfall events south of the forestation area (*i.e.* over the Guinean zone). Nevertheless, the decrease in the frequency of extreme rainfall events is higher in WRF (> 14 events per decade^{-1}) than RegCM (< 14 events decade^{-1}). On the other hand, forestation increases the frequency of non-extreme rainfall events (Figure 4.13c and Figure 4.13d) over the Guinean zone; although the increase is also higher in WRF (> 40 events decade^{-1}) than in RegCM (< 40 events per decade^{-1}). The above results suggest that while forestation in Savannah suppresses the occurrences of extreme rainfall events over the Guinean zone, it enhances more frequent non-extreme rainfall. The impact of these opposing influences on annual rainfall varies among the models. Although both models generally show that the influences will decrease the annual rainfall (in agreement with Abiodun *et al.*, 2012a; 2012b), RegCM shows some areas with a weak increase in rainfall within the zone. The decrease in frequency of extreme events south of the forestation area agrees with results of Abiodun *et al.*, (2012b), but the magnitude of the influences are higher than those in Abiodun *et al.*, (2012b). For instance, in Abiodun *et al.*, (2012b) the maximum decrease in the frequency of extreme rainfall is about 4 events decade^{-1}, but here it is up to 16 events decade^{-1} in RegCM and 24 events decade^{-1} in WRF. The difference may be attributed to the larger forestation area used in the present study.

Forestation generally increases the frequency of WEREs over the Savannah (Figure 4.15). The increase is in the range of 2 to 6 events decade^{-1} over the west and central Savannah. However, over the East Savannah, WRF projected a decrease in frequency of WEREs

(about 3 events decade^{-1}), while RegCM projects more frequent WEREs (about 1 event decade^{-1}). Moreover, the seasonal distribution of the changes suggest the highest change (increase and decrease) are likely to occur during the summer months (June-August).

Tables 4.1 and 4.2 below present the model simulations (RegCM and WRF) for forestation effects on weather events. The analysis describes mean (μ) and standard deviation (σ) of some climate variables for the present-day climate (PRS); the projected future climate change (GHG minus PRS, Δ); and the impacts of Savannah forestation on the future climate (FRS minus GHG, ψ). The climate variables considered are extreme rainfall threshold, frequency of extreme rainfall events and non-extreme rainfall events, total annual rainfall, latent heat flux and sensible heat flux. The significant climate change values (*i.e.* $\Delta > \sigma$) are in bold. If the impact of climate change is not significant, but the additional impact of forestation will make the overall future climate change signal significant (*i.e.* $\Delta + \psi > \sigma$), the impact of forestation value (ψ) is bolded.

Table 4.1: RegCM model simulations averaged over the forested zone (Savannah)

Variables	PRS			
	μ	σ	Δ	ψ
Extreme rainfall threshold (mm day^{-1})	25.95	-	-1.30	0.63
Extreme rain events (events per $year^{-1}$)	11.05	1.66	-1.01	1.01
Non-extreme rain events (events per $year^{-1}$)	209.6	8.88	-1.03	5.04
Total annual rainfall (mm per $year^{-1}$)	2207	204.5	-36.41	125.9
Latent heat flux (W m^{-2})	109.6	4.62	0.099	3.05
Sensible heat flux (W m^{-2})	40.59	3.44	2.89	0.47

Table 4.2: WRF model simulations averaged over the forested zone (Savannah)

Variables	PRS			
	μ	σ	Δ	ψ
Extreme rainfall threshold (mm day^{-1})	43.84	-	-1.26	0.016
Extreme rain events (events year^{-1})	8.07	0.94	-0.398	0.41
Non-extreme rain events (events year^{-1})	152.9	7.15	-3.798	**8.09**
Total annual rainfall (mm year^{-1})	2044	160.6	-90.58	**176.9**
Latent heat flux (W m^{-2})	67.44	1.98	0.53	**7.13**
Sensible heat flux (W m^{-2})	55.65	1.35	0.43	**2.62**

4.4.2 Impacts on Heatwave Characteristics

Both models (RegCM and WRF) show that forestation would alter the characteristics of projected heatwaves over the forested area (Figure 4.16, Figure 4.17 and Figure 4.18). RegCM generally simulates an increase of heatwave number (≈ 0.1 – 0.4 year^{-1}) and heatwave days (≈ 5 – 26 days year^{-1}) over the forested zone (Savannah). However, the magnitude and direction of the changes are not uniform over the forested zone, and the values also differ with both indices (EHF and TXI; Figure 4.17 and Figure 4.18). For instance, the results from RegCM show that with EHF (Figure 4.18), the increase of heatwave number occurs over the entire forested zone (except around 12°E where there is a small decrease, ≈ -0.1 event year^{-1}), and the maximum increase (≈ 1 event year^{-1}) is located at the western part of the zone. But with TXI (Figure 4.17), the increase is limited to west of 4°W (≈ 3 events year^{-1}) while a decrease (≈ -3 events year^{-1}) is projected over east of 4°W. However, with both indices, the model clearly shows that, on the average, forestation increases the number of heatwaves over the forested zone, in particular over the western part of Savannah. In addition, with both indices, the model show that heatwave duration and days increase over the forested zone, although the magnitude of the change in heatwave days is higher with TXI (≈ 25.9 days per year^{-1}) than with EHF (≈ 5.4 days per year^{-1}; Table 4.3). Moreover, RegCM also projects that forestation would increase extreme temperature thresholds (T95 and TX90) over the whole forested area (up to 1°C for T95 and 2°C for TX90; Figure 4.16).

The increase in heatwave number and days in RegCM is consistent with changes in others atmospheric variables following the forestation (Table 4.3 and Figure 4.19). In Figure 4.19a, the analysis of the annual distribution of the changes in heatwave days (induced by

the forestation), as simulated by RegCM, reveals that the impact of the forestation is most pronounced during the dry season (*i.e.* before the onset of monsoon rainfall system and after the cessation of the system) when the soil is dry. During this period, the decrease in surface albedo (≈ -0.02; Table 4.3) induced by forestation makes the surface to reflect less shortwave radiation and to absorb more radiation, thereby increasing the net solar radiation (≈ 6.5 W m^{-2}; Figure 4.19c) and making more energy available at the surface. As the soil is dry, the additional energy will be used to increase the sensible heat (≈ 8 W m^{-2}; Figure 4.19c), and hence the ground surface and boundary layer temperature during daytime (Figure 4.19b). The corresponding increase in maximum temperature is up to 1.3°C. These will create a more favourable condition for heatwaves occurrence over the forested area (Nairn and Fawcett, 2013). However, as the monsoon rainfall system sets in, the impact of forestation on sensible heat and maximum temperature gradually moves from an increase (in March) to a decrease (in June), while the impact on evaporation moves from a decrease to an increase over the same periods. Moreover, the combined increase of relative humidity (Table 4.3 and Figure 4.19b) and maximum temperature (especially, in March; Figure 4.19b) over the forested area constitutes some of the climatic factors that can enhance the risk on human health and security (Fischer and Schär, 2010). Also, the decrease in wind speed (≈ -0.14; Table 4.3) over the forested area may slow down the mixing of the warmer air with the surrounding cooler air. These conditions may induce a stagnant warmer environment over the forested area. The pattern of changes here is consistent with that of Abiodun *et al.*, (2012b), which found that forestation over the Savannah zone in Nigeria will increase the number of heatwave events over the western part of the forested area but decrease these over the eastern part. However, the present study shows that extending the

forestation over the entire Savannah zone in West Africa will lower the heatwaves number over the whole Savannah zone in Nigeria.

Table 4.3 below presents the RegCM model simulations for forestation effects on heatwave events. The analysis describes the mean (μ) and standard deviation (σ) of some climate variables for the present-day climate (PRS); the projected future climate change (GHG - PRS; Δ); and the impacts of Savannah forestation on the future climate (FRS - GHG; ψ). The climate variables are heatwave number (HWN), heatwave days (HWF), maximum temperature (Tmax), minimum temperature (Tmin), daily mean temperature (T_i), ground surface temperature (TS), foliage canopy temperature (TF), surface net shortwave energy flux (RSS), surface net longwave energy flux (RSNL), latent heat flux (LHF), sensible heat flux (SHF), near surface air specific humidity (QAS), near surface relative humidity (RH), moisture content of the soil layers (SMOIS), surface albedo (ALBEDO) and wind speed at 10 m height (WIND). The significant climate change values (*i.e.* $\Delta > \sigma$) are in bold. If a climate change value is significant, but the additional impact of forestation will make the overall future climate change signal not significant (*i.e.* $\Delta + \psi < \sigma$), the impact of forestation value (ψ) is underlined. If the impact of climate change is not significant, but the additional impact of forestation will make the overall future climate change signal significant (*i.e.* $\Delta + \psi > \sigma$), the impact of forestation value (ψ) is in bold.

Table 4.3: The RegCM simulations, averaged over the forested zone (Savannah)

Variables		PRS		Δ	Ψ
		μ	σ		
HWN (events per year^{-1})	EHF	2.17	0.57	**4.33**	0.42
	TX90	4.02	0.81	**4.89**	0.11
HWF (days per year^{-1})	EHF	16.17	6.27	**70.79**	5.38
	TX90	29.73	7.67	**70.15**	25.87
Tmax (°C)		32.13	0.39	**1.93**	0.06
Tmin (°C)		20.88	0.32	**1.94**	-0.18
T_i (°C)		26.51	0.30	**1.94**	-0.06
TS (°C)		26.03	0.32	**2.05**	**0.59**
TF (°C)		25.04	0.31	**2.00**	-0.11
RSS (W m^2)		231.3	2.34	0.57	**4.19**
RSNL (W m^2)		79.11	3.14	-2.42	0.57
LHF (W m^2)		109.6	4.62	0.099	3.05
SHF (W m^2)		40.59	3.44	2.89	0.47
QAS (g g^{-1})		12.39	0.44	**1.14**	**0.52**
RH (%)		57.28	1.98	-0.60	0.48
SMOIS, 0.1 m (kg m^{-2})		22.2	0.66	-0.29	**5.00**
SMOIS, 1 m (kg m^{-2})		450.8	7.91	-11.53	**105.4**
ALBEDO		0.093	0.00	0.00	**-0.02**
WIND (m s^{-1})		1.199	0.14	0.12	**-0.14**

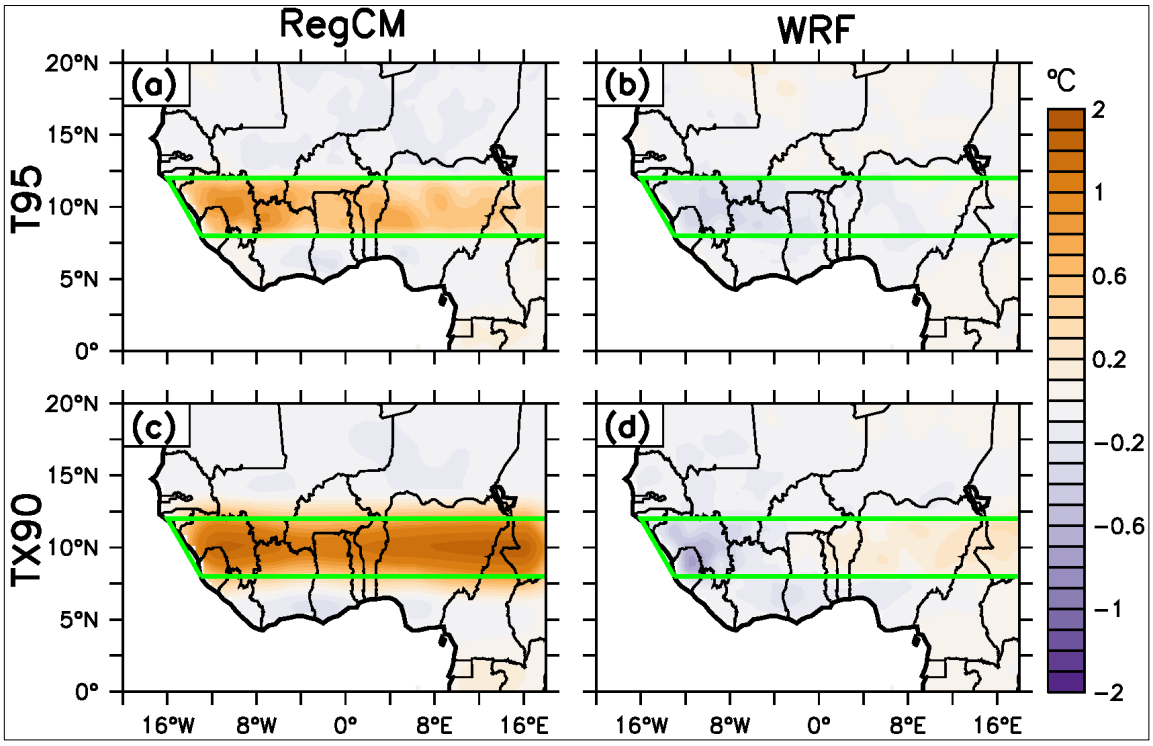

Figure 4.16: Potential impacts of forestation on the projected extreme temperature thresholds: T95 (a, b; °C) and TX90 (c, d; °C)

The results from WRF differ from that of RegCM. In general, the impacts of forestation on heatwave characteristics are weaker in WRF than in RegCM, and in some cases the directions of the changes are opposed in the models. For instance, RegCM projects increases of extreme temperature thresholds over the forested area, while WRF generally tends to simulate the reverse impact of forestation of T95 and TX90 over the Savannah in future (Figure 4.16). However, with TX90, WRF projects that forestation would have a dipole impact on the forested area with a decrease west of 4°W (up to -1°C) and an increase east of 4°W (about +0.3°C). Also, with EHF, RegCM indicates that the forestation would increase the number of heatwave events by 0.42 events $year^{-1}$ and increase the number of heatwave days by about 5.4 days per $year^{-1}$, whereas WRF suggests that the forestation will have no impact on heatwave number, but will decrease heatwave days by about 1.95 days $year^{-1}$ (Table 4.4). With TXI, while RegCM simulates more heatwave events (≈ 0.11 event per $year^{-1}$) following forestation, WRF simulates fewer (-0.05 events per $year^{-1}$), although both model agree on the increase of heatwave days (25.87 days per $year^{-1}$ for RegCM and 0.23 day per $year^{-1}$ for WRF).

In addition, the analysis of the spatial distribution of the changes in heatwave number and days over the forested area also shows some disagreement in the RCMs. For example, while RegCM generally projects an increase of heatwave number and days over the western part of the forested area, WRF generally produces a decrease. Although with EHF both RegCM and WRF project decreases of heatwave duration over the forested area, except RegCM displays three local increases at the north west, south east parts of the forested area and at 4°E (Figure 4.18). With TXI, the main difference is that, while RegCM projects a widespread increase of heatwave duration east of 4°W, WRF substitutes it with local and

weaker increase east of 4°W and a decrease over the western part of the forested zone (Figure 4.17). Nevertheless, on the average, the simulated impacts of forestation on heatwave characteristics are more consistent and agree better with other atmospheric variables in RegCM results (Table 4.3) than in WRF results (Table 4.4).

Both models show that the influence of forestation on the characteristics of heatwaves is not limited to the forested area; it extends to the surrounding areas (Figure 4.17 and Figure 4.18). North of the forested area (over the Sahel), forestation generally induces decreases of most heatwave characteristics. The decrease of heatwave events and days over the Sahel zone is generally higher and more spread in RegCM than WRF. In WRF, the decreases are located in west and east Sahel while RegCM tends to project widespread decreases over the Sahel zone (Figure 4.17 and Figure 4.18). However, along the Guinea coast both RCMs generally disagree in their future projections of the impacts of forestation on heatwave characteristics. While in RegCM forestation decreases heatwave number and days along the Guinea coast, it increases them in WRF; although, with TXI, the number of heatwave days also decreases in WRF along the Guinea coast. But, both temperature thresholds (T95 and TX90) decrease along the Guinean coast and over the Sahel (Figure 4.16), while over the south east coast (near the Equator); forestation increases all heatwave characteristics irrespective of the RCM and the heatwave index. With TXI, changes in heatwave characteristics north and south of the forested area are generally higher and more widely spread than with EHF, with the exception of changes in heatwave duration. In fact, in both RCMs, forestation generally decreases heatwave duration over the Sahel and along the Guinean coast but the change is usually higher with EHF than with TXI (Figure 4.17 and Figure 4.18). Table 4.4 below presents the WRF model simulations for forestation effects

on heatwave events. The analysis describes mean (μ) and standard deviation (σ) of some climate variables for the present-day climate (PRS); the projected future climate change (GHG - PRS; Δ); and the impacts of Savannah forestation on the future climate (FRS – GHG; ψ). The climate variables are heatwave number (HWN), heatwave days (HWF), maximum temperature (Tmax), minimum temperature (Tmin), daily mean temperature (T_i), surface net shortwave energy flux (RSS), surface net longwave energy flux (RSNL), latent heat flux (LHF), sensible heat flux (SHF), surface albedo (ALBEDO) and wind speed at 10 m height (WIND). The significant climate change values (*i.e.* $\Delta > \sigma$) are in bold. If a climate change value is significant, but the additional impact of forestation will make the overall future climate change signal not significant (*i.e.* $\Delta + \psi < \sigma$), the impact of forestation value (ψ) is underlined. If the impact of climate change is not significant, but the additional impact of forestation will make the overall future climate change signal significant (*i.e.* $\Delta + \psi > \sigma$), the impact of forestation value (ψ) is in bold.

Table 4.4: The WRF simulations, averaged over the forested zone (Savannah)

Variables		PRS			
		μ	Σ	Δ	ψ
HWN (events per year^{-1})	EHF	2.19	0.79	**1.94**	0.00
	TX90	4.52	1.09	**2.46**	-0.05
HWF (days per year^{-1})	EHF	14.76	8.86	**45.07**	-1.95
	TX90	27.03	9.82	**41.83**	0.23
Tmax (°C)		30.41	0.39	**1.65**	0.03
Tmin (°C)		20.67	0.395	**1.57**	-0.09
T_i (°C)		25.54	0.38	**1.61**	-0.03
RSS (W m^2)		198.1	1.17	0.48	**7.24**
RSNL (W m^2)		82.30	1.78	-0.66	**-2.66**
LHF (W m^2)		67.44	1.98	0.53	**7.13**
SHF (W m^2)		55.65	1.35	0.43	**2.62**
ALBEDO		0.199	0.00	0.00	**-0.03**
WIND (m s^{-1})		3.00	0.06	-0.06	**-0.65**

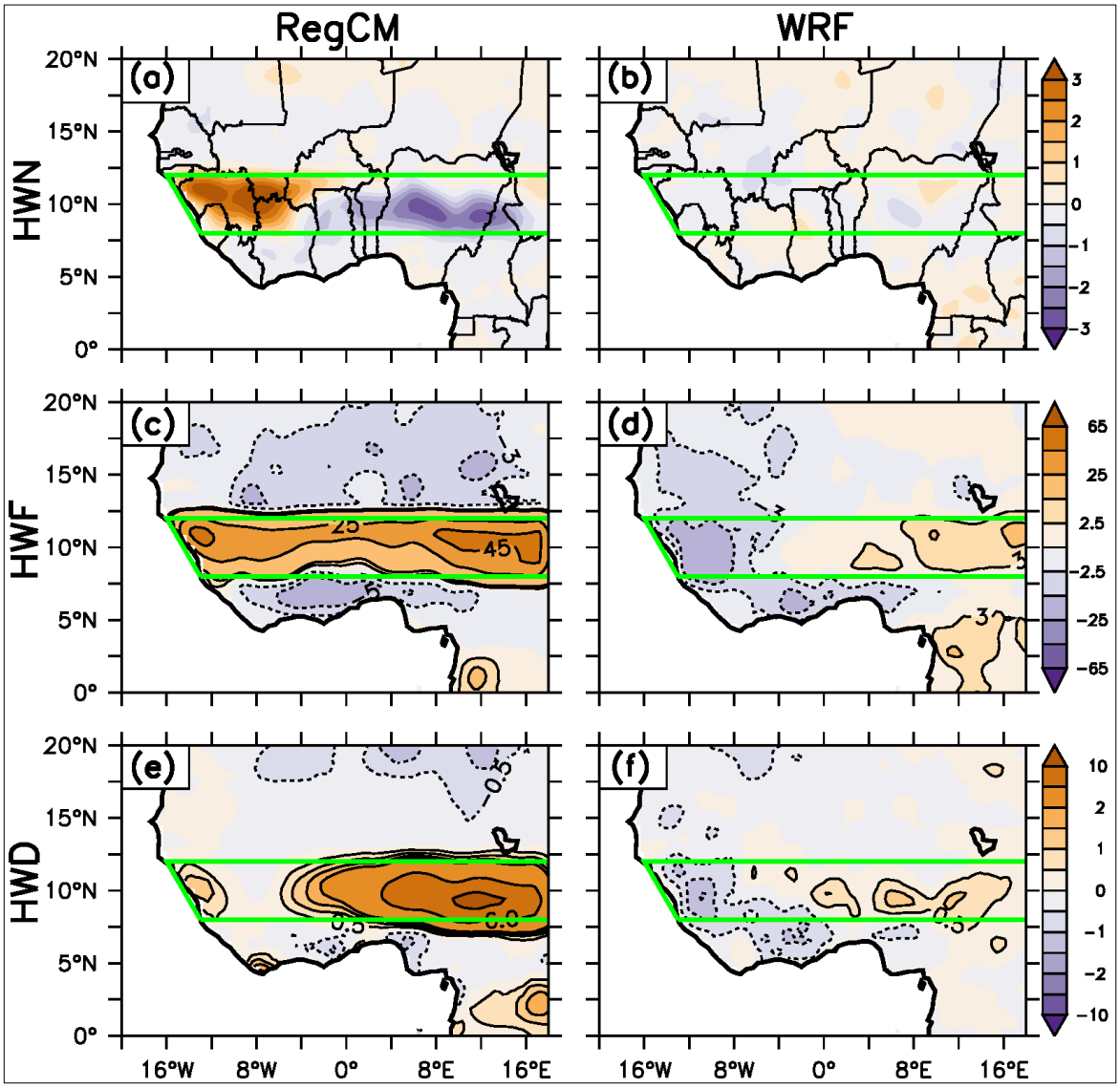

Figure 4.17: Potential impacts of forestation on the projected heatwave characteristics: heatwave number (HWN: event year^{-1}; a - b), heatwave days (HWF: day year^{-1}; c - d) and heatwave duration (HWD: days event^{-1}; e - f) with TXI

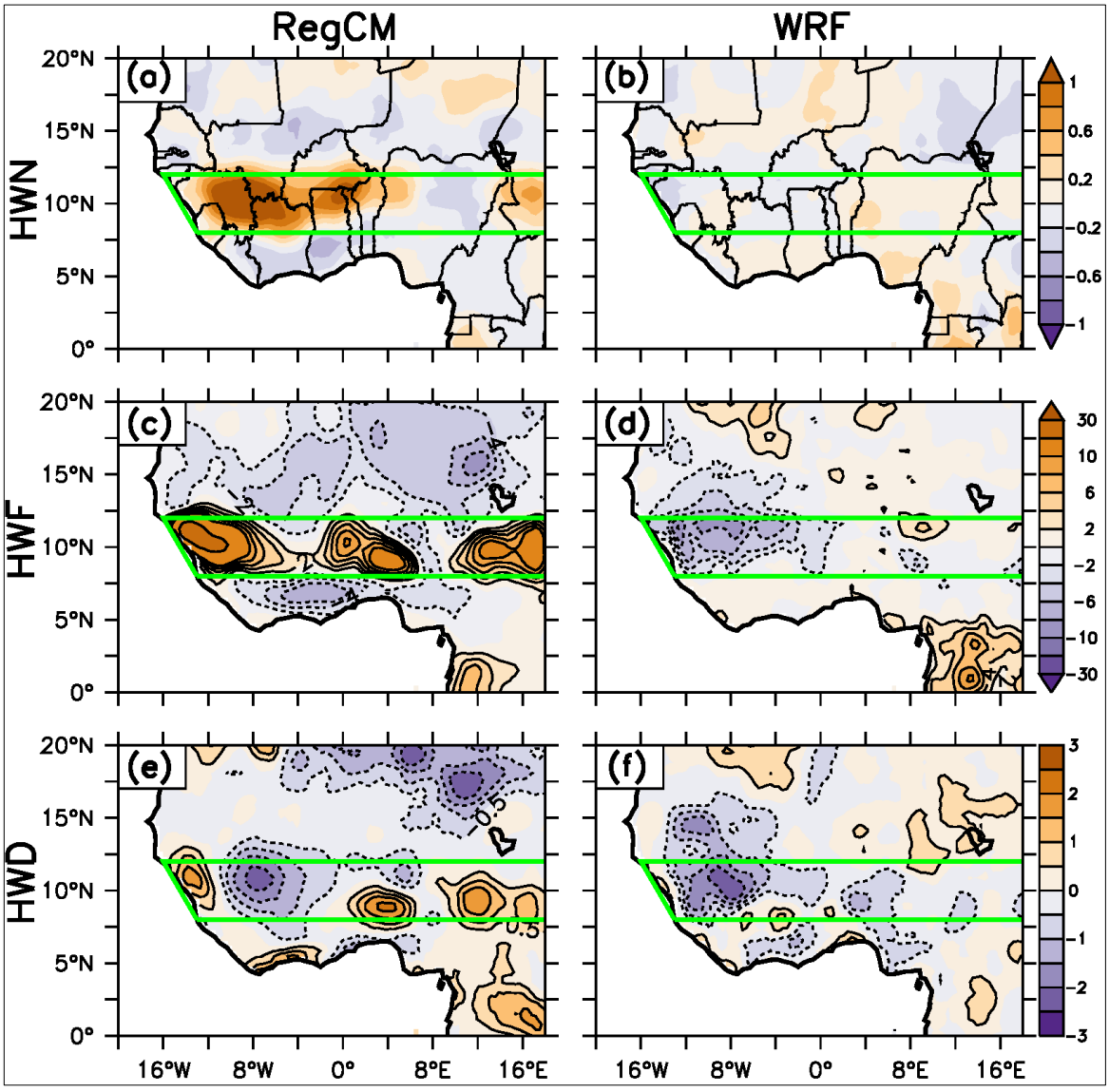

Figure 4.18: Potential impacts of forestation on the projected heatwave characteristics: heatwave number (HWN: event year^{-1}; a - b), heatwave days (HWF: day year^{-1}; c - d) and heatwave duration (HWD: days event^{-1}; e - f) with EHF

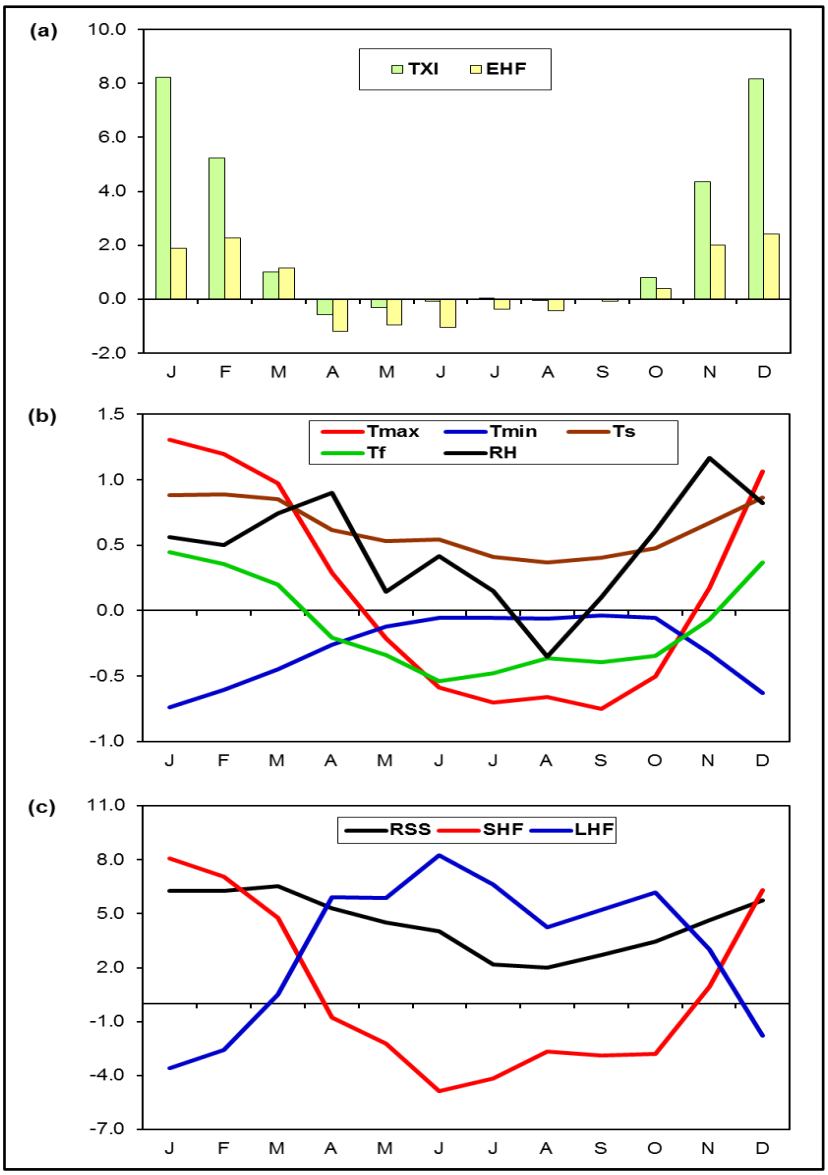

Figure 4.19: Projected future (2031-2064) changes (as simulated by RegCM) in the annual distribution of (a) heatwave days; (b) maximum and minimum temperatures (Tmax and Tmin respectively; °C), ground surface temperature (TS; °C), foliage canopy temperature (TF; °C) and relative humidity (RH; %); and (c) surface net shortwave energy flux (RSS; W m^{-2}), sensible heat flux (SHF; W m^{-2}) and latent heat flux (LHF; W m^{-2}) due to the impacts of forestation averaged over the forested zone (Savannah) in West Africa

CHAPTER FIVE

CONCLUSIONS AND RECOMMENDATIONS

5.1 CONCLUSIONS

This study has investigated extreme climate events, in the form of extreme rainfall and heatwaves, over West Africa and responses to global warming and changes in land surface conditions using simulations from RCMs. The study applies two RCMs (RegCM and WRF) forced with different GCMs in three numerical experiments simulating the present-day climate (1970-2004) and the future climate (2030-2064) with and without forestation (FRS and GHG). The simulations account for the potential impacts of forestation in the Savannah zone (8°N - 12°N) of West Africa. For each climate extreme (extreme rainfall and heatwave events), first the performance of the RCMs (using PRS experiment) is evaluated, and then the projected future changes (GHG minus PRS) are presented, before discussing the impacts of forestation (FRS minus GHG) on their respective characteristics.

The first research question was to investigate the capability of two regional climate models to simulate extreme climate events over West Africa. To achieve this, an extreme rainfall event was defined in this study as any grid point when the daily rainfall (greater than 0.5 mm) is greater than the extreme rainfall threshold (95^{th} percentile of daily rainfall) calculated at that point using all rainy days of the year during the present-day climate (PRS, 1971-2004). Also a Widespread Extreme Rainfall Event (WERE) is defined over three selected areas of the Savannah zone as a simultaneous occurrence of extreme rainfall events over at least 50% (*i.e.* 102 grid points) of each of the areas. This definition helped to

eliminate localised extreme events and retain those induced by synoptic scale features. Before assessing the future changes in extreme rainfall events, first the capability of the RCMs to reproduce the characteristics of extreme rainfall over West Africa for the present-day climate over West Africa was evaluated. The observation datasets used for the evaluation were daily rainfall data from the Global Precipitation Climatology Project (GPCP) and the Tropical Rainfall Measuring Mission (TRMM 3B42). To analyse heatwave characteristics, two different indices were considered to identify heatwaves over West Africa. The first index is the excess heat factor (EHF) while the second index (TXI) used the 90th percentile (TX90) of daily maximum temperature (Tmax). A heatwave event occurs in each case at any point when EHF > 0 (or Tmax > TX90) for at least three (3) consecutive days. For the evaluation of the RCMs in simulating heatwave characteristics over West Africa, maximum and minimum daily temperatures data from the Princeton University Global Meteorological Forcing Dataset for land surface modelling (PGFD) were used.

Both models provided realistic simulations of extreme rainfall thresholds (95^{th} percentile) over West Africa and WERE over Savannah, but with some biases. They generally overestimate the threshold of extreme rainfall, especially over coastal areas and highlands, and simulated WERE earlier than previously observed. Both RCM models gave realistic simulations of extreme temperature thresholds (T95 and TX90) over West Africa, but with some biases when compared to PGFD. They generally underestimate T95 and TX90 across the region, and poorly capture the spatial distribution of heatwave frequency, duration, and days over West Africa.

The second research question investigated the potential impacts of climate change and land cover change (forestation) on extreme rainfall events over West Africa. The models projected a future decrease in the frequency of extreme rainfall over the Savannah and Sahel zones, but an increase over the Guinea coast. In RegCM, the increase of extreme rainfall events over Savannah is associated with more frequent non-extreme rainfall events, but in WRF, it is due to less frequent wet days. Both RCMs projected that climate change would increase the frequency of WEREs over the Savannah in future. The study found that forestation would enhance the frequency and intensity of future extreme rainfall events over the forested area, but reduces them over the Guinea coast. It could also increase the frequency of WEREs over Savannah zones.

The third research question investigated the potential impacts of climate change and forestation on heatwave characteristics over West Africa. The research found that the models project increases in all heatwave characteristics over West Africa under RCP4.5, with high increase of heatwave days over the Sahel zone. This suggests a strong and consistent impact of climate change on heatwave characteristics over the region. However, the magnitude and location of the changes vary according to the heatwave index (EHF or TXI) and the RCM used. The difference in the results from both indices may arise from the fact that EHF considers both Tmax and Tmin to define heatwaves while TXI used only Tmax. RegCM simulates that, on average, forestation would increases the projected heatwave frequency, duration and days over most parts of the forested area but decreases them elsewhere. Moreover, the location and direction of the change depend on the heatwave indices used in the study. Finally, the WRF model does not show a consistent

impact of the forestation on heatwave characteristics, and the magnitude of the simulated impact is generally lower in WRF than in RegCM.

5.2 LIMITATIONS OF THE STUDY

In this study, the performance of two RCMs in simulating extreme climate events (extreme rainfall and heatwaves) characteristics was evaluated as well as their sensitivity to climate change and forestation. The results are model-dependant to some extent, but also depend on the definition of extreme events used (only for heatwaves). Although the RCMs show good ability in simulating some of the characteristics of extreme events over West Africa as in the observation data, they also struggle to resolve other inconsistencies. For instance, with extreme rainfall events, both models capture well the spatial distribution of extreme rainfall events frequency and seasonal distribution of WEREs, but struggle to represent the horizontal distribution of extreme rainfall thresholds over the study domain. The reasons are certainly linked to shortcomings in the RCMs. The disagreement among the observation datasets (TRMM and GPCP) also creates more uncertainty in the model evaluation. Additionally, with heatwaves, the RCMs reproduce very well the extreme temperature thresholds values over the West African domain as in the observation but fail to resolve other characteristics of heatwaves, such as heatwave number, days and duration for the present-day climate. If the discrepancy between models and observation derive mainly from shortcomings in the RCMs; it may also partly come from the nature of the observation data used. In fact, the PGFD is a hybrid observation reanalysis which is created with the combination of a set of global observation-based datasets with the NCEP-NCAR reanalysis. Subsequently, the PGFD might reproduce well the extreme temperature

thresholds but may not be able to sufficiently capture their spatial distribution over West Africa.

Another limitation of the present study is that it does not implement any statistical inference to test the significance of the impacts of climate change and forestation on the future characteristics of climate extremes. The reason for such limitation is that the study focuses more on the changes in extreme climate events' frequency rather than on the changes in intensity. Moreover, a statistically significant event might not be significant in terms of the impact it may have on human health, security and communities, while a statistically insignificant event may reveal itself to produce significant damages to humans and their surrounding environment.

5.3 RECOMMENDATIONS FOR FUTURE RESEARCH

For more robust conclusions, future studies can improve the results of this study in many ways. For instance, future studies on extreme rainfall events could include in their experiments more RCMs and forced each with different GCM simulations under different future climate scenarios, similar to CORDEX but with focus on the impacts of forestation in Africa. In addition, the discrepancy between the two models regarding the impacts of forestation on heatwave characteristics, which may be due to differences in the representation of land surface processes in the models, is a gap to be addressed by further studies. These studies could use a combination of more GCM and RCM simulations under various climate change scenarios. Since the magnitude of the impacts also depends on the indices used to characterise heatwaves, employing several heatwave definitions in

analysing results from the multi-ensemble, multi-model simulations could also help to quantify the uncertainties associated with the projected impacts and improve robustness of the results. These would provide insight into the conflicts between the two RCMs used in the present study and make the results more robust for policy makers. However, the results of the present study have shown that the use of forestation to mitigate global warming in West Africa could enhance the frequency and intensity of extreme rainfall events, make widespread extreme rainfall events more frequent and could further increase heatwave number, days and duration over the sub-continent. This may further escalate climate risks to human health and security. Hence, there is a need to further investigate the potential impacts of forestation on extreme climate and weather events before embarking on any large-scale forestation in West Africa.

REFERENCES

Abba Omar, S. (2014). Capability of CORDEX RCMs in simulating extreme rainfall events over Southern Africa. University of Cape Town. Retrieved from https://open.uct.ac.za/bitstream/item/9285/thesis_sci_2014_omar_sa.pdf?sequence=1

Abiodun, B. J., Abba Omar, S., Lennard, C., & Jack, C. (2016). Using regional climate models to simulate extreme rainfall events in the Western Cape, South Africa. International Journal of Climatology, 36(2): 689–705. doi:10.1002/joc.4376

Abiodun, B. J., Adeyewa, Z. D., Oguntunde, P. G., Salami, A. T., & Ajayi, V. O. (2012). Modeling the impacts of reforestation on future climate in West Africa. Theoretical and Applied Climatology, 110(1-2): 77–96. doi:10.1007/s00704-012-0614-1

Abiodun, B. J., Lawal, K. A., Salami, A. T., & Abatan, A. A. (2013). Potential influences of global warming on future climate and extreme events in Nigeria. Regional Environmental Change, 13: 477–491. doi:10.1007/s10113-012-0381-7

Abiodun, B. J., Pal, J. S., Afiesimama, E. A., Gutowski, W. J., & Adedoyin, A. (2008). Simulation of West African monsoon using RegCM3 Part II: impacts of deforestation and desertification. Theoretical and Applied Climatology, 93(3-4): 245–261. doi:10.1007/s00704-007-0333-1

Abiodun, B. J., Salami, A. T., Matthew, O. J., & Odedokun, S. (2012). Potential impacts of afforestation on climate change and extreme events in Nigeria. Climate Dynamics, 41(2): 277–293. doi:10.1007/s00382-012-1523-9

Afiesimama, E. A., Pal, J. S., Abiodun, B. J., Gutowski, W. J., & Adedoyin, A. (2006). Simulation of West African monsoon using the RegCM3. Part I: Model validation and

interannual variability. Theoretical and Applied Climatology, 86(1-4): 23–37. doi:10.1007/s00704-005-0202-8

Anderson, G. B., & Bell, M. L. (2011). Heat waves in the United States: Mortality risk during heat waves and effect modification by heat wave characteristics in 43 U.S. communities. Environmental Health Perspectives, 119(2): 210–218. doi:10.1289/ehp.1002313

AUC. (2006). The Green Wall for the Sahara Initiative: A Concept Note. Addis Ababa.

Basu, R., & Samet, J. M. (2002). Relation between Elevated Ambient Temperature and Mortality: A Review of the Epidemiologic Evidence. Epidemiologic Reviews, 24(2): 190–202. doi:10.1093/epirev/mxf007

Beniston, M., & Stephenson, D. B. (2004). Extreme climatic events and their evolution under changing climatic conditions. Global and Planetary Change, 44(1-4): 1–9. doi:10.1016/j.gloplacha.2004.06.001

Britannica Encyclopaedia. (2016). West African monsoon: Wind and rainfall patterns of the West African monsoon. In Encyclopaedia Britannica. Retrieved from http://www.britannica.com/science/West-African-monsoon/images-videos

Browne, N. A. K., & Sylla, M. B. (2012). Regional Climate Model Sensitivity to Domain Size for the Simulation of the West African Summer Monsoon Rainfall. International Journal of Geophysics, Cher. doi:10.1155/2012/625831

Browne, N. A. K., Sylla, M. B., Diallo, I., Sarr, A., Dosio, A., Diedhiou, A., Kamga, A., Lamptey, B., Ali, A., Gbobaniyi, E. O., Owusu, K., Lennard, C., Hewitson, B., Nikulin, G., Panitz, H.-J., & Büchner, M. (2015). Daily characteristics of West African summer monsoon precipitation in CORDEX simulations. Theoretical and

Applied Climatology, 1–18. doi:10.1007/s00704-014-1352-3

Charney, J. G. (1975). Dynamics of deserts and drought in the Sahel. Quarterly Journal of the Royal Meteorological Society, 101: 193–202.

Charney, J., Quirk, W. J., Chow, S.-H., & Kornfield, J. (1977). A Comparative Study of the Effects of Albedo Change on Drought in Semi-Arid Regions. Journal of the Atmospheric Sciences, 34: 1366–1385.

Chen, C.-S., Chen, Y.-L., Liu, C.-L., Lin, P.-L., & Chen, W.-C. (2007). Statistics of Heavy Rainfall Occurrences in Taiwan. Weather and Forecasting, 22(5): 981–1002. doi:10.1175/WAF1033.1

Chen, F., & Dudhia, J. (2001). Coupling an advanced land surface-hydrology model with the Penn State-NCAR MM5 modeling system. Part I: Model implementation and sensitivity. Monthly Weather Review, 129(4): 569–585. doi:http://dx.doi.org/10.1175/1520-0493(2001)129<0569:CAALSH>2.0.CO;2

Christensen, J. H., Hewitson, B., Busuioc, A., Chen, A., Gao, X., Held, I., Jones, R., Kolli, R. K., Kwon, W.-T., Laprise, R., Magaña Rueda, V., Mearns, L., Menéndez, C. G., Räisänen, J., Rinke, A., Sarr, A., & Whetton, P. (2007). Regional Climate Projections. In S. Solomon, D. Qin, M. Manning, Z. Chen, M. Marquis, K. B. Averyt, M. Tignor, & H. L. Miller (Eds.), Climate Change 2007: The Physical Science Basis. Contribution of Working Group I to the Fourth Assessment Report of the Intergovernmental Panel on Climate Change (Vol. 27, pp. 847–940). Cambridge: Cambridge University Press. doi:10.1080/07341510601092191

Chung, U., Gbegbelegbe, S., Shiferaw, B., Robertson, R., Yun, J. I., Tesfaye, K., Hoogenboom, G., & Sonder, K. (2014). Modeling the effect of a heat wave on maize

production in the USA and its implications on food security in the developing world. Weather and Climate Extremes, 5-6: 67–77. doi:10.1016/j.wace.2014.07.002

Ciais, P., Reichstein, M., Viovy, N., Granier, A., Ogée, J., Allard, V., Aubinet, M., Buchmann, N., Bernhofer, C., Carrara, A., Chevallier, F., De Noblet, N., Friend, a D., Friedlingstein, P., Grünwald, T., Heinesch, B., Keronen, P., Knohl, A., Krinner, G., Loustau, D., Manca, G., Matteucci, G., Miglietta, F., Ourcival, J. M., Papale, D., Pilegaard, K., Rambal, S., Seufert, G., Soussana, J. F., Sanz, M. J., Schulze, E. D., Vesala, T., & Valentini, R. (2005). Europe-wide reduction in primary productivity caused by the heat and drought in 2003. Nature, 437(7058): 529–533. doi:10.1038/nature03972

Coles, S. (2001). An introduction to statistical modeling of extreme values. Springer Series in Statistics. London: Springer Series in Statistics. doi:10.1007/978-1-4471-3675-0

Collins, W. J., Bellouin, N., Doutriaux-Boucher, M., Gedney, N., Halloran, P., Hinton, T., Hughes, J., Jones, C. D., Joshi, M., Liddicoat, S., Martin, G., O'Connor, F., Rae, J., Senior, C., Sitch, S., Totterdell, I., Wiltshire, A., & Woodward, S. (2011). Development and evaluation of an Earth-system model – HadGEM2. Geoscientific Model Development, 4: 1051–1075. doi:10.5194/gmd-4-1051-2011

Cook, K. H., & Vizy, E. K. (2012). Impact of climate change on mid-twenty-first century growing seasons in Africa. Climate Dynamics, 39(12): 2937–2955. doi:10.1007/s00382-012-1324-1

Cornforth, R. (2012). Overview of the West African Monsoon 2011. Weather, 67(3): 59–65. doi:10.1002/wea.1896

Diasso, U. J. (2015). Impacts of Climate Change and Reforestation on Droughts over West

Africa using Regional Climate Models. Federal University of Technology, Akure.

Dickinson, R. E., Henderson-Sellers, A., & Kennedy, P. J. (1993). Biosphere-atmosphere transfer scheme (BATS) version 1 as coupled to the NCAR Community Climate Model. NCAR Tech Note. Boulder, Colorado: National Centre for Atmospheric Research (NCAR).

Dole, R., Hoerling, M., Perlwitz, J., Eischeid, J., Pegion, P., Zhang, T., Quan, X.-W., Xu, T., & Murray, D. (2011). Was there a basis for anticipating the 2010 Russian heat wave? Geophysical Research Letters, 38(L06702). doi:10.1029/2010GL046582

Dudhia, J. (1989). Numerical study of convection observed during the winter monsoon experiment using a mesoscale two-dimensional model. Journal of the Atmospheric Sciences, 46(20): 3077–3107. doi:http://dx.doi.org/10.1175/1520-0469(1989)046<3077:NSOCOD>2.0.CO;2

Dyson, L. L. (2009). Heavy daily-rainfall characteristics over the gauteng province. Water SA, 35(5): 627–638. doi:10.4314/wsa.v35i5.49188

Easterling, D. R., Meehl, G. A., Parmesan, C., Changnon, S. a, Karl, T. R., & Mearns, L. O. (2000). Climate extremes: observations, modeling, and impacts. Science (New York, N.Y.), 289(5487): 2068–2074. doi:10.1126/science.289.5487.2068

Elguindi, N., Bi, X., Giorgi, F., Nagarajan, B., Pal, J., Solmon, F., Rauscher, S., Zakey, A., & Giuliani, G. (2011). Regional climatic model RegCM user manual version 4.1. Trieste: ITCP.

Emanuel, K. A. (1991). A Scheme for Representing Cumulus Convection in Large-Scale Models. Journal of the Atmospheric Sciences, 48(21): 2313–2329. doi:http://dx.doi.org/10.1175/1520-0469(1991)048<2313:ASFRCC>2.0.CO;2

Enger, L., & Tjernstrom, M. (1991). Estimating the Effetcs on the Regional Precipitation Climate in a Semiarid Region Caused by an Artificial Lake Using a Mesoscale Model. Journal of Applied Meteorology, 30: 227–250.

FAO. (2009). FAO's Role in the Burkina Faso Flash Appeal 2009. Food and Agriculture Organization of the United Nations (FAO).

Fontaine, B., Trzaska, S., & Janicot, S. (1998). Evolution of the relationship between near global and Atlantic SST modes and the rainy season in West Africa: statistical analyses and sensitivity experiments. Climate Dynamics, 14(5): 353–368. doi:Article

Fragoso, M., & Tildes Gomes, P. (2008). Classification of daily abundant rainfall patterns and associated large-scale atmospheric circulation types in Southern Portugal. International Journal of Climatology, 28: 537–544. doi:10.1002/joc.1564

Frich, P., Alexander, L. V., Della-Marta, P., Gleason, B., Haylock, M., Tank Klein, A., & Peterson, T. (2002). Observed coherent changes in climatic extremes during the second half of the twentieth century. Climate Research, 19(3): 193–212. doi:10.3354/cr019193

Galiano, S. G. G., & Osorio, J. D. G. (2011). Non stationary analysis of spatial patterns of extreme rainfall events trends in West Africa. In Hydro-climatology: Variability and Change (pp. 75–81). Melbourne.

García-Herrera, R., Díaz, J., Trigo, R. M., Luterbacher, J., & Fischer, E. M. (2010). A Review of the European Summer Heat Wave of 2003. Critical Reviews in Environmental Science and Technology, 40(4): 267–306. doi:10.1080/10643380802238137

Giorgetta, M. A., Jungclaus, J., Reick, C. H., Legutke, S., Bader, J., Böttinger, M., Brovkin,

V., Crueger, T., Esch, M., Fieg, K., Glushak, K., Gayler, V., Haak, H., Hollweg, H.-D., Ilyina, T., Kinne, S., Kornblueh, L., Matei, D., Mauritsen, T., Mikolajewicz, U., Mueller, W., Notz, D., Pithan, F., Raddatz, T., Rast, S., Redler, R., Roeckner, E., Schmidt, H., Schnur, R., Segschneider, J., Six, K. D., Stockhause, M., Timmreck, C., Wegner, J., Widmann, H., Wieners, K.-H., Claussen, M., Marotzke, J., & Stevens, B. (2013). Climate and carbon cycle changes from 1850 to 2100 in MPI-ESM simulations for the Coupled Model Intercomparison Project phase 5. Journal of Advances in Modeling Earth Systems, 5(3): 572–597. doi:10.1002/jame.20038

Giorgetta, M. A., Roeckner, E., Mauritsen, T., Bader, J., Crueger, T., Esch, M., Rast, S., Kornblueh, L., Schmidt, H., Kinne, S., Hohenegger, C., Möbis, B., Krismer, T., Wieners, K.-H., & Stevens, B. (2013). The atmospheric general circulation model ECHAM6: Model description. (Max-Planck-Institut für Meteorologie, Ed.)Reports on Earth System Science. Hamburg: Max-Planck-Institut für Meteorologie.

Giorgi, F., Coppola, E., Solmon, F., Mariotti, L., Sylla, M., Bi, X., Elguindi, N., Diro, G., Nair, V., Giuliani, G., Turuncoglu, U., Cozzini, S., Güttler, I., O'Brien, T., Tawfik, A., Shalaby, A., Zakey, A., Steiner, A., Stordal, F., Sloan, L., & Brankovic, C. (2012). RegCM4: model description and preliminary tests over multiple CORDEX domains. Climate Research, 52: 7–29. doi:10.3354/cr01018

Giorgi, F., Jones, C., & Asrar, G. R. (2009). Addressing climate information needs at the regional level: the CORDEX framework. Bulletin - World Meteorological Organization, 58(3): 175–183.

Groisman, P. Y., Knight, R. W., & Karl, T. R. (2001). Heavy precipitation and high streamflow in the contiguous United States: Trends in the twentieth century. Bulletin

of the American Meteorological Society, 82: 219–246. doi:10.1175/1520-0477(2001)082<0219:HPAHSI>2.3.CO;2

Guy, B. N. (2012). Regional Analysis of Convective Systems during the West African Monsoon. Colorado State University.

Hémon, D., Jougla, E., Clavel, J., Laurent, F., Bellec, S., & Pavillon, G. (2003). Surmortalité liée à la canicule d'Août 2003 en France. BEH, 45-46(221): 225.

Holtslag, A. A. M., De Bruijn, E. I. F., & Pan, H.-L. (1990). A high resolution air mass transformation model for short-range weather forecasting. Monthly Weather Review, 118(8): 1561–1575. doi:http://dx.doi.org/10.1175/1520-0493(1990)118<1561:AHRAMT>2.0.CO;2

Hong, S.-Y., Dudhia, J., & Chen, S.-H. (2004). A Revised Approach to Ice Microphysical Processes for the Bulk Parameterization of Clouds and Precipitation. Monthly Weather Review, 132(1): 103–120. doi:http://dx.doi.org/10.1175/1520-0493(2004)132<0103:ARATIM>2.0.CO;2

Hong, S.-Y., Noh, Y., & Dudhia, J. (2006). A New Vertical Diffusion Package with an Explicit Treatment of Entrainment Processes. Monthly Weather Review, 134(9): 2318–2341. doi:http://dx.doi.org/10.1175/MWR3199.1

Hounkpè, J., Diekkrüger, B., Badou, D., & Afouda, A. (2015). Non-Stationary Flood Frequency Analysis in the Ouémé River Basin, Benin Republic. Hydrology, 2(4): 210–229. doi:10.3390/hydrology2040210

Houze, R. A., Smull, B. F., & Dodge, P. (1990). Mesoscale Organization of Springtime Rainstorms in Oklahoma. Monthly Weather Review. doi:10.1175/1520-0493(1990)118<0613:MOOSRI>2.0.CO;2

Huffman, G. J., Adler, R. F., Bolvin, D. T., Gu, G., Nelkin, E. J., Bowman, K. P., Hong, Y., Stocker, E. F., & Wolff, D. B. (2007). The TRMM Multisatellite Precipitation Analysis (TMPA): Quasi-global, multiyear, combined-sensor precipitation estimates at fine scales. Journal of Hydrometeorology, 8(1): 38–55. doi:http://dx.doi.org/10.1175/JHM560.1

Huffman, G. J., Adler, R. F., Morrissey, M. M., Bolvin, D. T., Curtis, S., Joyce, R., McGavock, B., & Susskind, J. (2001). Global Precipitation at One-Degree Daily Resolution from Multisatellite Observations. Journal of Hydrometeorology, 2(1): 36–50. doi:http://dx.doi.org/10.1175/1525-7541(2001)002<0036:GPAODD>2.0.CO;2

IFRC. (2014). World Disasters Report: Focus on culture and risk. Geneva: International Federation of Red Cross and Red Crescent Societies.

Ilyina, T., Six, K., Segschneider, J., Maier-Reimer, E., Li, H., & Núñez-Riboni, I. N. (2013). Global ocean biogeochemistry model HAMOCC: Model architecture and performance as component of the MPI-Earth System Model in different CMIP5 experimental realizations. Journal of Advances in Modeling Earth Systems, 5(2): 287–315. doi:10.1029/2012MS000178

IPCC. (2001). Climate Change 2001. The IPCC Third Assessment Report. Volumes I (Science), II (Impacts and Adaptation) and III (Mitigation Strategies). Cambridge: Cambridge University Press.

IPCC. (2007). Climate change 2007: mitigation of climate change. (L. A. Metz, O. R. Davidson, P. R. Bosch, R. Dave, & L. A. Meyer, Eds.). CambridgePress: Cambridge University Press.

IPCC. (2013). Climate Change 2013: The Physical Science Basis. Contribution of Working

Group I to the Fifth Assessment Report of the Intergovernmental Panel on Climate Change. (T. F. Stocker, D. Qin, G.-K. Plattner, M. Tignor, S. K. Allen, J. Boschung, A. Nauels, Y. Xia, V. Bex, & P. M. Midgley, Eds.). Cambridge University Press, Cambridge, United Kingdom and New York, NY, USA. doi:10.1029/2000JD000115

IPCC. (2014). Climate Change 2014: Impacts, Adaptation, and Vulnerability. Part A: Global and Sectoral Aspects. Contribution of Working Group II to the Fifth Assessment Report of the Intergovernmental Panel on Climate Change. (L. L. Field, C.B., Barros, V.R., Dokken, D.J., Mach, K.J., Mastrandrea, M.D., Bilir, T.E., Chatterjee, M., Ebi, K.L., Estrada, Y.O., Genova, R.C., Girma, B., Kissel, E.S., Levy, A.N., MacCracken, S., Mastrandrea, P.R., White, Ed.). Cambridge University Press, Cambridge, United Kingdom and New York, NY, USA,.

Jenkins, G. S., Gaye, A. T., & Sylla, B. (2005). Late 20th century attribution of drying trends in the Sahel from the Regional Climate Model (RegCM3). Geophysical Research Letters, 32(22): -. doi:10.1029/2005GL024225

Jones, C. D., Hughes, J. K., Bellouin, N., Hardiman, S. C., Jones, G. S., Knight, J., Liddicoat, S., O'Connor, F. M., Andres, R. J., Bell, C., Boo, K.-O., Bozzo, a., Butchart, N., Cadule, P., Corbin, K. D., Doutriaux-Boucher, M., Friedlingstein, P., Gornall, J., Gray, L., Halloran, P. R., Hurtt, G., Ingram, W., Lamarque, J.-F., Law, R. M., Meinshausen, M., Osprey, S., Palin, E. J., Parsons Chini, L., Raddatz, T., Sanderson, M., Sellar, a. a., Schurer, a., Valdes, P., Wood, N., Woodward, S., Yoshioka, M., & Zerroukat, M. (2011). The HadGEM2-ES implementation of CMIP5 centennial simulations. Geoscientific Model Development Discussions, 4(1): 689–763. doi:10.5194/gmdd-4-689-2011

Jungclaus, J. H., Fischer, N., Haak, H., Lohmann, K., Marotzke, J., Matei, D., Mikolajewicz, U., Notz, D. S., & von Storch, J. (2013). Characteristics of the ocean simulations in MPIOM, the ocean component of the MPI-Earth System Model. Journal of Advances in Modeling Earth Systems, 5(2): 422–446. doi:10.1002/jame.20023

Kain, J. (2004). The Kain-Fritsch convective parameterization: An update. Journal of Applied Meteorology and Climatology, 43(1): 170–181. doi:http://dx.doi.org/10.1175/1520-0450(2004)043<0170:TKCPAU>2.0.CO;2

Kalkstein, L. S., & Davis, R. E. (1989). Weather and human mortality: An evaluation of demographic and inter-regional responses in the U.S. Ann. Assoc. Amer. Geogr., 79, 4–64. Karl, T. R., H. F. Diaz, and G. Kukla, 1988: Urbanization: Its detection and effect in the United States climate record. Journal of Climate, 1: 1099–1123.

Keggenhoff, I., Elizbarashvili, M., & King, L. (2015). Heat Wave Events over Georgia Since 1961: Climatology, Changes and Severity. Climate, 3(2): 308–328. doi:10.3390/cli3020308

Kiehl, J. T., Hack, J. J., Bonan, G. B., Boville, B. A., Breigleb, B. P., Williamson, D. L., & Rasch, P. J. (1996). Description of the NCAR community climate Model (CCM3). NCAR Tech Note (Vol. NCAR0TN-42). Boulder, Colorado: National Centre for Atmospheric Research.

Klein Tank, A. M. G., Zwiers, F. W., & Zhang, X. (2009). Guidelines on Analysis of Extremes in a Changing Climate in Support of Informed Decisions for Adaptation. WMO-TD no. 1500, WCDMP no.72. Geneva, Switzerland.

Laing, A. G., Fritsch, J. M., & Negri, A. J. (1999). Contribution of Mesoscale Convective

Complexes to Rainfall in Sahelian Africa: Estimates from Geostationary Infrared and Passive Microwave Data. Journal of Applied Meteorology, 38(7): 957–964. doi:10.1175/1520-0450(1999)038<0957:COMCCT>2.0.CO;2

Lanning, S. B., Siebenmorgen, T. J., Counce, P. A., Ambardekar, A. A., & Mauromoustakos, A. (2011). Extreme nighttime air temperatures in 2010 impact rice chalkiness and milling quality. Field Crops Research, 124(1): 132–136. doi:10.1016/j.fcr.2011.06.012

Laurent, H., D'Amato, N., & Lebel, T. (1998). How important is the contribution of the mesoscale convective complexes to the Sahelian rainfall? Physics and Chemistry of the Earth, 23(5-6): 629–633. doi:10.1016/S0079-1946(98)00099-8

Lenton, T. M., & Vaughan, N. E. (2009). The radiative forcing potential of different climate geoengineering options. Atmospheric Chemistry and Physics Discussions, 9(1): 2559–2608. Retrieved from http://www.atmos-chem-phys-discuss.net/9/2559/2009/

Mapa, R. B. (1995). Effect of Reforestation Using Tectona-Grandis on Infiltration and Soil-Water Retention. Forest Ecology and Management, 77(1-3): 119–125. doi:10.1016/0378-1127(95)03573-S

Martin, G. M., Bellouin, N., Collins, W. J., Culverwell, I. D., Halloran, P. R., Hardiman, S. C., Hinton, T. J., Jones, C. D., McDonald, R. E., McLaren, A. J., O'Connor, F. M., Roberts, M. J., Rodriguez, J. M., Woodward, S., Best, M. J., Brooks, M. E., Brown, A. R., Butchart, N., Dearden, C., Derbyshire, S. H., Dharssi, I., Doutriaux-Boucher, M., Edwards, J. M., Falloon, P. D., Gedney, N., Gray, L. J., Hewitt, H. T., Hobson, M., Huddleston, M. R., Hughes, J., Ineson, S., Ingram, W. J., James, P. M., Johns, T. C.,

Johnson, C. E., Jones, A., Jones, C. P., Joshi, M. M., Keen, A. B., Liddicoat, S., Lock, a. P., Maidens, a. V., Manners, J. C., Milton, S. F., Rae, J. G. L., Ridley, J. K., Sellar, A., Senior, C. A., Totterdell, I. J., Verhoef, A., Vidale, P. L., & Wiltshire, A. (2011). The HadGEM2 family of Met Office Unified Model climate configurations. Geoscientific Model Development, 4(3): 723–757. doi:10.5194/gmd-4-723-2011

Mathon, V., Laurent, H., & Lebel, T. (2002). Mesoscale Convective System Rainfall in the Sahel. Journal of Applied Meteorology, 41(11): 1081–1092. doi:10.1175/1520-0450(2002)041<1081:MCSRIT>2.0.CO;2

Mlawer, E., Taubman, S., Brown, P., Iacono, M., & Clough, S. (1997). Radiative transfer for inhomogeneous atmosphere: RRTM, a validated correlated-k model for the longwave. Journal of Geophysical Research, 102(D14): 16663–16682. doi:10.1029/97JD00237

Moufouma-Okia, W., & Rowell, D. P. (2010). Impact of soil moisture initialisation and lateral boundary conditions on regional climate model simulations of the West African monsoon. Climate Dynamics, 35: 213–229. doi:10.1007/s00382-009-0638-0

Mouhamed, L., Traore, S. B., Alhassane, A., & Sarr, B. (2013). Evolution of some observed climate extremes in the West African Sahel. Weather and Climate Extremes, 1: 19–25. doi:10.1016/j.wace.2013.07.005

Mounkaila Saley, M. (2015). Impacts of Climate Change and Reforestation on Rainfall Onset and Cessation over West Africa using Regional Climate Models. Federal University of Technology, Akure.

Naik, M., & Abiodun, B. J. (2016). Potential impact of forestation on the future climate change on Southern Africa. International Journal of Climatology.

doi:10.1002/joc.4652

Nairn, J., & Fawcett, R. (2013). Defining heatwaves : heatwave defined as a heat- impact event servicing all community and business sectors in Australia. CAWCR technical report.

Nairn, J., & Fawcett, R. (2015). The Excess Heat Factor: A Metric for Heatwave Intensity and Its Use in Classifying Heatwave Severity. International Journal of Environmental Research and Public Health, 12: 227–253. doi:10.3390/ijerph120100227

National Academy of Sciences. (1992). Policy Implications of Greenhouse Warming: Mitigation, Adaptation, and the Science Base Panel. Public Policy. Retrieved from http://www.nap.edu/openbook.php?isbn=0309043867

Nicholson, S. E., & Grist, J. P. (2001). A Conceptual Model for Understanding Rainfall Variability in the West African Sahel on interannual and interdecadal timescales. International Journal of Climatology, 21(14): 1733–1758.

Omotosho, J. B. (1985). The separate contributions of line squalls, thunderstorms and the monsoon to the total rainfall in nigeria. Journal of Climatology, 5(5): 543–552. doi:10.1002/joc.3370050507

Paeth, H., Fink, A. H., Pohle, S., Keis, F., Mächel, H., & Samimi, C. (2011). Meteorological characteristics and potential causes of the 2007 flood in sub-Saharan Africa. International Journal of Climatology, 31(13): 1908–1926. doi:10.1002/joc.2199

Pal, J. S., Giorgi, F., Bi, X., Elguindi, N., Solmon, F., Rauscher, S. A., Gao, X., R., F., Zakey, A., Winter, J., Ashfaq, M., Syed, F. S., Sloan, L. C., Bell, J. L., Diffenbaugh, N. S., Karmacharya, J., Konare, A., Martinez, D., da Rocha, R. P., & Steiner, A. L.

(2007). Regional Climate Modeling for the Developing World: The ICTP RegCM3 and RegCNET. Bulletin of the American Meteorological Society, 88(9): 1395–1409. doi:http://dx.doi.org/10.1175/BAMS-88-9-1395

Pal, J. S., Small, E. E., & Eltahir, E. A. B. (2000). Simulation of regional scale water and energy budgets: representation of subgrid cloud and precipitation processes within RegCM. Journal of Geophysical Research, 105(D24): 29579–29594. doi:10.1029/2000JD900415

Panthou, G., Vischel, T., Lebel, T., Blanchet, J., Quantin, G., & Ali, A. (2012). Extreme rainfall in West Africa: A regional modeling. Water Resources Research, 48(8): n/a–n/a. doi:10.1029/2012WR012052

Patricola, C. M., & Cook, K. H. (2010). Northern African climate at the end of the twenty-first century: an integrated application of regional and global climate models. Climate Dynamics, 35: 193–212. doi:10.1007/s00382-009-0623-7

Perkins, S. E., Alexander, L. V., & Nairn, J. R. (2012). Increasing frequency, intensity and duration of observed global heatwaves and warm spells. Geophysical Research Letters, 39(20): n/a–n/a. doi:10.1029/2012GL053361

Peter, M., & Tetzlaff, G. (1988). The structure of West African squall lines and their environmental moisture budget. Meteorol Atmos Phys, 39: 74–84.

Rafferty, J. P. (2015). India-Pakistan heat wave of 2015 | Britannica.com. Encyclopaedia Britannica. Retrieved 5 December 2015, from http://global.britannica.com/event/India-Pakistan-heat-wave-of-2015

Reick, C. H., Raddatz, T., Brovkin, V., & Gayler, V. (2013). The representation of natural and anthropogenic land cover change in MPI-ESM. Journal of Advances in Modeling

Earth Systems, 5(3): 459–482. doi:10.1002/jame.20022

Russo, S., Dosio, A., Graversen, R. G., Sillmann, J., Carrao, H., Dunbar, M. B., Singleton, A., Montagna, P., Barbola, P., & Vogt, J. V. (2014). Magnitude of extreme heat waves in present climate and their projection in a warming world. Journal of Geophysical Research: Atmospheres, 119: 12500–12512. doi:10.1002/2014JD022098

Scheer, D., & Renn, O. (2014). Public Perception of geoengineering and its consequences for public debate. Climatic Change, 125: 305–318. doi:10.1007/s10584-014-1177-1

Schneck, R., Reick, C. H., & Raddatz, T. (2013). The land contribution to natural CO2 variability on time scales of centuries. Journal of Advances in Modeling Earth Systems2, 5(2): 354–365. doi:10.1002/jame.20029

Sheffield, J., Goteti, G., & Wood, E. F. (2006). Development of a 50-year high-resolution global dataset of meteorological forcings for land surface modeling. Journal of Climate, 19(13): 3088–3111. doi:10.1175/JCLI3790.1

Skamarock, W. C., & Klemp, J. B. (2008). A time-split nonhydrostatic atmospheric model for weather research and forecasting applications. Journal of Computational Physics, 227: 3465–3485. doi:10.1016/j.jcp.2007.01.037

Skamarock, W. C., Klemp, J. B., Dudhia, J., Gill, D. O., Barker, D. M., Duda, M. G., Huang, X.-Y., Wang, W., & Powers, J. G. (2008). A Description of the Advanced Research WRF Version 3. (National Centre for Atmospheric Research (NCAR), Ed.)NCAR Tech Note (Vol. TN-475+STR). Boulder, Colorado.

Stephenson, D. B. (2008). Definition, diagnosis and origin of extreme weather and climate events. Climate Extremes and Society, 340. doi:10.1017/CBO9780511535840.003

Stevens, B., Giorgetta, M., Esch, M., Mauritsen, T., Crueger, T., Rast, S., Salzmann, M.,

Schmidt, H., Bader, J., Block, K., Brokopf, R., Fast, I., Kinne, S., Kornblueh, L., Lohmann, U., Pincus, R., Reichler, T., & Roeckner, E. (2013). Atmospheric component of the MPI-M Earth System Model: ECHAM6. Journal of Advances in Modeling Earth Systems, 5(2): 146–172. doi:10.1002/jame.20015

Sylla, M. B., Diallo, I., & Pal, J. S. (2013). West African Monsoon in State-of-the-Science Regional Climate Models. Climate Variability - Regional and Thematic Patterns, 3–36. doi:http://dx.doi.org/10.5772/55140

Sylla, M. B., Gaye, a. T., & Jenkins, G. S. (2012). On the Fine-Scale Topography Regulating Changes in Atmospheric Hydrological Cycle and Extreme Rainfall over West Africa in a Regional Climate Model Projections. International Journal of Geophysics, 2012: 1–15. doi:10.1155/2012/981649

Sylla, M. B., Gaye, A. T., Pal, J. S., Jenkins, G. S., & Bi, X. Q. (2009). High-resolution simulations of west African climate using regional climate model (RegCM3) with different lateral boundary conditions. Theoretical and Applied Climatology, 98: 293–314.

Sylla, M. B., Giorgi, F., Coppola, E., & Mariotti, L. (2013). Uncertainties in daily rainfall over Africa: assessment of gridded observation products and evaluation of a regional climate model simulation. International Journal of Climatology, 33(7): 1805–1817. doi:DOI: 10.1002/joc.3551

The Royal Society. (2009). Geoengineering the climate: Science, governance, and uncertainty. Design (Vol. 12). London: Royal Society Press. Retrieved from https://royalsociety.org/~/media/Royal_Society_Content/policy/publications/2009/8693.pdf

Thompson, M. P., Adams, D., & Sessions, J. (2009). Radiative forcing and the optimal rotation age. Ecological Economics, 68(10): 2713–2720.

Thomson, A. M., Calvin, K. V., Smith, S. J., Kyle, G. P., Volke, A., Patel, P., Delgado-Arias, S., Bond-Lamberty, B., Wise, M. A., Clarke, L. E., & Edmonds, J. A. (2011). RCP4.5: A pathway for stabilization of radiative forcing by 2100. Climatic Change, 109(1): 77–94. doi:10.1007/s10584-011-0151-4

Trail, M., Tsimpidi, A. P., Liu, P., Tsigaridis, K., Hu, Y., Nenes, A., Stone, B., & Russell, A. G. (2013). Potential impact of land use change on future regional climate in the Southeastern U.S.: Reforestation and crop land conversion. Journal of Geophysical Research: Atmospheres, 118(20): 11,577–11,588. doi:10.1002/2013JD020356

Tschakert, P., Sagoe, R., Ofori-Darko, G., & Codjoe, S. N. (2010). Floods in the Sahel: An analysis of anomalies, memory, and anticipatory learning. Climatic Change, 103(3): 471–502. doi:10.1007/s10584-009-9776-y

Vizy, E. K., & Cook, K. H. (2012). Mid-Twenty-First-Century Changes in Extreme Events over Northern and Tropical Africa. Journal of Climate, 25(17): 5748–5767. doi:10.1175/JCLI-D-11-00693.1

Wang, G., & Eltahir, E. A. B. (2000). Ecosystem dynamics and the Sahel drought. Geophysical Research Letters, 27(6): 795–798. doi:10.1029/1999GL011089

WMO. (2013). The global climate 2001-2010: A decade of climate extremes. Summary report. WMO-No. 1119, World Meteorological Organization (WMO), Geneva, Switzerland. Retrieved from http://www.unep.org/pdf/wmo_report.pdf

WMO. (2014). Atlas of Mortality and Economic Losses from Weather, Climate and Water Extremes 1970-2012. doi:ISBN 978-92-63-11123-4

Xue, Y., & Shukla, J. (1993). The Influence of Land Surface Properties on Sahel Climate. Part I: Desertification. Journal of Climate, 6: 2232–2245.

Zhang, X., Alexander, L., Hegerl, G. C., Jones, P., Tank, A. K., Peterson, T. C., Trewin, B., & Zwiers, F. W. (2011). Indices for monitoring changes in extremes based on daily temperature and precipitation data. Wiley Interdisciplinary Reviews Climate Change, 2(6): 851–870. doi:10.1002/wcc.147

Zheng, X., & Eltahir, E. A. B. (1997). The response to deforestation and desertification in a model of West African monsoons. Geophysical Research Letters, 24(2): 155–158.

Zwiers, F. W., Alexander, L. V, Hegerl, G. C., Knutson, T. R., Kossin, J. P., Naveau, P., Nicholls, N., Schär, C., Seneviratne, S. I., & Zhang, X. (2013). Climate Extremes: Challenges in Estimating and Understanding Recent Changes in the Frequency and Intensity of Extreme Climate and Weather Events (pp. 339–389). doi:10.1007/978-94-007-6692-1

Zwiers, F. W., & Kharin, V. V. (1998). Changes in the Extremes of the Climate Simulated by CCC GCM2 under CO2 Doubling. Journal of Climate, 11(9): 2200–2222. doi:10.1175/1520-0442(1998)011<2200:CITEOT>2.0.CO;2

APPENDICES

APPENDIX A: ETCCDI INDICES

The definitions for a core set of 27 descriptive indices of extremes defined by the Joint CCl/CLIVAR/JCOMM Expert Team on Climate Change Detection and Indices (ETCCDI, http //etccdi.pacificclimate.org/list_27_indices.shtml) are provided below.

Temperature indices:

1. FD, frost days count of days where TN (daily minimum temperature) < 0°C Let TNij be the daily minimum temperature on day i in period j. Count the number of days where TNij < 0°C.

2. SU, summer days count of days where TX (daily maximum temperature) > 25°C Let TXij be the daily maximum temperature on day i in period j. Count the number of days where TXij > 25°C.

3. ID, icing days count of days where TX < 0°C Let TXij be the daily maximum temperature on day i in period j. Count the number of days where TXij < 0°C.

4. TR, tropical nights count of days where TN > 20°C Let TNij be the daily minimum temperature on day i in period j. Count the number of days where TNij > 20°C.

5. GSL, growing season length annual count of days between first span of at least six days where TG (daily mean temperature) > 5°C and first span in second half of the year of at least six days where TG < 5°C.

Let TGij be the daily mean temperature on day i in period j. Count the annual (1 Jan to 31 Dec in Northern Hemisphere, 1 July to 30 June in Southern Hemisphere) number of days between the first occurrence of at least six consecutive days where TGij > 5°C and the first occurrence after 1 July (1 Jan in Southern Hemisphere) of at least six consecutive days where TGij < 5°C.

6. TXx monthly maximum value of daily maximum temperature:

Let TXik be the daily maximum temperature on day i in month k. The maximum daily maximum temperature is then TXx = max (TXik).

7. TNx monthly maximum value of daily minimum temperature

Let TNik be the daily minimum temperature on day i in month k. The maximum daily minimum temperature is then TNx = max (TNik).

8. TXn monthly minimum value of daily maximum temperature

Let TXik be the daily maximum temperature on day i in month k. The minimum daily maximum temperature is then TXn = min (TXik).

9. TNn monthly minimum value of daily minimum temperature

Let TNik be the daily minimum temperature on day i in month k. The minimum daily minimum temperature is then TNn = min (TNik).

10. TN10p, cold nights count of days where TN < 10th percentile

Let TNij be the daily minimum temperature on day i in period j and let TNin10 be the calendar day 10^{th} percentile of daily minimum temperature calculated for a five-day window centred on each calendar day in the base period n (1961-1990). Count the number of days where TNij < TNin10.

11. TX10p, cold day-times count of days where TX < 10th percentile

Let TXij be the daily maximum temperature on day i in period j and let TXin10 be the calendar day 10^{th} percentile of daily maximum temperature calculated for a five-day window centred on each calendar day in the base period n (1961-1990). Count the number of days where TXij < TXin10.

12. TN90p, warm nights count of days where TN > 90th percentile

Let TNij be the daily minimum temperature on day i in period j and let TNin90 be the calendar day 90^{th} percentile of daily minimum temperature calculated for a five-day

window centred on each calendar day in the base period n (1961-1990). Count the number of days where TNij > TNin90.

13. TX90p, warm day-times count of days where TX > 90th percentile

Let TXij be the daily maximum temperature on day i in period j and let TXin90 be the calendar day 90^{th} percentile of daily maximum temperature calculated for a five-day window centred on each calendar day in the base period n (1961-1990). Count the number of days where TXij > TXin90.

14. WSDI, warm spell duration index count of days in a span of at least six days where TX > 90^{th} percentile

Let TXij be the daily maximum temperature on day i in period j and let TXin90 be the calendar day 90^{th} percentile of daily maximum temperature calculated for a five-day window centred on each calendar day in the base period n (1961-1990). Count the number of days where, in intervals of at least six consecutive days TXij > TXin90.

15. CSDI, cold spell duration index count of days in a span of at least six days where TN > 10^{th} percentile

Let TNij be the daily minimum temperature on day i in period j and let TNin10 be the calendar day 10^{th} percentile of daily minimum temperature calculated for a five-day window centred on each calendar day in the base period n (1961-1990). Count the number of days where, in intervals of at least six consecutive days TNij < TNin10.

16. DTR, diurnal temperature range mean difference between TX and TN (°C)

Let TXij and TNij be the daily maximum and minimum temperature on day i in period j. If I represents the total number of days in j then the mean diurnal temperature range in period j DTRj = sum (TXij - TNij) / I.

Precipitation indices:

17. RX1day, maximum one-day precipitation highest precipitation amount in one-day period

Let RRij be the daily precipitation amount on day i in period j. The maximum one-day value for period j is RX1dayj = max (RRij).

18. RX5day, maximum five-day precipitation highest precipitation amount in five-day period

Let RRkj be the precipitation amount for the five-day interval k in period j, where k is defined by the last day. The maximum five-day values for period j are RX5dayj = max (RRkj).

19. SDII, simple daily intensity index mean precipitation amount on a wet day

Let RRij be the daily precipitation amount on wet day w (RR ≥ 1 mm) in period j. If W represents the number of wet days in j then the simple precipitation intensity index SDIIj = sum (RRwj) / W.

20. R10mm, heavy precipitation days count of days where RR (daily precipitation amount) ≥ 10 mm

Let RRij be the daily precipitation amount on day i in period j. Count the number of days where RRij ≥ 10 mm.

21. R20mm, very heavy precipitation days count of days where RR ≥ 20 mm

Let RRij be the daily precipitation amount on day i in period j. Count the number of days where RRij ≥ 20 mm.

22. Rnnmm count of days where RR ≥ user-defined threshold in mm

Let RRij be the daily precipitation amount on day i in period j. Count the number of days where RRij ≥ nn mm.

23. CDD, consecutive dry days maximum length of dry spell (RR < 1 mm)

Let RRij be the daily precipitation amount on day i in period j. Count the largest number of consecutive days where RRij < 1 mm.

24. CWD, consecutive wet days maximum length of wet spell (RR ≥ 1 mm)

Let RRij be the daily precipitation amount on day i in period j. Count the largest number of consecutive days where RRij ≥ 1 mm.

25. R95pTOT precipitation due to very wet days (> 95th percentile)

Let RRwj be the daily precipitation amount on a wet day w (RR ≥ 1 mm) in period j and let RRwn95 be the 95th percentile of precipitation on wet days in the base period n (1961-1990). Then R95pTOTj = sum (RRwj), where RRwj > RRwn95.

26. R99pTOT precipitation due to extremely wet days (> 99th percentile)

Let RRwj be the daily precipitation amount on a wet day w (RR ≥ 1 mm) in period j and let RRwn99 be the 99th percentile of precipitation on wet days in the base period n (1961-1990). Then R99pTOTj = sum (RRwj), where RRwj > RRwn99.

27. PRCPTOT total precipitation in wet days (> 1 mm)

Let RRwj be the daily precipitation amount on a wet day w (RR ≥ 1 mm) in period j. Then PRCPTOTj = sum (RRwj).

APPENDIX B: POLICY BRIEF

POLICY BRIEF

MODELLING THE POTENTIAL IMPACTS OF FORESTATION ON EXTREME CLIMATE EVENTS OVER WEST AFRICA

Romaric Christel ODOULAMI

KEY MESSAGES TO POLICY MAKING COMMITTEES

1. Governments need to support research activities prior to the implementation of any climate change mitigation strategy;
2. Governments need to enhance the resilience capacity of people living in West African countries to the damaging impacts of climate extremes over the region; and
3. Government need to create and develop financial instruments to:
    i. to cover the damages caused by extreme climate events and increase the resilience capacity to extremes in West Africa; and
    ii. to support research activities on climate change adaptation and mitigation.

June 2016

INTRODUCTION

Extreme climate events (extreme rainfall and heatwaves) can have devastating impacts on society, the environment and economy. In West Africa, extreme climate events generally lead to loss of lives and property, due to the high vulnerability of most communities in this region to the impacts of weather and climate extremes. For instance, in 1997, floods and inundations induced by extreme rainfall events over West Africa rendered more than 800,000 people homeless in 14 different countries (Tschakert *et al.*, 2010). More recently in September 2009, floods induced by an extreme rainfall event (>260 mm/day) in Ouagadougou destroyed about 300 hectares of crops, wrecked nearly 25,000 houses and rendered more than 100,000 people homeless (FAO, 2009). Also, In West Africa, the World Meteorological organisation (WMO, 2013) reported during the boreal summer of 2002, extremely hot events in the region, with abnormally high temperature (up to 50.6 °C) in the Sahara. As the anthropogenic influence on the climate have affected the frequency and intensity of extreme climate and weather events (*i.e.* extreme temperatures, extreme precipitation, and droughts) (IPCC, 2014), it is expected that the ongoing climate change may affect the intensity and frequency of extreme climate events in the future (Abiodun *et al.*, 2012, 2013; Russo *et al.*, 2014; Vizy & Cook, 2012).

Moreover, considering the widely reported threat that climate change may pose to human and natural systems, it is important to reliably estimate future climate change scenarios, in order to develop suitable adaptation and mitigation strategies (such as forestation) for implementation, at regional and local scales (Giorgi *et al.*, 2009). However, before implementing any adaptation and/or mitigation strategy such as forestation, it is important

to understand its direct and potential side effects, the ethical issues and the risks associated with the option (National Academy of Sciences, 1992).

Therefore, it is necessary to provide useful and reliable information at the regional and local scale on the potential impacts of forestation on the climate in West Africa especially on climate extremes in future, so as to provide policy makers and end-users, a solid decision support mechanism to guide response options (Giorgi *et al.*, 2009). This may help to enhance the adaptive capability of the population to the impacts of extreme climate events in future and to lower their negative impacts on society, human health and security.

The present brief provides key messages that came out from a study entitled "Modelling the Potential Impacts of Forestation on Extreme Climate Events over West Africa". It aims to provide policy makers and end-users with appropriate information on the use of a large scale forestation activity (as proposed in the Great Green Wall Initiative by the African Union Commission) to mitigate the impacts of future climate change on extreme climate events (extreme rainfall and heatwaves) over West Africa. The Great Green Wall is an initiative of the African Union Commission aiming to stop the advance of the Sahara desert and to answer the multi-sectorial problems (including climate change) affecting people lives in the Sahel and Sahara regions of Africa by enhancing their livelihood (African Union Commission, 2006).

RISK AND VULNERABILITY ASSOCIATED WITH FORESTATION ON CLIMATE EXTREMES OVER WEST AFRICA IN FUTURE

Assessing the impacts of large scale forestation activities based on the proposed Great Green Wall Initiative in West Africa, using regional climate models, revealed that forestation would alter the characteristics of future climate extremes (extreme rainfall and heatwave events) over the region. These impacts of foresting the Savannah zone (area between 8°N - 12°N) in West Africa can be summarised as follow:

i. Forestation would enhance the frequency and intensity of future extreme rainfall events over the forested area, but reduce them outside the forested area (over the Guinea coast);

ii. Forestation would also increase the frequency of widespread extreme rainfall events over forested zone in West Africa; and

iii. Forestation would increase the projected heatwave number and days over the forested area but would decrease them elsewhere (outside the forested area).

This indicates that using forestation to mitigate the impacts of climate change over West Africa could enhance the frequency and intensity of future extreme climate events over the sub-continent. This would affect in many ways people living in the West African countries by increasing the risk on their health and security, affecting the environmental sustainability and the economy of the region.

KEY MESSAGES TO POLICY MAKING COMMITTEES

(1) Support to research activities prior to the implementation of any mitigation strategy

Governments need to support and encourage research activities on climate change mitigation options especially on the potential impacts of forestation on extreme climate and weather events. This will help to fully understand all the mechanisms by which forestation could alter the characteristics of extreme climate events and also to identify which of the mitigation options are more appropriate in West Africa. The support to research activities is crucial to identify suitable climate change mitigation strategies (such as forestation) that are adequate for the region before making any robust and self-sustaining recommendation on the impacts of forestation on extreme climate events.

(2) Enhance the resilience capacity to extremes in West Africa

Before coming to more robust and self-sustaining conclusions on the potential impacts of forestation on climate extremes; it is imperative that governments improve the resilience capacity of people living in West Africa to the damaging impacts of extreme climate events in the region. This also includes the establishment of early warning systems that would help to inform communities about the imminence of a potential disaster and prepare them to face it more appropriately.

(3) Creation and development of financial instruments

Governments need to consider the creation, development and maintenance of financial instruments such as:

- ***Climate disasters fund***: to cover the damages caused by extreme climate events and increase the resilience of capacity of people living in West Africa to the damaging impacts of extreme climate events
- ***Research and Development fund***: to support research activities which focused on the development and implementation of climate change adaptation and mitigation strategies and also on the understanding of the side effects associated with them.

REFERENCE

Abiodun, B. J., Lawal, K. A., Salami, A. T., & Abatan, A. A. (2013). Potential influences of global warming on future climate and extreme events in Nigeria. Regional Environmental Change, 13: 477–491. doi:10.1007/s10113-012-0381-7

Abiodun, B. J., Salami, A. T., Matthew, O. J., & Odedokun, S. (2012). Potential impacts of afforestation on climate change and extreme events in Nigeria. Climate Dynamics, 41(2): 277–293. doi:10.1007/s00382-012-1523-9

African Union Commission (2006). The Green Wall for the Sahara Initiative: A Concept Note. Addis Ababa.

FAO. (2009). FAO's Role in the Burkina Faso Flash Appeal 2009. Food and Agriculture

Organization of the United Nations (FAO).

Giorgi, F., Jones, C., & Asrar, G. R. (2009). Addressing climate information needs at the regional level: the CORDEX framework. Bulletin - World Meteorological Organization, 58(3): 175–183.

IPCC. (2014). Climate Change 2014: Impacts, Adaptation, and Vulnerability. Part A: Global and Sectoral Aspects. Contribution of Working Group II to the Fifth Assessment Report of the Intergovernmental Panel on Climate Change. (L. L. Field, C.B., Barros, V.R., Dokken, D.J., Mach, K.J., Mastrandrea, M.D., Bilir, T.E., Chatterjee, M., Ebi, K.L., Estrada, Y.O., Genova, R.C., Girma, B., Kissel, E.S., Levy, A.N., MacCracken, S., Mastrandrea, P.R., White, Ed.). Cambridge University Press, Cambridge, United Kingdom and New York, NY, USA,.

National Academy of Sciences. (1992). Policy Implications of Greenhouse Warming: Mitigation, Adaptation, and the Science Base Panel. Public Policy. Retrieved from http://www.nap.edu/openbook.php?isbn=0309043867

Russo, S., Dosio, A., Graversen, R. G., Sillmann, J., Carrao, H., Dunbar, M. B., Singleton, A., Montagna, P., Barbola, P., & Vogt, J. V. (2014). Magnitude of extreme heat waves in present climate and their projection in a warming world. Journal of Geophysical Research: Atmospheres, 119: 12500–12512. doi:10.1002/2014JD022098

Tschakert, P., Sagoe, R., Ofori-Darko, G., & Codjoe, S. N. (2010). Floods in the Sahel: An analysis of anomalies, memory, and anticipatory learning. Climatic Change, 103(3): 471–502. doi:10.1007/s10584-009-9776-y

Vizy, E. K., & Cook, K. H. (2012). Mid-Twenty-First-Century Changes in Extreme Events

over Northern and Tropical Africa. Journal of Climate, 25(17): 5748–5767. doi:10.1175/JCLI-D-11-00693.1

WMO. (2013). The global climate 2001-2010: A decade of climate extremes. Summary report. WMO-No. 1119, World Meteorological Organization (WMO), Geneva, Switzerland. Retrieved from http://www.unep.org/pdf/wmo_report.pdf